

Growth and biomechanics of plant epidermal cells

Inaugural-Dissertation

zur

Erlangung des Doktorgrades

der Mathematisch-Naturwissenschaftlichen Fakultät

der Universität zu Köln

vorgelegt von

Aleksandra Sapała

aus Stettin, Polen

Köln, 2018

Die vorliegende Arbeit wurde am Max-Planck-Institut für Pflanzenzüchtungsforschung in Köln in der Abteilung für Vergleichende Entwicklungsgenetik (Direktor: Prof. Dr. Miltos Tsiantis), in der Arbeitsgruppe von Dr. Richard S. Smith angefertigt.



Berichterstatter:	Prof. Dr. Miltos Tsiantis
	Prof. Dr. Martin Hülskamp
Schriftführer:	Dr. Peter Huijser
Prüfungsvorsitzender:	Prof. Dr. Achim Tresch
Tag der Disputation:	03.09.2018

Table of contents

ABSTRACT	I
ZUSAMMENFASSUNG	III
LIST OF FIGURES	V
LIST OF TABLES	VII
LIST OF ABBREVIATIONS	VII
1. INTRODUCTION	1
1.1. Organization of the thesis	3
2. BACKGROUND	5
2.1. The plant cell and the cell wall	5
2.1.1 The plant cell	5
2.1.2 The cell wall	6
2.2. Mechanics of plant cells – how to view a plant cell as a physical system	7
2.2.1 Cell geometry and size influences mechanical stress on the cell wall	7
2.2.2 Measuring material properties of cell wall	8
2.2.3 Cell wall stiffness limits cell growth	10
2.2.4 Osmotic potential (turgor pressure) drives cell expansion	11
2.2.5 Measuring turgor pressure	11
2.2.6 Plant cells are able to sense mechanical signals	14
2.3. Growth	15
2.3.1 Types of growth	15
2.3.2 Measuring cell shape and growth	17
2.3.3 Mechanical stress feeds back on growth	19
2.4. Jigsaw- puzzle – shaped cells in leaf epidermis as an example of a mechanical feedback in creating forms	19

2.4.1 Molecular networks driving puzzle cell formation	21
2.4.2 Methods for measuring puzzle shapes and their growth	22
2.4.3. Mechanical feedback facilitates puzzle cell formation	24
2.4.4 Potential functions of the puzzle shapes	25
3. CELLULAR GROWTH PATTERNS IN ISOTROPICALLY AND ANISOTROPICALLY GROWING ORGANS	27
3.1. A round organ grows isotropically: <i>A.thaliana</i> cotyledon	29
3.2. An elliptical organ grows anisotropically: <i>A. thaliana</i> sepal	33
3.2.1 Growth patterns in wild type sepals	34
3.2.2. Growth patterns in <i>lgo</i> sepals	36
3.2.3.A mechanical feedback restricts sepal growth and shape in <i>A. thaliana</i>	41
3.3. Summary of the results	42
3.4. Materials and methods	45
3.5. Acknowledgement	45
4. MECHANICAL PROPERTIES OF GROWING PLANT CELLS	47
4.1. Cellular Force Microscope	48
4.2. Combining the Cellular Force Microscope technology with a confocal laser scanning microscope	51
4.3.Osmotic treatment for quantifying cell wall elasticity in the sepal of <i>Arabidopsis thaliana</i>	54
4.4. On the micro-indentation of plant cells in a tissue context	59
4.5 The correlation between cell wall elasticity, ROS levels and cell maturation	62
4.6. Summary of the results	64
4.7. Materials and methods	66
4.7.1. Onion CFM	66
4.7.2. CFM setup mounted on the confocal microscope	66
4.7.3. Osmotic treatment	67
4.7.4. Integrating the CFM and osmotic treatment data into a mechanical model	68
4.7.5. Comparing stiffness in sepal epidermal cells between wild type and <i>fish4-5</i> mutant	68
4.7.6. Acknowledgement	69

5. WHY PLANTS MAKE PUZZLE CELLS AND HOW THEIR SHAPE EMERGES	71
5.1. Cell shape predicts mechanical stress magnitude	73
5.2. Cell shape measures	75
5.3. A mechanistic model for puzzle shape emergence	76
5.4. Isotropic tissue growth is correlated with puzzle-shaped cell formation	80
5.5. Lobeyness allows cells to increase their size while avoiding excessive stress	84
5.6. Experimental evidence that stress needs to be managed	89
5.7. Cell shape and size across species	90
5.8 Summary of the results	92
5.9. Materials and methods	94
5.9.1 FEM modelling of mechanical stress	94
5.9.2 2D mass-spring model of cell growth	94
5.9.3 Live imaging of cotyledons	95
5.9.4 Creating transgenic lines	95
5.9.5 Analysis of fruit and exocarp cell shape	95
5.9.6 Imaging cell shapes in mature leaves of IQD lines	96
5.9.7 Pharmacological treatment	96
5.9.8 Multi-species leaf cell shape analysis	96
5.10. Acknowledgement	97
6. CONCLUSION	99
6.1. Summary of the findings	99
6.2. Discussion of research contributions	100
6.2.1. Mechanical properties of the cell wall reflect cellular growth rates in wild type and <i>fish4</i> sepals	100
6.2.2. Cellular Force Microscopy coupled with confocal microscopy and computational modeling as a good method to measure turgor pressure <i>in vivo</i>	102
6.2.3. The relationship between cell and organ shape	103
6.2.4. Puzzle cells minimize mechanical stress on the cell wall	104
6.2.5. Local growth restrictions and curvature sensing reproduce puzzle cell shapes	106
6.2.6. Experimental evidence of the stress minimizing mechanism in plant epidermis	109

6.2.7. A role for mechanical or geometric cues in cell shape formation	110
6.2.8. Could cells sense stress through geometry?	111
6.2.9. Acknowledgement	112
6.3. Directions for future work	112
6.3.1. Biomechanics	112
6.3.2. Regulation of growth directions on cell, tissue and organ level	112
6.3.3. The stress minimization mechanism in plants	113
6.4. Closing remarks	114
BIBLIOGRAPHY	115
ACKNOWLEDGEMENTS	129
LEBENS LAUF	131
AFFIDAVIT / EIDESSTAATLICHE ERKLÄRUNG	135

Abstract

Since plant cells are encased in rigid cell walls, approaching them as physical systems is necessary to fully understand the multi-level mechanisms controlling developmental processes. Therefore, in my thesis I tried to combine physical and biological methods to study the morphogenetic processes in the plant epidermis.

I quantified growth of the *Arabidopsis thaliana* sepal, an elliptical floral organ which is comprised of small, square cells and large, elongated ‘giant cells’ randomly interspersed between the small ones. I detected a wave of high anisotropic growth (growing predominantly in one direction): along the proximo-distal starting at the tip of the sepal, gradually moving to its base as the organ develops. Interestingly, replacing the giant cells with files of small cells (observed in the *Igo* mutant) does not change the overall growth rate tendencies. In contrast, the *Arabidopsis* cotyledon, which has a round shape, grows much more isotropically (at the same rate in all directions), even though its cells have very elaborate, jigsaw puzzle-like shapes.

I used Cellular Force Microscopy (CFM) to measure stiffness (or, indirectly, turgor pressure) of sepal cells. A Finite Element Method (FEM) mechanical model showed that observed differences in measured stiffness values between small and giant cells can be explained by cell geometry. Furthermore, using osmotic treatments I demonstrated *in vivo* that the cell wall is softer in the fast-growing areas than in the slow-growing areas. By comparing osmotic treatment results in wild type and the *ftsh4* mutant, I speculated that Reactive Oxygen Species play an important role in cell maturation by locally stiffening the cell wall.

Finally, I focused on more complex cell shapes as I employed genetic engineering, cell growth and shape quantification and computational modelling to answer the question why epidermal cells in leaves and cotyledons make jigsaw puzzle-like shapes. Cell shapes are adjusted to growth direction according to self-enhancing growth restriction, as proven by a growing mechanical model. I proposed puzzle cells minimize mechanical stress on the cell wall and therefore prevent it from bursting or needing to introduce additional structural reinforcements. Finally, I demonstrated several lines of evidence that plants of different cell shape and size, as well as different species, have an active mechanism of keeping this stress low.

Taken together, my results contribute to the understanding of the role of cell shape in the epidermal tissue. They also provide novel input on mechanical properties of the cell wall during growth supported by in vivo experiments performed using state-of-the-art biomechanical methods.

Zusammenfassung

Da Pflanzenzellen in starren Zellwänden eingeschlossen sind, ist es notwendig, sie als physikalische Systeme zu betrachten, um die Mechanismen, die die Entwicklungsprozesse auf verschiedenen Ebenen steuern, vollständig zu verstehen. In meiner Doktorarbeit kombiniere ich physikalische und biologische Methoden, um diese morphogenetischen Prozesse in der Pflanzenepidermis zu untersuchen.

Ich quantifizierte das Wachstum des *Arabidopsis thaliana* Sepalum (Kelchblatt), eines elliptischen Blütenorgans, das aus kleinen, quadratischen Zellen und großen, länglichen Riesenzellen besteht, die zufällig zwischen den kleinen Zellen eingestreut sind. Ich entdeckte einen Bereich mit hohem anisotropen Wachstum (hauptsächlich in einer Richtung wachsend) entlang der proximo-distalen Achse, welcher sich wie eine Welle beginnend an der Spitze des Kelchblattes allmählich zur Basis bewegt, wenn sich das Organ entwickelt. Interessanterweise ändert sich das beobachtete Wachstum nicht, wenn die Riesenzellen durch kleine Zellen ersetzt werden (beobachtet in der *lgo*-Mutante). Im Gegensatz dazu wächst das rund geformte Keimblatt (Kotyledone) sehr viel isotroper (mit gleicher Geschwindigkeit in allen Richtungen), obwohl seine Zellen sehr komplexe Formen, ähnlich den von Puzzleteilen, haben.

Ich verwendete Cellular Force Microscopy (CFM), eine Methode um physikalische Größen wie die Formsteifigkeit oder indirekt den Turgordruck von Pflanzenzellen zu messen, um die Eigenschaften der Kelchblattzellen zu bestimmen. Ein mechanisches Modell der Finite-Elemente-Methode (FEM) zeigte, dass beobachtete Unterschiede in den gemessenen Steifigkeiten zwischen kleinen und großen Zellen durch die Zellgeometrie erklärt werden können. Darüber hinaus demonstrierte ich *in vivo* mit osmotischen Behandlungen, dass die Zellwand in den schnell wachsenden Bereichen weicher ist als in den langsam wachsenden Bereichen. Durch den Vergleich der Ergebnisse der osmotischen Behandlung mit dem Wildtyp und der *ftsh4*-Mutante spekulierte ich, dass reaktive Sauerstoffspezies eine wichtige Rolle bei der Maturation der Zellen spielen, indem sie die Zellwand lokal versteifen.

Schließlich beschäftigte ich mich mit komplexeren Zellformen, indem ich Gentechnik, Zellwachstum, Formquantifizierung sowie Computermodelle einsetzte, um die Frage zu beantworten, warum epidermale Zellen in Blättern und Keimblättern puzzleartige Formen

bilden. Die Zellformen werden gemäß selbstverstärkender Wachstumsbeschränkung an die Wachstumsrichtung angepasst, wie durch ein mechanisches Modell bewiesen wird, welches das Zellwachstum simuliert. Ich habe vorgeschlagen, dass die Form der puzzleartigen Zellen die mechanische Belastung der Zellwand minimiert und verhindert, dass sie platzen oder zusätzliche strukturelle Verstärkungen benötigen. Abschliessend zeige ich auf, dass verschiedene Arten von Pflanzen mit unterschiedlichen Zellformen und -größen einen aktiven Mechanismus haben diesen Stress niedrig zu halten.

Zusammengefasst tragen meine Ergebnisse zum Verständnis der Rolle der Zellform im Epidermisgewebe bei. Sie liefern auch neue Informationen über mechanische Eigenschaften der Zellwand während des Wachstums, unterstützt durch *in vivo* Experimente, die mit modernsten biomechanischen Methoden durchgeführt wurde.

List of figures

Figure 2.1. Stress directions on a sphere and a cylinder.	8
Figure 2.2. AFM and CFM operate on different force magnitudes.	13
Figure 2.3. Selected plant growth types and their modalities.	16
Figure 2.4. Two mathematical representations of growth.	17
Figure 2.5. Confocal image analysis using MorphoGraphX.	18
Figure 2.6. Cell shape in the epidermis of <i>Arabidopsis thaliana</i> cotyledon.	20
Figure 3.1. Isotropically and anisotropically shaped organs of <i>Arabidopsis thaliana</i> .	28
Figure 3.2. Heteroblasty in <i>Arabidopsis thaliana</i> rosette leaves.	31
Figure 3.3. Evolution of the cotyledon epidermal cells in the first days after germination.	31
Figure 3.4. Growth tracking of an <i>Arabidopsis</i> cotyledon from 2 to 6 days after germination.	32
Figure 3.5. The schematic morphology of an <i>Arabidopsis thaliana</i> flower.	34
Figure 3.6. Growth patterns in a developing abaxial sepal of <i>Arabidopsis thaliana</i> .	38
Figure 3.7. The abaxial sepal is created from a small band of cells.	39
Figure 3.8. Heat maps of a growing <i>lgo</i> sepal.	40
Figure 4.1. Results of Cellular Force Microscopy experiments on turgid onion epidermis.	50
Figure 4.2. A scheme of the CFM-confocal setup.	51
Figure 4.3. CFM measurements on sepal epidermis performed using the CFM-confocal setup.	53
Figure 4.4. The principle of an osmotic treatment experiment.	55
Figure 4.5. Submergence of the sepal in pure water in order to achieve full turgidity of the cells (starting point for osmotic treatment experiments).	56

Figure 4.6. Plasma membrane (marked by YFP, yellow) and cell wall (stained with PI, red). 57

Figure 4.7. Cell wall shrinkage upon osmotic treatment in wild type sepal. 58

Figure 4.8. CFM indentation and osmotic treatments on an *A. thaliana* sepal implemented in the FEM model. 61

Figure 4.9. Comparison of cell wall elasticity between wild type and *ftsh4-5* at developmental stages 8–9. 64

Figure 5.1. Epidermis of a mature leaf of *Arabidopsis thaliana*. 72

Figure 5.2. Cellular stress patterns in finite element method (FEM) simulations. 73

Figure 5.3. Principal stresses generated by turgor *in vivo* simulated in an FEM model. 74

Figure 5.4. The 2D puzzle cell model. 77

Figure 5.5. Geometric-mechanical model of puzzle cell emergence. 79

Figure 5.6. Stresses in modeled cell shapes. 80

Figure 5.7. Correlation between growth direction and shape on the cell and organ level. 83

Figure 5.8. The predicted relationship between cell size and LEC size. 85

Figure 5.9. Different epidermal cell shapes in adult leaves of transgenic lines (Bürstenbinder et al., 2017). 86

Figure 5.10. Geometric features of cell populations. 87

Figure 5.11. Distribution of LEC area vs. cell area for all cells. 88

Figure 5.12. Depolymerization of cortical microtubules by oryzalin treatment causes cells of NPA-treated meristems to expand without division, ultimately leading to the rupture of the cell wall due to increased mechanical stress. 90

Figure 5.13. Multi-species cell shape analysis. 91

Figure 5.14. Correlation of lobeyness and cell area. 92

Figure 6.1. Cell shape as a means of minimizing mechanical stress on the cell wall. 106

Figure 6.2. The proposed molecular network driving puzzle cell formation.

107

Figure 6.3. Cell wall reinforcements follow stress directions in the periclinal cell walls.

111

List of tables

Table 2.1. Basic terminology used in pavement cell studies.	20
Table 2.2. Puzzle cell quantification tools developed in recent years.	23
Table 3.1. Stages of flower development.	35
Table 4.1. Experimental and simulated indentation stiffness results fitted between 2–1.5 μm indentation depth for the points in figure 4.8.	61
Table 4.2. Average stiffness values for small and giant cells (Table 4.1) and relative stiffness variation between them. Adapted from (Mosca et al., 2017).	62

List of abbreviations

%	percent
2D	two-dimensional
3D	three-dimensional
ABP	Auxin Binding Protein
ACR	ACT-domain Repeat
AFM	Atomic Force Microscopy
<i>A. thaliana</i>	<i>Arabidopsis thaliana</i>
ATML	<i>Arabidopsis thaliana</i> Meristem Layer
ATX	<i>Arabidopsis</i> Trithorax
CDS	coding DNA sequence

CESA	Cellulose Synthase
CFM	Cellular Force Microscopy
CLASP	CLIP-associated Protein
cm	centimeter
CMT	cortical microtubules
Col-0	<i>Arabidopsis thaliana</i> Columbia accession
CUC	Cup-shaped Cotyledon
DAB	3,3'-diaminobenzidine
DAG	days after germination
DEK	Defective Kernel
DNA	deoxyribonucleic acid
E	Young's modulus (measure of stiffness)
e.g	exempli gratia
F	force
FEM	Finite Element Method
FtsH	FTSH protease
HDG	Hedgehog
IQD	IQ67-domain
KRP	Kip-related Protein
LEC	Largest Empty Circle
LGO	Loss of Giant Cells in Organs
LNG	Longifolia
LOCO-EFA	Lobe Contribution Elliptic Fourier Analysis
M	Molar
MEMS	microelectromechanical system
MPa	megapascal

NA	numerical aperture
nm	nanometer
NPA	1-N-naphtylphthalamic acid (NPA),
NBT	nitroblue tetrazolium
<i>P</i>	pressure
PCR	polymerase chain reaction
PDG	principal growth directions
PI	propidium iodide
PIN	Pin-formed
PPM	plant protective medium
p35S	Cauliflower Mosaic Virus 35S promoter
<i>r</i>	Pearson correlation coefficient
RCO	Reduced Complexity
RIC	ROP-interactive CRIB motif-containing Proteins
ROP	Rho of Plants
ROS	reactive oxygen species
SAM	Shoot Apical Meristem
SD	standard deviation
TRM	TON1-recruiting Motif
Ws-2	<i>Arabidopsis thaliana</i> Wassilewskaja accession
WT	wild type
vos	Variable Organ Size and Shape
<i>x</i>	displacement
YFP	Yellow Fluorescent Protein
μl	microliter
μM	micromolar

ν

Poisson's ratio(measure of compressibility)

1. Introduction

Three processes are considered to be the canonical events in the creation of a functional plant: cell proliferation, cell differentiation, and growth. The pluripotent meristematic cells multiply and eventually differentiate into cell types of specific identities. After cell identity is established, cells continue to grow to achieve their final form and size. In my work I study the third process – the growth. While after differentiation the overall function of a cell has already been decided, there are still many levels on which the development of a plant is controlled in the growth phase.

In this thesis I discuss the primary plant growth, which entails creation of primary tissue: stems, roots, leaves and reproductive organs. I do not consider secondary growth, i.e. growing in thickness by creating wood. Two features very important for controlling the primary growth of plant cells (in the green tissue) are: the cell wall, which provides structural strength to the tissue, and the turgor pressure which exerts forces on the wall from inside the cell. Growth occurs when turgor pressure causes elastic (reversible) expansion of the cell wall, and this expansion is then made plastic (irreversible) by cell wall remodeling enzymes (Lockhart, 1965, 1967). Therefore, material properties of the cell wall (its ability to irreversibly expand) and turgor pressure are the backbone of cell growth, and the genetic and physical components regulating them are secondary factors.

The cell wall is a very important part of plant morphogenetic studies because it bears the mechanical stress induced by turgor pressure. It is made of several kinds of biopolymers (cellulose, hemicelluloses, pectins) and has to be very durable but at the same time able to expand (Cosgrove, 2005). Due to complex interdependencies between the different components, the cell wall is not a trivial system to study. It requires both biochemical, biological and physical expertise. So far, the most common and most successful approach has been to investigate the molecular aspects of growth. This is understandable because using modern genetics it is possible to decipher a role of each structural component of the system by knocking it out, enhancing its activity or disrupting any related biochemical pathway (Bilborough et al., 2011; Scarpella et al., 2010). This kind of work can be combined with precise growth quantification in order to understand the effect of these genetic changes (Barbier de Reuille et al., 2015).

The problem with this approach is that it is extremely unlikely that a process as complex as growth can be determined by a single component. The cell wall is a very inhomogenous system built of a number of diverse biochemical compounds. Therefore, it is influenced by a variety of enzymes and transcription factors. Water transport between the cell and its surroundings, which determines turgor pressure, is also a complex phenomenon. In fact, it encompasses active water transport as well as passive distribution of ions across cell membranes which in turn influences osmosis. An integrative perspective is needed, which would approximate cells to hydraulic systems (elastic material under pressure) (Bidhendi and Geitmann, 2018) and, at the same time, include more specific molecular effects such as proteins responsible for growth repression (Bilborough et al., 2011).

In this thesis I adopt a biomechanical approach in order to investigate plant growth. This means neglecting the fine details of cell wall biochemistry and approximating it to a material of certain physical properties such as elasticity as well as simplifying the cytosol to a liquid with a certain osmotic potential which exerts a certain pressure on the cell wall. Given the fact that growth as an observable can be effectively measured on tissue or cell level (not lower), if we describe growth of cells, approximate cell wall elasticity to the same dimension and couple all this with genetics, we can reasonably state how a gene/group of

genes is acting on a cell in order to modify growth in a specific manner (Barbier de Reuille et al., 2015; Hervieux et al., 2016; Hofhuis et al., 2016; Kierzkowski et al., 2012; Kuchen et al., 2012; Vlad et al., 2014).

In the research field of plant development, both a genetic and a physical expertise is required. Previous studies have shown that neither of those approaches is really effective without the other (Coen et al., 2004). However, since biology and physics are two rather distant disciplines, it has required major effort to combine them not only in plant science, but in any other research area. It has been my aim to build a bridge between molecular biology and physics in order to better understand shape establishment in plants on cell, tissue and organ level. With that in mind, I have optimized and improved existing protocols in order to customize them to answer specific biological questions.

1.1. Organization of the thesis

At the beginning of this thesis (Chapter 2) I introduce all the biological and physical concepts necessary to understand the results of my work. In the following chapters I will present my work regarding:

- a detailed description of cellular growth patterns in two organs of *Arabidopsis thaliana* which have different organ and cell shape: the isotropic cotyledon and the anisotropic sepal (Chapter 3)
- measuring physical properties of plant cells such as turgor pressure and cell wall elasticity and putting them in context of different biological studies. I mostly use the sepal as study system because of the relatively simple shape of its cells (Chapter 4)
- proposing a mechanics-based explanation of how cell shape is established in an externally imposed growth field, namely that cells adjust their shape to minimize the mechanical stress exerted on the periclinal cell walls. I demonstrate it on jigsaw-puzzle-shaped epidermal cells in cotyledons and leaves, as they are an extreme case of complex shapes in plant cells and require the most sophisticated shape coordination while growing (Chapter 5)

Finally, I will discuss my results in the context of other work. Given that cellular growth happens when the cell wall gives into turgor pressure in a controlled way, I propose that a

very important component of this control is cell geometry itself, which is a part of a shape-stress-growth feedback loop. I also hypothesize that cell geometry, via cortical microtubules, may be involved in sensing of mechanical stress in plant cells (Chapter 6).

2. Background

2.1. The plant cell and the cell wall

2.1.1 The plant cell

As plants do not have the ability to move from one place to another, one possibility for them to accommodate to the environment is by adapting their growth. They need a way to keep a certain architecture and posture of their bodies (which can be very large) and perform small scale movements (tropisms). Since the non-woody plants do not have muscles or skeletons, they strongly rely on turgor in maintaining their form and function.

Plant cells are surrounded by the cell wall – a rigid case which serves as a scaffolding for their bodies. This scaffolding, however, needs to be supported by high pressure (turgor) coming from within the cell in order to keep its form (Gramüller et al., 2015; Guiducci et al., 2014; Li and Wang, 2015). This is achieved by water stored in the vacuole, but also by high water content in the cytoplasm. Neighboring cells are connected through plasmodesmata and share walls with each other, therefore pressure exerted on the wall by one cell can be counteracted by pressure in the neighboring cell (Sager and Lee, 2014). For special cell types such as trichomes and cotton fibers, plasmodesmata can close causing the increase in turgor pressure leading to increased local outgrowth (Ruan et al., 2001).

The presence of the cell wall is extremely important in the developmental biology of plants because, compared to animal cells, it serves as an additional factor regulating cell and tissue growth. Any growth signal, independently of its nature (biochemical, genetic, abiotic), has to influence not only the content of the cell (cytosol, vacuole and genetic material), but also the cell wall (Wolf et al., 2012).

2.1.2 The cell wall

The primary cell wall has three major components: cellulose, hemicelluloses and pectins (Cosgrove, 2005). The secondary cell wall is created in mature tissues and is not investigated in this thesis, where I focus on young, developing cells. Therefore, throughout this chapter I will only discuss the primary cell wall. Cellulose is constituted of unbranched microfibrils of polysaccharides which are very stiff and relatively resistant to enzymatic activities. Hemicelluloses bind to cellulose and branch, while pectins cross-link with each other. The latter group forms a hydrated gel that enables cellulose microfibrils to slip sideways as the cell is growing and keep them in place after growth is finished (Vincken et al., 2003; Willats et al., 2001). It has also been proposed that cellulose microfibrils are connected by specific junctions called ‘biomechanical hotspots’ that facilitate cell wall expansion in a more refined way (Cosgrove, 2014; Park and Cosgrove, 2012).

While cellulose is produced by large enzymatic complexes close to the cell wall in the plasma membrane (Kimura et al., 1999), the matrix polysaccharides are produced inside the cell by the Golgi apparatus, packed in small vesicles and driven towards the wall by turgor pressure (one of the main drivers of growth) (Cosgrove, 2005; Proseus and Boyer, 2005). Cellulose microfibrils are created by large proteins called CESA (plant cellulose synthase). They are very stiff and account for the structural integrity of the cell wall. Although these fibers are only 3-5 nm wide, their length can be in the micrometer range, and can go around the circumference of a cell a few times (Cosgrove, 2005). CESA are guided by microtubules embedded in the plasma membrane (Lloyd and Chan, 2004; Paredez et al., 2006). Since microtubules are known to orient along the direction of high stress in the cell wall (Hamant et al., 2008; Hejnowicz et al., 2000), this is a primary link to a large body of work showing that cell wall structure adjusts to geometry and mechanical stress, which I will discuss later in this thesis.

The displacement of the cellulose fibers is controlled by selective loosening of linkages between the cell wall components (Marga et al., 2005). Depending on the chemical bond being cleaved or created, the cell wall extension can be fast (within a second or less) or slow (within hours or days, for example when growth gradually slows down upon tissue maturation). It needs to be underlined that actual growth (increase in volume) happens not due to the scission of the cross-link chemical bonds, but due to yielding of the ‘newly softened’ cell wall upon turgor pressure (Cosgrove, 2005). This means that cell wall elasticity and turgor pressure are both very important for growth processes, with the difference that cell wall can also define growth direction while pressure by definition is equal in all directions.

2.2. Mechanics of plant cells – how to view a plant cell as a physical system

In the previous section I listed the main features of the cell wall composition and how they influence cell growth. Two key components of cellular growth are: material properties of the wall and turgor pressure. In this section I am going to introduce experimental methods used to measure these properties and present an overview of information gathered using these methods. Before that, I am going to explain a crucial concept in biomechanics, that is mechanical stress, how it is determined and what its implications are on the growth of plant cells.

2.2.1 Cell geometry and size influences mechanical stress on the cell wall

Plant cells are like small balloons inflated with considerable turgor pressure, up to 10 bar in *A. thaliana* leaf cells (Forouzesh et al., 2013), although it can be as high as 50 bar in specialized cells such as stomata (Franks et al., 1995, 2001, measured in species other than *A. thaliana*). Turgor pressure exerts internal forces on the cell wall. The magnitude of these forces is called mechanical stress and it is defined as the ratio of internal force acting on a cross-section of the material to the area resisting (area of this cross-section). Therefore, if the wall were made of a homogeneous material, the mechanical stress could be predicted by the cell's size and shape (Geitmann and Ortega, 2009; Niklas, 1992; Schopfer, 2006).

If a cell were a sphere, stress would be equal in all directions because a sphere is a uniform structure. If a cell were a cylinder, stress would be higher along the circumferential direction than along the longitudinal direction (Fig. 2.1) (Geitmann and Ortega, 2009; Niklas, 1992). Bassel et al. (2014) have shown that upon pressurization (introducing internal pressure similarly to a balloon), a square cuboid cell is going to expand less than a rectangular cuboid cell if they have identical volumes and cell wall thickness. The reason for that is that as cell wall length increases (cell shape changes from cube to brick), the area of the wall which holds stress increases as a linear function of length, while stress increases as a quadratic function of length. This demonstrates that initial cell geometry can influence growth (Bassel et al., 2014).

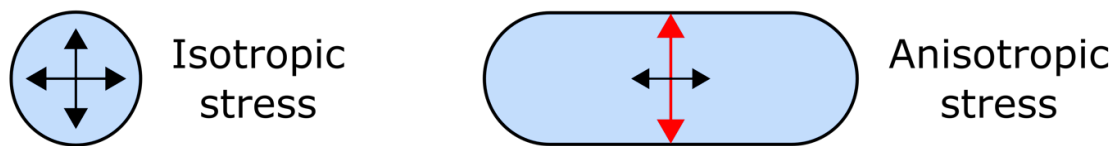


Figure 2.1. Stress directions on a sphere and a cylinder. (Left) In an inflated sphere stress is uniform in all directions. (Right) In an inflated cylinder stress is higher in the radial direction (red arrow) because the radial cross section has lower area than the longitudinal cross section (black arrow). Therefore, the pressure is distributed on a smaller surface and stress is higher.

Apart from the shape, cell size also affects cell wall stress. It has been demonstrated with physical simulations that a large square cuboid cell is going to expand more than a small square cuboid cell (under the same pressure and cell wall material properties). This indicates that in general, large cells are under more mechanical stress than small cells (Bassel et al., 2014).

2.2.2 Measuring material properties of cell wall

Atomic Force Microscopy (AFM) is a method which can be used to study mechanical properties of different materials. Its applications range from material sciences (Yu et al., 2001), through studies on single biomolecules such as proteins (Rico et al., 2013) or DNA (Sakai et al., 2011), to single living cells (Guillaume-Gentil et al., 2014; Shibata et al., 2015) and entire organisms such as *Caenorhabditis elegans* worms (Allen et al., 2015; Essmann et al., 2017; Várkuti et al., 2012). Finally, AFM has been used in many studies in

plant development (Beauzamy et al., 2015a; Fernandes et al., 2012; Forouzesht et al., 2013; Hayot et al., 2012; Milani et al., 2011; Peaucelle et al., 2011; Sampathkumar et al., 2014).

AFM uses a cantilever to probe the sample with very low forces and a laser beam which is deflected off the cantilever. Deflection of the laser beam is calibrated according to the cantilever stiffness so that it can be translated to how much the cantilever displaces the tissue. This, in turn, can uncover information about topology and stiffness using different mathematical models, depending on setup and sample properties (Redmacher, 1997).

Apart from AFM, another technique which has been used to measure the elastic modulus of the cell wall is fluorescence emission – Brillouin scattering imaging (Elsayad et al., 2016). It entails probing the sample with laser recording scattered light, and the light frequency is proportional to the speed of sound waves in the sample (Ballmann et al., 2015).

The aforementioned methods have a limited ability to measure cell wall stiffness in the in-plane direction of the cell wall, the direction that is presumed to be the most relevant for growth and morphogenesis. The most reliable methods in this respect are ones using an extensometer which pulls the tissue in the in-plane directions. However, it has only been applied *in planta* in very limited situations for actual force measurements (Park and Cosgrove, 2012; Robinson et al., 2017) or for less precise assessment of tissue response to mechanical forces (Bringmann and Bergmann, 2017).

Osmotic treatments offer the possibility to measure in-plane cell wall stiffness in living plant cells (Hong et al., 2016; Kierzkowski et al., 2012; Wang et al., 2006; Weber et al., 2015) in a relatively direct manner. Like an extensometer, osmotic treatments are based on changing the stress on the cell wall and recording the deformation that occurs as a result. Cells are imaged with a confocal laser scanning microscope and the change in their surface area is quantified using the 3D image processing software MorphoGraphX (Barbier de Reuille et al., 2015; Kierzkowski et al., 2012). The change in stress is accomplished by manipulating the cell's turgor pressure through osmosis. The turgor pressure in plant cells results from the difference in osmotic potential between the cell cytosol and the extracellular space. Since the cell cytosol has a higher osmolarity than extracellular space, the cell will take up water through osmosis until the physical pressure balances the

difference in osmotic potential. The increase of osmotic potential of the extracellular space is achieved by immersing the sample in a solution with an osmolarity higher than the cytosol. This will cause the cells to deflate as a process called plasmolysis and can be used to estimate the turgor pressure of the cells (reviewed by Oparka, 1994). While this method is less direct than an extensometer, it is more direct than indentation-based methods as well as Brillouin imaging. Furthermore, it does not require specific equipment apart from a confocal microscope and image quantification software.

2.2.3 Cell wall stiffness limits cell growth

The wall of a plant cell is often softer (more prone to plastic and elastic deformation) in fast-growing regions than in the slow-growing regions. This has been demonstrated using experimental methods such as Atomic Force Microscopy (AFM) (Milani et al., 2011), or combination of high-resolution growth tracking and cell wall elasticity measurements by osmotic treatment (Kierzkowski et al., 2012). Not only are elastic properties of cells responsible for tissue expansion, but they are also critical in new organ primordia formation at the shoot apical meristem (Peaucelle et al., 2011; Pien et al., 2001).

Milani et al. (2011) reported that the central zone of shoot apical meristem (SAM) was stiffer than the peripheral zone, which overlaps with growth rates – central zone is known to grow slower than peripheral zone as new leaf primordia are created (Kierzkowski et al., 2012). This supports the generally agreed on viewpoint that cell wall needs to loosen in order for the cells to grow (Cosgrove, 2005). Peaucelle et al. (2011) used a slightly different methodology. They performed AFM measurements using a cantilever with beads of different sizes attached to its tip to investigate SAM cells. They claimed that this gave them access to stiffness of both the epidermal cell layer (a smaller bead) and the sub-epidermal cell layers inside the meristem (a larger bead). This led them to hypothesize that cell wall loosening via demethylesterification of pectin is initiated in the subepidermal layers and then propagates to the epidermis to allow new primordia to grow out.

Epidermal cell wall architecture in *A. thaliana* cotyledons was analyzed with AFM by Sampathkumar et al. (2014). They reported that the direction of cellulose fibers on the periclinal wall overlapped with the orientation of cortical microtubules and direction of

calculated stress patterns within the jigsaw-puzzle-shaped pavement cells. This is in line with other studies that point to the fact that the microtubules are able to sense mechanical stress and direct cellulose deposition to reinforce the cell wall against this stress (Hamant et al., 2008).

2.2.4 Osmotic potential (turgor pressure) drives cell expansion

The most widely used physical theory of plant growth was constructed by Lockhart. He linked osmotic pressure inside a plant cell (influenced by water movement from mature cells to younger, growing cells) and the elastic properties of the wall as two factors driving cell expansion (Lockhart, 1965, 1967; Lockhart et al., 1961).

Turgor pressure caused by water uptake exerts force on the cell wall perpendicular to its plane, which results in the cell expanding in directions imposed by the cell walls. Material properties of the cell wall determine how much it yields to pressure (Geitmann and Ortega, 2009). The relationship between the directionality of cellulose deposition, cell geometry and growth will be discussed further on. In the following section I am going to focus on methods of measuring turgor pressure available to date and how they have contributed to understanding growth processes in plants. They are usually a combination of laboratory setups and computer simulations.

2.2.5 Measuring turgor pressure

Indentation techniques can be an experimental approach for measuring both cell wall elasticity and turgor pressure by directly or indirectly recording force exerted on a sensor by the sample upon indentation and fitting these values to mathematical models. However, it is difficult to measure these two properties with exactly the same experimental setup, because cell wall elasticity measurements require much smaller forces than turgor pressure measurements. Therefore, the first can be measured by AFM, but usually forces available in this technique are too low to measure the latter (Routier-Kierzkowska and Smith, 2013).

Apart from the experiments described in section 2.2.2, AFM was also used for turgor pressure measurements in plants. Forouzesh et al. (2013) used a Finite Element Method

(FEM) simulation to extract cell wall elasticity and turgor pressure from relaxation experiments performed with AFM. This work, however, only simulated a spherical membrane, not a real cell or group of cells. They were able to measure different turgor pressure values for different conditions: lowest in salt (plasmolysis), medium in air and highest in water (turgid). Another example is work of Beauzamy et al. (Beauzamy et al., 2015a). They proposed a mathematical model in which both turgor pressure and cell wall elasticity can be inferred from one AFM dataset. This is not a trivial task since these two properties involve force of different scales. The method used by Beauzamy et al. (2015a) was applied to onion epidermal cells which are much bigger than meristematic cells of *A.thaliana*.

Another way of measuring turgor pressure inside plant cells is cell pressure probe. This method is much more straightforward and does not require mathematical models, since it measures hydrostatic pressure in the cell directly (Tomos and Leigh, 1999; Wang et al., 2006). However, a big disadvantage of this method is that it requires the probe to be inserted inside the cell rather than touch the cell from the outside, thereby being much more invasive to the system.

The two methods presented above have two disadvantages. Firstly, it is not clear if AFM measures in-plane stiffness of expandable cellulose fibrils specifically (which can bundle, according for instance to AFM images provided by Sampathkumar et al. (2014) or Zhang et al. (2014)) or the stiffness of the cellulose matrix in general. Secondly, inserting a glass needle of the pressure probe into a cell has its size limitations – it is very difficult to obtain good measurements in the smallest cells, which are the most interesting from the perspective of morphogenesis. Cellular Force Microscopy (CFM) is another indentation method for measuring turgor pressure in systems such as onion epidermis (Routier-Kierzkowska et al., 2012). It can be seen as a simplified version of AFM because it is also based on analyzing force/displacement curves upon indentation. The force detection method is simpler because it directly measures force acting on the sensor, instead of tracking the deflection of a laser beam off the cantilever as is the case in AFM. The CFM uses a simple MEMS (micro-electro-mechanical system) sensor which detects force using microscopic capacitors that move in one dimension while the sensor is indenting the sample

(Felekis et al., 2011; Routier-Kierzkowska et al., 2012). Due to the hardware differences mentioned above, CFM detects higher forces (micronewton to millinewton scale) than AFM, which is more flexible: it can detect forces from piconewton to micronewton (Fig. 2.2).

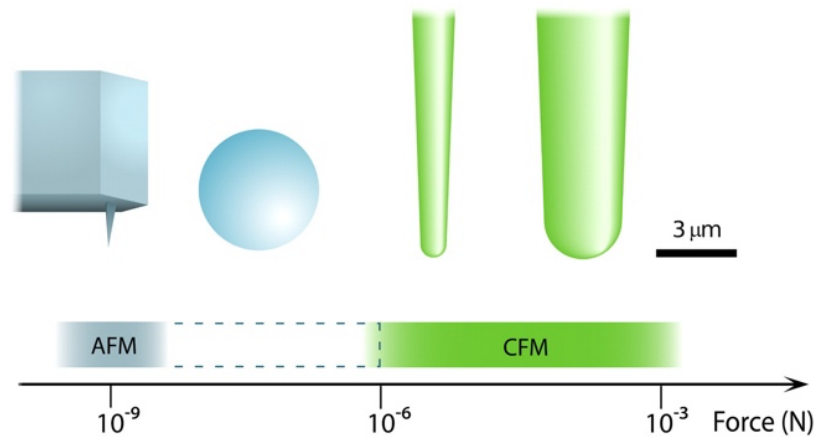


Figure 2.2. AFM and CFM operate on different force magnitudes. AFM has been primarily designed to detect very low forces (piconewton scale) with a sharp indenter (left). In specific cases, the detected forces can be extended, as was done by Peaucelle et al. (2011) who glued a glass bead to the indenter (middle). Finally, the CFM can detect forces from micro- to nanonewton scale. Therefore, it cannot detect subtle topographical features or elasticity of the cell wall as AFM does, but it is more suitable for creating coarse surface maps (cellular resolution) and measuring turgor pressure. Image adapted from (Routier-Kierzkowska et al., 2012).

The output of a CFM experiment is stiffness, understood as the slope of force acting on the sensor as a function of displacement (during a vertical indentation). In other words, this value is the answer to the question: how much force is needed to displace a material by a given distance? However, it is important to keep in mind that this raw readout is influenced by a number of factors. In the case of CFM, mechanical simulations (Finite Element Method, FEM) of the indentation experiments were performed in order to understand which features of the cells and the setup influences the output stiffness values the most (Mosca et al., 2017; Weber et al., 2015). It turned out that stiffness measured by CFM is mostly sensitive to turgor pressure, indentation depth and cell radius. Features such as elasticity and shear modulus of the cell wall did not influence the output stiffness values significantly (Weber et al., 2015). Therefore, CFM indentations can be used to indirectly measure turgor pressure inside cells, ideally if coupled with cell wall elasticity (derived from osmotic

treatments) and fed into a mechanical model (Mosca et al., 2017; Weber et al., 2015). This kind of work will be discussed in Chapter 3.

2.2.6 Plant cells are able to sense mechanical signals

Plant cells have been known to sense mechanical signals. Apart from obvious abiotic factors influencing plants in their natural environment, such as rain, wind, insects etc., turgor pressure is believed to be the main (or even the only) intrinsic cause of mechanical stress (Hamant and Haswell, 2017).

One proposed way of responding to mechanical stress is orienting the cell division plane in a way that reduces the amount of tension on the cell wall (Lintilhac and Vesecky, 1984; Louveaux et al., 2016). This results in reducing mechanical stress on the cell walls (see sec. 2.2.1).

More precisely, cortical microtubules (CMTs) are believed to be the structures sensing stress (Green, 1962). Hejnowicz et al. (2000) were the first to demonstrate it in sunflower hypocotyls which have anisotropic (elongated) epidermal cells, which can be approximated to cylinders. They showed that the CMTs are oriented along the highest stress direction, which means - along the radial axis of the cylinder (see sec. 2.2.1). This finding was followed by multiple studies on other organs (mostly the shoot apical meristem), which put CMTs forward as an important stress sensor (Hamant et al., 2008). Consequently, they are now used as a proxy for studying the dependence of other phenomena (hormone response, gene expression and others) on mechanics (Heisler et al., 2010; Landrein et al., 2015; Nakayama et al., 2012).

Apart from the cellular level described in the previous paragraph, plant cells are also able to sense forces on the molecular level, where molecular mechanoreceptors change their conformation as a response to forces (e. g. mechanosensitive ion channels, reviewed by Hamilton et al. (2015)). However, the main focus of this thesis are cells as individual units and components constituting the tissue. Therefore, I am going to refer to the CMTs as the primary force-sensing mechanism. More information about how CMTs might sense cell

wall stress and geometry is included in section 2.4 as well as in Chapter 5, where I introduce the intricate jigsaw puzzle-like shaped epidermal cells. Since they are probably the most elaborate shapes occurring in plants (with complicated stress patterns), studying microtubule orientation in this system can provide a lot of information on stress-related microtubule alignment.

2.3. Growth

2.3.1 Types of growth

Developmental biologists are highly interested in the process of growth (evolution of form over time) in single cells and tissues and how this process is guided by genetics. This is especially important in plants where cells cannot create shapes by moving around, since they are constrained by the cell wall. One of the biggest challenges of these studies is the need for an accurate way of describing growth as a physical process to be coupled with information about growth factor transportation, gene expression or others. This description is not trivial from a mathematical point of view. Over the years, a few (not mutually exclusive) ways of classifying growth have emerged. Below I describe the most popular ones.

- A) Isotropic/anisotropic growth – based on directions of growth. An object is considered to be growing isotropically if it is expanding at the same rate in all directions, and anisotropically if there is one predominant direction of growth (Fig. 2.3).
- B) Uniform/non-uniform – based on the distribution of growth. An object grows uniformly if all its parts expand at the same rate and in the same direction. If, instead, some parts of the object expand at different rates than others (e. g. some parts of the cell wall grow faster), growth is non-uniform (Fig. 2.3).
- C) Tip/diffuse growth – based on the localization of growth within an object. Tip growth is observed when growth of an object is concentrated in one point, that is a peak of a lobe or another kind of elongated structure, and the rest of the cell is not growing (Geitmann and Ortega, 2009; Qin and Yang, 2011). It can also be considered as a specific case of non-uniform growth. Diffuse growth is observed when the growth is not concentrated in a specific part of the object (Fig. 2.3). It can be uniform or non-uniform.

D) Eulerian/Lagrangian – two alternative mathematical representations of a growing structure. The difference between them lies in the perception of the coordinate system. In the Eulerian perspective, the grid coordinate system does not change, and material points ‘flow through it’ as they grow. In the Lagrangian approach, the coordinate system is assigned to a material point (in other words, to the growing structure) and not to a point in space. Therefore, as the object grows, the Lagrangian coordinate system deforms (Fig. 2.4). The choice of approach for a specific growth simulation depends on its specific assumptions, as none of these approaches is perfect (Coen et al., 2004). However, from a very general point of view, the Eulerian approach is more suitable for growing plant cells because it allows adding new material instead of just stretching the old one. This, in turn, was one of the main assumptions of the Lockhart’s model (Lockhart, 1965).

As these terms are often interchanged, in Fig. 2.3 I include selected examples of plant cells and how their growth is usually designated (Guerriero et al., 2014).

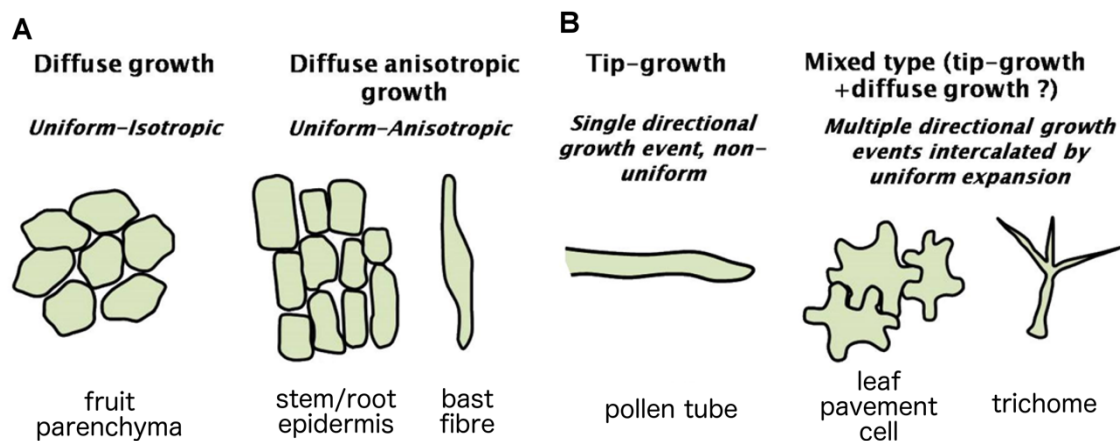


Figure 2.3. Selected plant growth types and their modalities. (A) Diffuse (uniform) growth. (B) Differential (non-uniform) growth. Adapted from (Guerriero et al., 2014).

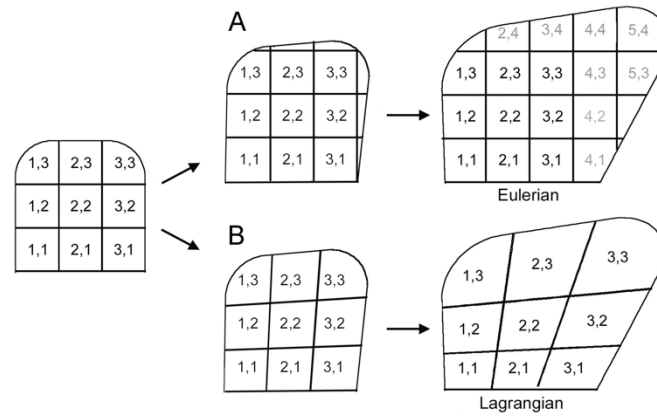


Figure 2.4. Two mathematical representations of growth. (A) Eulerian representation in which the growing object 'passes through' the coordinate system. (B) Lagrangian representation in which the coordinate system deforms together with the growing object. Adapted from (Coen et al., 2004).

2.3.2 Measuring cell shape and growth

Historically, the pace of the evolution of organ shape measurement methods has been dictated by the development of imaging techniques and molecular biology. In the first half of the 20th century adult leaves were divided into small squares and their shape was calculated from that. However, it was not possible to make any conclusion about growth since all this was done on fixed tissue (organs were detached from the plant itself) (Avery, 1933).

The emergence of clonal analysis has been a relevant step forward because it allowed the creation of reference points on the leaf (clones of cells) which could be used to measure tissue expansion (Dolan and Poethig, 1998; Kuchen et al., 2012; Poethig and Sussex, 1985; Serna et al., 2002). Later on, when laser scanning confocal microscopy became available, it became possible to shift this analysis to the single cell level. Moreover, scientific image analysis software able to track growth such as ImageJ (Rueden et al., 2017), Fiji (Schindelin et al., 2012), Imaris (Bitplane AG) and MorphoGraphX (Barbier de Reuille et al., 2015) became available to track cellular growth on all levels of precision and sophistication, including growth in three dimensions in some cases.

In my work I used the software MorphoGraphX to quantify organ growth on the cellular level. In this software, the confocal laser scanning microscope images (Fig. 2.5A) are converted into meshes which precisely retain the surface shape of the imaged sample (Fig. 2.5B, C). Next, a portion of the fluorescent signal is projected onto this mesh in order to get clear epidermal cell outlines (Fig. 2.5D). Finally, the mesh is segmented into single cells (Fig. 2.5E, F). In order to calculate growth rate between time points, corresponding cells (or their lineage, if cell divisions occur) are assigned to each other.

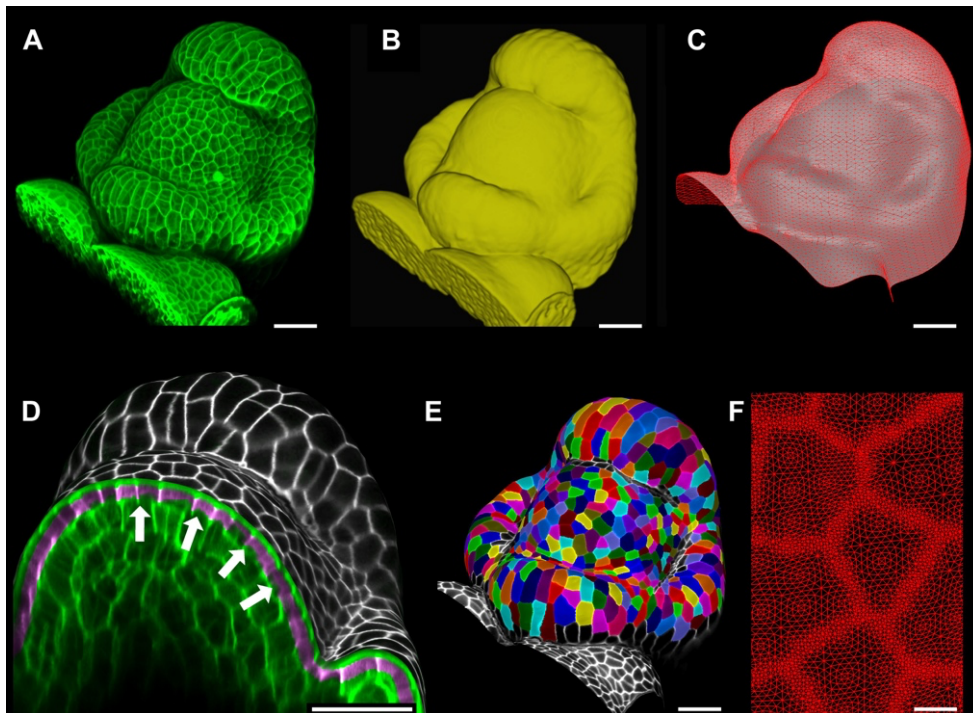


Figure 2.5. Confocal image analysis using MorphoGraphX. (A) An example confocal image used for quantification (a developing flower of *Arabidopsis thaliana*). (B) Shape of the flower extracted. (C) A 2D mesh created based on the shape of the flower. (D) A portion of the fluorescent signal is projected onto the mesh to get cell outlines (white). (E) The mesh is segmented into individual cells. (F) The mesh is additionally refined around cell borders. Scale bars, 20 μm (A-E) and 2 μm (F). Adapted from (Barbier de Reuille et al., 2015).

Cell junctions are used as landmarks to calculate displacement in the growth field, therefore the type of growth that can be measured with MorphoGraphX is uniform growth within a cell. In other words, this software can calculate expansion of cells as individual units but cannot capture the sub-cellular level differences which would be observed, for instance, in

non-uniform growth at the sub-cellular level (see sec. 2.3.1). By using this software, I consciously neglect the possible heterogeneity in cell wall structure and expansion rates, which have been reported for the puzzle-shaped epidermal cells (Elsner et al., 2012, 2017; Majda, 2017). I view growth as turgor-driven expansion and the subcellular features are not very important on this level.

2.3.3 Mechanical stress feeds back on growth

As I mentioned in section 2.6, plant cells can sense mechanical stress and cortical microtubules are believed to organize themselves along the principle direction of this stress (Hamant et al., 2008; Hejnowicz et al., 2000).

Since microtubules guide cellulose synthases (CESA) (Paredez et al., 2006), they can trigger anisotropic reinforcement of the cell wall along the direction of stress, limiting growth in this direction (Julien and Boudaoud, 2018; Sassi and Traas, 2015; Suslov and Verbelen, 2006). This can alter the shape of the cell, which in a pressurized structure is a primary determinant of stress (Beauzamy et al., 2015b; Mosca et al., 2017; Sapala et al., 2018). This suggests a feedback where stress patterns orient microtubules (and thereby cellulose), causing changes in growth and the shape of the cell, which in turn affects stress. Such a feedback has been proposed as primary driver of formation of the puzzle-shaped pavement cells (Belteton et al., 2017). In section 2.4 as well as in Chapter 5 I am going to elaborate on the feedback of stress (through geometry) on growth, using the puzzle cells as a case study.

2.4. Jigsaw- puzzle – shaped cells in leaf epidermis as an example of a mechanical feedback in creating forms

Cells with an elaborate, jigsaw puzzle-like shape appear in the epidermis of many plant species, including the model plant *Arabidopsis thaliana*. Progressing from simple polygon-shaped meristematic cells, they develop into large cells with many interlocking lobes (convex areas) and indentations (concave areas), that often resemble puzzle pieces (Fig. 2.6, Table 2.1.). Because of this dramatic change in form during development, puzzle cells are an attractive system for investigating cell shape control. I used them in my thesis to

investigate how cells adjust to externally imposed growth direction. Furthermore, I proposed a new function for those cell shapes, that is to minimize mechanical stress on the cell wall (Sapala et al., 2018).

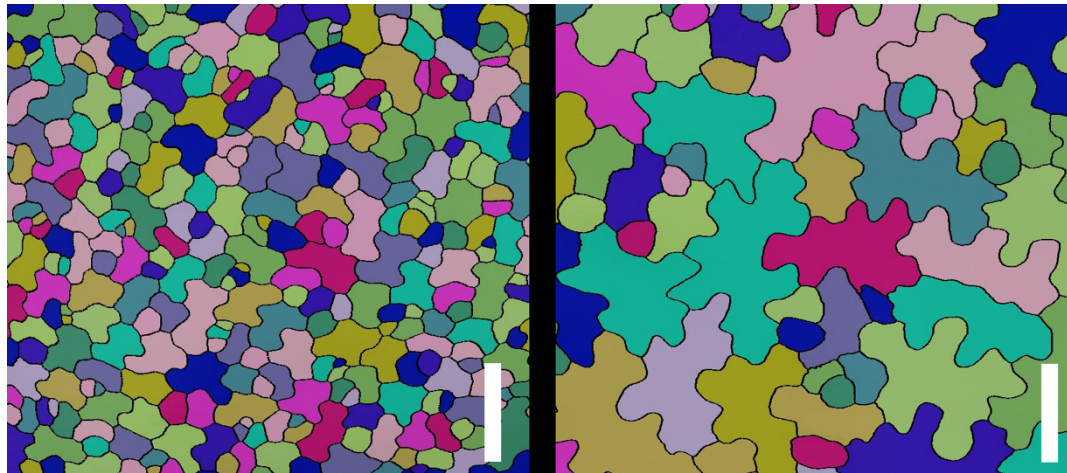


Figure 2.6. Cell shape in the epidermis of *Arabidopsis thaliana* cotyledon. Small cells (2 days after germination, left) have relatively isodiametric shapes, while larger cells (6 days after germination, right) display very complex, jigsaw puzzle-like shapes. The emergence of the puzzle shape is established early in organ development. Scale bars, 50 μm . Image adapted from (Sapala et al. 2019).

Table 2.1. Basic terminology used in pavement cell studies. Adapted from (Sapala et al., 2019).

Term	Definition
Lobe	a convex (protruding) portion of the cell contour in a puzzle-shaped epidermal cell
Indentation	a concave (indented) portion of the cell contour in a puzzle-shaped epidermal cell. Indentations facing each other across the cell form a ‘neck’. A lobe on one cell is matched with an indentation in a neighboring cell
Circularity	a shape measure of how closely an object resembles a perfect circle ($4\pi \text{ Area/Perimeter}^2$)
Largest Empty Circle (LEC)	the largest empty circle that can fit into a cell; provides a proxy for mechanical stress
Convex hull	the smallest convex shape that contains an object
Lobeyness	a scalar cell shape measure indicating how lobed or puzzle shaped a cell is. Measures such as convexity, solidity or lobe number can be used for this purpose

Understanding puzzle cell development has been challenging, as it appears to involve feedbacks and interactions at several scales. These feedbacks include various self-organizing components that act at the sub-cellular scale. Molecular interactions for cell wall partitioning (Fu et al., 2002, 2005, 2009; Higaki et al., 2016, 2017; Lin et al., 2013; Xu et al., 2010), sub-cellular cytoskeleton organization (Chakraborty et al., 2018; Mirabet et al., 2018; Zhang et al., 2011) and differential cell wall properties (Armour et al., 2015; Majda, 2017; Sampathkumar et al., 2014; Sotiriou et al., 2018) all interact to produce the lobes and indentations. Since a lobe in one puzzle cell must fit into the corresponding indentation in its neighbor, coordination of these processes must occur at the supra-cellular level. Possible candidates to provide this coordination are extra-cellular signaling molecules (Chen et al., 2015), mechanical or geometric cues (Sampathkumar et al., 2014; Sapala et al., 2018; Verger et al., 2018) or a combination of the two.

2.4.1 Molecular networks driving puzzle cell formation

Much work has been put into deciphering the molecular components driving puzzle cell formation. Current thinking is that Rho of Plants (ROP) proteins interact with ROP-interactive CRIB motif-containing proteins (RIC) proteins to direct the cytoskeleton and thereby locally regulate cell growth. Specifically, it appears that ROP6 accumulates in indentations and recruits cortical microtubules through RIC1, inhibiting growth in that region (Fu et al., 2009), while ROP2 recruits actin filaments through RIC4 in lobes to promote further outgrowth (Fu et al., 2005). ROP6 and ROP2 are believed to mutually inhibit each other, thereby creating an alternating pattern along the anticlinal cell wall. Simulation models of a ROP2-ROP6 style co-repression network can partition cells into sub-cellular domains. Intra-cellular coordination of these domains can be accounted for by an extracellular signal (Abley et al., 2013a). This means that the model of Abley et al. suggests that the ROP2-ROP6 network requires an external signal (a signaling molecule) to be plausible. Several authors have proposed that auxin could be such a signal, acting in concert with AUXIN BINDING PROTEIN 1 (ABP1) and the PIN-FORMED (PIN) auxin transporters (Fu et al., 2005; Li et al., 2011; Xu et al., 2010). However, recent work of Gao et al. (2015) have undermined the function of ABP1 as a key component in auxin signaling (Gao et al., 2015). In addition, Belteton et al. (2017) showed that PIN proteins, which are expressed during pavement cell development, have no apparent influence on lobe

patterning. Consequently, the hypothesis that auxin controls the ROP2/ROP6 patterning of lobes and indentations via PIN and ABP1 (Xu et al., 2010) has been put in question.

2.4.2 Methods for measuring puzzle shapes and their growth

Puzzle cells have complex recognizable shapes that nevertheless are highly variable. This has made it challenging to reliably quantify cell shape changes during development or identify cell shape differences between various mutants (Möller et al., 2017; Sánchez-Corrales et al., 2018; Sapala et al., 2018; Wu et al., 2016). Shape measures provide a means to determine specific geometric aspects of cell shape. The simplest measure is circularity, which indicates how close a cell shape is to a circle (see Table 2.1 for definitions). The perimeter or area of a cell can be compared to its convex hull to give a measure of the convexity of a cell representing the amount of indentations or concave regions the cell has. Conversely, one can take the ratio of the largest empty circle (LEC) that fits inside a cell and compare it to the cell area, giving another simple measure of how the cell deviates from a circular shape (Sapala et al., 2018). These simple to compute measures are useful in coarsely evaluating differences in cell shape, focusing on the general degree of lobeyness. Although most are not directly related to the mechanism of pavement cell formation, the LEC by itself (without the area ratio) provides a proxy for stress in the cell (Sapala et al., 2018). It follows that measures related to the mechanism controlling pavement cell morphogenesis may be especially useful in characterizing the phenotypes of various puzzle cell shape mutants.

For more advanced quantification, measures characterizing the number and geometry of lobes and indentations are required. These measures are often directly relevant to proposed mechanisms, for example the number of lobes at a given cell size could indicate the periodicity of an intra-cellular partitioning mechanism. Several methods for puzzle cell quantification have been proposed. They can be roughly divided into two categories: those that focus on the cell contour and those that use skeletons to approximate the overall form of the cell (Table 2.2).

Table 2.2. Puzzle cell quantification tools developed in recent years. Adapted from (Sapala et al., 2019).

Name	Definition
LobeFinder (Wu et al., 2016)	Contour-based. A MatLab application focused on extraction of lobes based on the convex hull (lobe number, distance to convex hull). Extracts lobes and can track their development.
PaCeQuant (Möller et al., 2017)	An ImageJ tool that provides a suite of measures based on both the cell contour and skeleton. The tool calculates many simple measures, but also puzzle cell specific measures such as lobe number
LOCO-EFA (Sánchez-Corrales et al., 2018)	Contour-based. Extends traditional Elliptical-Fourier-Analysis (decomposes the contour into waves of different frequencies) to provide rotation-invariance. These coefficients can then be used to analyze cell shape.
Custom MorphoGraphX features (Sapala et al., 2018)	Plugins to calculate largest empty circle fitting into the cell (LEC), circularity and both perimeter- and area-based convex hull measures. Quantification can be performed on both flat images and curved surfaces.

Due to the fact that puzzle cell shapes are very complicated, it is an even bigger challenge to measure their growth. In my work I am using MorphoGraphX, which assumes that cellular growth is uniform. It is a fair approximation if one is interested in turgor-driven cell expansion and overall growth coordination on tissue level, however, differential growth has been detected in those cells using different methods.

At the sub-cellular level, puzzle cells have complicated patterns of growth that, nonetheless, occurs within the context of the broadly coordinated tissue growth shaping organs (Elsner et al., 2012; Wu et al., 2016; Zhang et al., 2011). To track sub-cellular growth, recent studies have used microbead labeling to randomly mark the outer wall of cells in the epidermis with fluorescent beads and monitored the positions of beads over time (Armour et al., 2015; Elsner et al., 2017). Both of these studies confirm that individual puzzle cells grow heterogeneously in a pattern related to lobe outgrowth but suggest different patterns of sub-cellular growth. Armour et al. (2015) report that growth in puzzle cells is isotropic, but lobe creation is enhanced by higher growth rates in the convex sides of the cell wall. Whereas, Elsner et al.'s observations suggest lobe outgrowth is not limited

to the lobe tip, but involves anisotropic extension of the entire lobe (i.e. diffuse anisotropic growth) (Elsner et al., 2017). These inconsistencies may stem from the sparse covering of fluorescent beads, or differences in the computational techniques used to infer growth.

2.4.3. Mechanical feedback facilitates puzzle cell formation

In the previous sections I mentioned that cells can sense mechanical stress *via* cortical microtubules and that this stress can feed back on growth by reinforcing the cell wall against it. This idea has been explored in the case of puzzle cells as well. Sampathkumar et al. (2014) calculated stress patterns within puzzle cells and showed that these patterns overlap with microtubule orientation as well as cellulose fiber orientation. Even though they speculated that this might demonstrate mechanical feedback, they did not provide a model of growing cells, so it was impossible to confirm that the geometry sensing at a given state really influences future shapes.

Nevertheless, modeling work has proposed that cell geometry itself may account for microtubule orientations (Chakraborty et al., 2018; Gomez et al., 2016). Based on simple rules derived from observation of microtubule behaviour, Chakraborty et al. (2018) simulated the interaction of microtubules with each other and the curvature of the cell wall. They were able to reproduce patterns resembling those observed *in planta*. Similar simulations by Mirabet et al. (2018) indicate that highly curved cell shapes (i.e. with sharp edges) have more anisotropic microtubule distribution than those with smooth edges, which may lead to more focused cell wall reinforcement by CESA. The alignment of microtubules perpendicular to sharp-edged corners can be overcome by CLASP (cytoplasmic linker-associated proteins) which accumulate in corners and create microtubule bundles (Ambrose et al., 2011). The tendency for microtubules to bundle when they interact may provide an additional mechanism for the accumulation of microtubules in indentations. This could work in concert with the self-enhancing behavior of the membrane bound form of ROP6 proposed in molecular models of pavement cell patterning (Abley et al., 2013; Fu et al., 2009) with ROP2 in the lobes promoting enhanced growth rates (Armour et al., 2015).

2.4.4 Potential functions of the puzzle shapes

When unusual cell shapes are observed in nature, it is natural to wonder about their function, as form often follows function in biology (recently reviewed by Brophy et al., 2018). Several hypotheses have been proposed to explain the interlocking puzzle shape of these cells. It has been proposed that puzzle shapes may be important for the correct spacing of other epidermal cell types such as stomata and trichomes (Glover, 2000) or to help the leaf to remain flat and thereby optimize light capture (Galletti and Ingram, 2015). Another hypothesis is that the interlocking shapes may increase adhesive strength between cells, increasing the stability of the epidermis (Jacques and Vissenberg, 2014; Lee, 2000) that is often under considerable tension from internal cells (Kutschera and Niklas, 2007). A related idea is that puzzle cells might help the tissue to undergo large reversible deformations, such as when the tissue is stretched or bent (Sotiriou et al., 2018).

In my work (Chapter 5) I propose an alternative function for these intricate shapes, namely that they minimize the amount of mechanical stress exerted on the cell wall. According to my theory, they achieve this by adjusting the size of large open spaces and thereby lower the amount of resources necessary to reinforce the cell wall and prevent it from bursting under turgor pressure.

3. Cellular growth patterns in isotropically and anisotropically growing organs

Plants display a large variety of organ shapes between species. However, differences in organ geometry within one plant are also commonly observed. For instance, the root and stem of a plant are usually elongated (meaning they have expanded more in one preferential direction compared to others). In some cases (including *Arabidopsis thaliana*) the fruit is an elongated organ, but between species and families its shapes can greatly differ (Fig. 3.1). Leaves of *Arabidopsis thaliana* are heteroblastic – their shape depends on the position on the developmental age of the plant. Juvenile leaves (ones that appear at the beginning of the life of a plant) are round while adult leaves (ones that appear when a plant is more mature) are more elongated (Fig. 3.2). In other words, even though most plant organs originate from a similar group of small, polygonal meristematic cells (called organ primordia), in order for a plant to develop from a seedling to a fully functional organism capable of reproducing, a few different growth regimes have to be employed. The two most

basic ones are: isotropic growth (no predominant direction) and anisotropic growth (one predominant direction) (Fig. 2.3).

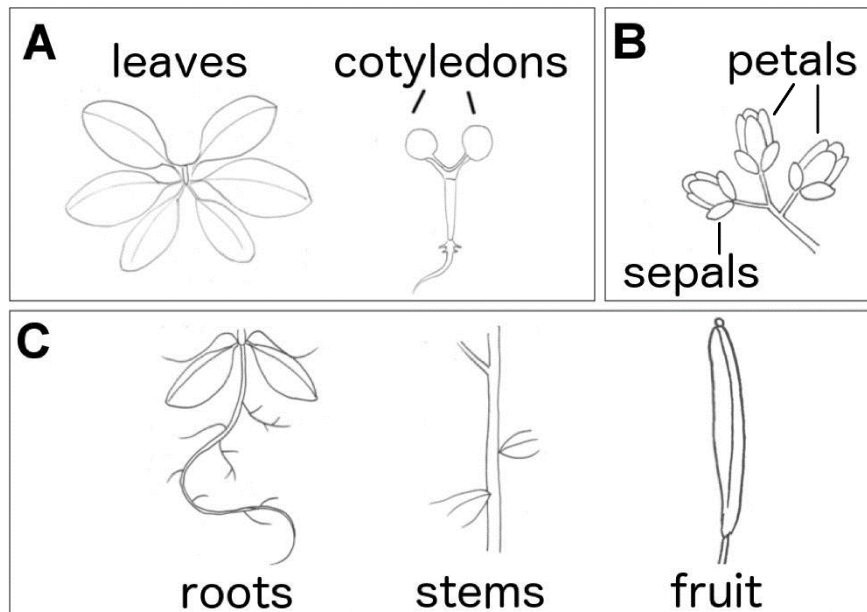


Figure 3.1. Isotropically and anisotropically shaped organs of *Arabidopsis thaliana*. (A) Isotropic organs: leaves (in mature plants) and cotyledons (in seeds and seedlings). (B) Elliptical organs: sepals and petals. (C) Elongated organs: roots, stems, fruit. Image courtesy: Helen Ai He.



Figure 3.2. Heteroblasty in *Arabidopsis thaliana* rosette leaves. The shape progresses from round in juvenile leaves (left) to elongated in adult leaves (right). Adapted from (Hunter et al., 2006).

Since epidermis limits growth (Savaldi-Goldstein et al., 2007), it is reasonable to expect at least a qualitative connection between epidermal cell shape and organ shape. However, from the experimental point of view it is still not clear if growth is controlled by one global signal or by a sum of local signals. If the latter assumption applies, a correlation between cell shape and organ shape is not necessarily granted to occur. For instance, in the root the scenario is clear: a highly elongated organ is comprised of simple, cylindrical cells (or

cubic, if they are still dividing). Conversely, the leaf (or cotyledon) of *Arabidopsis thaliana* has a rather isotropic, round shape while its epidermal cells have jigsaw puzzle-like shapes (called ‘puzzle cells’ for the remainder of this thesis). They are likely to result in an overall isotropic growth, but some local anisotropy is required for creating individual lobes (Armour et al., 2015; Majda, 2017; Sotiriou et al., 2018).

A detailed description of the different growth regimes and their genetic basis can allow scientists to better understand growth of plants. As I discussed in Chapter 2, different types (directions) of growth result in a variety of cell shapes, from elongated, cylinder-like pollen tubes (Chebli et al., 2012; Hepler et al., 2013), through polygonal meristematic cells (Kierzkowski et al., 2012), to complex shapes resulting from a mixture of subcellular growth patterns such as puzzle cells (Armour et al., 2015; Elsner et al., 2017) or trichomes (Hervieux et al., 2017; Hülkamp et al., 1994) (Fig. 2.3).

There are two ways to compare different growth regimes in plants. Usually growth is compared in the same organ of different species/mutants (such as in Hong et al., 2016; Vlad et al., 2014). In this Chapter, I chose a different possibility and studied two organs of the same species (*A. thaliana*) which display different shapes: the round cotyledon and the more elliptically shaped sepal. I employed confocal laser scanning microscopy and image analysis software MorphoGraphX (Barbier de Reuille et al., 2015) to decipher cellular growth rates in both organs. Since these are two archetypical organ shapes, their detailed growth characterization can serve as a starting point for numerous studies in developmental biology.

3.1. A round organ grows isotropically: *A.thaliana* cotyledon

The cotyledon is an organ created at a very early stage of plant development. Its primary function is to store nutritional resources for the embryo. Since its anatomy resembles a leaf, it serves as the first source of photosynthesis which enables the shoot apical meristem to create proper leaves, stems and flowers (Chandler, 2008). A plant can have one or two cotyledons, which is an important morphological feature used in taxonomy to divide plants into monocotyledonous (monocots) and dicotyledonous (dicots). *Arabidopsis thaliana* has two cotyledons and is therefore classified as a dicot.

The *A.thaliana* cotyledon is a good system for studying growth on cell, tissue and organ level because it is much more easily accessible for imaging than a young leaf. It has a round shape similar to that of the juvenile leaf and therefore I used it to study growth patterns in isotropically shaped organs. The epidermis of the cotyledon is mainly composed of large, endoreduplicated jigsaw puzzle-shaped pavement cells. Stomatal guard cells are randomly interspersed between them. While the puzzle cells have largely irregular contours, they are considered to be isotropic shapes because in order for them to be created, the initially square meristematic cells need to grow in many different directions in plane in order to reach this jigsaw puzzle shape. It was one of my objectives to confirm if growth of these cells is generally isotropic, despite the irregular lobes and indentations.

I imaged wild type cotyledons from 1 day after germination (DAG) until 8 DAG in order to qualitatively assess the time window in which puzzle cells are created. The cotyledon epidermal cells have slight lobes even before the plants germinate which makes it impossible to track the shape evolution from a purely polygonal shape in cotyledons (as observed in meristematic cells, for instance at the shoot apical meristem). However, I observed that the most visible shape changes happen between 2 and 6 DAG. After 6 DAG, the cells still expand, but it is uniform and just maintains their shape while increasing in size (Fig. 3.3).

The cotyledon is a very round, isotropic organ. Therefore, isotropic growth on the cellular level can be hypothesized. As I mentioned earlier in this section, the puzzle-like epidermal cells have very irregular shapes and it cannot be taken for granted that local growth anisotropy results in global isotropy. Therefore, I wanted to prove that the epidermis indeed grows isotropically using MorphoGraphX. Based on the data presented in Fig. 3.3, I decided that the most suitable time window for performing the time lapse imaging will be between 2 and 6 DAG, since this is when the most dramatic cell shape changes occur. I imaged cotyledons every 48 hours for 4 days and kept the plants in a growth medium in long day conditions in between the measurements (Fig. 3.4A). The morphology of the cotyledon is similar throughout the whole surface of the organ (it does not have bilateral symmetry as the leaf, which has a midvein along its apico-basal axis that changes the shape of epidermal cells). I therefore decided to only image a section of the cotyledon instead of

the whole organ. I segmented the time series and calculated growth anisotropy using MorphoGraphX. As expected, the epidermal cells of the cotyledon grow isotropically (Fig. 3.4B). It is worth noticing that at that stage of cotyledon development, the puzzle-shaped epidermal cells expand but do not divide. The majority of cells that undergo divisions are the ones belonging to the stomatal lineage (Fig. 3.4C).

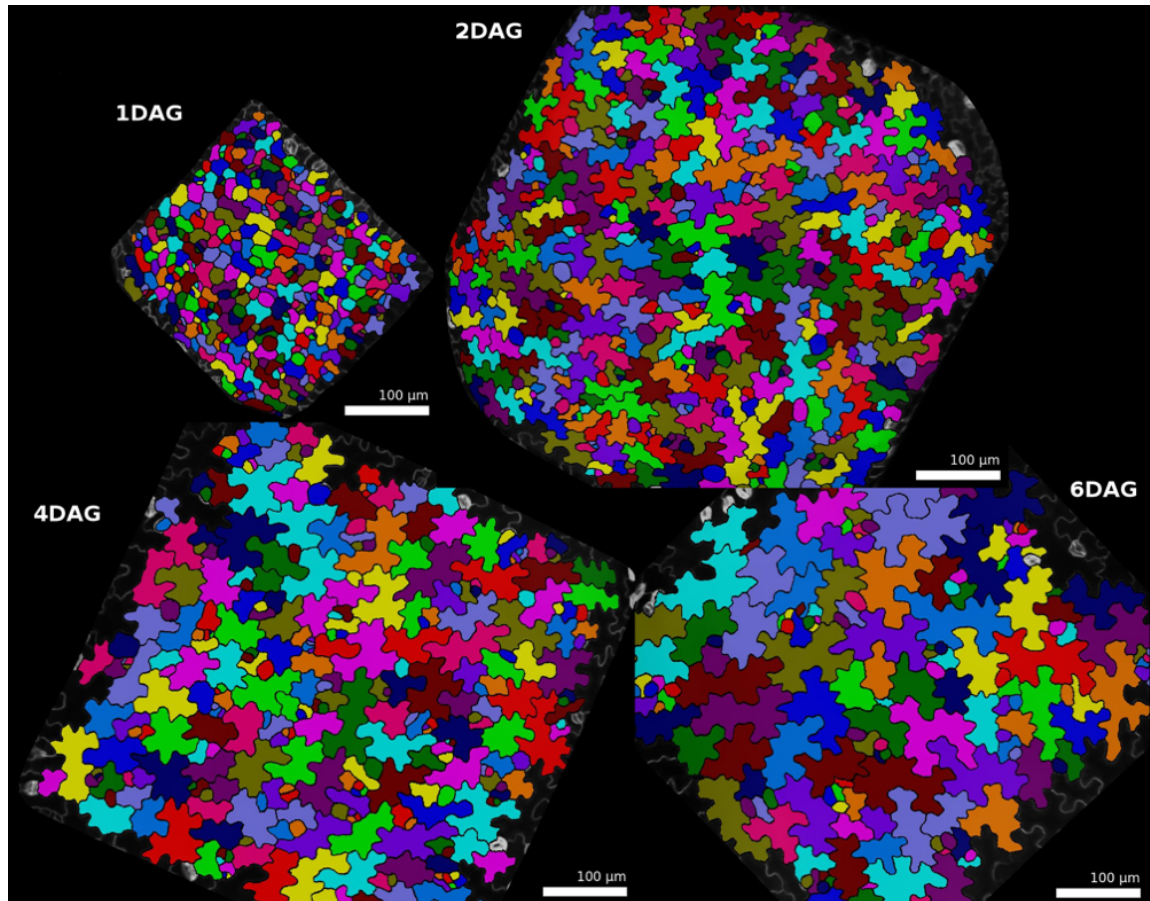


Figure 3.3. Evolution of the cotyledon epidermal cells in the first days after germination. Outlines of epidermal cells 1, 2, 4 and 6 days after germination (DAG), segmented in MorphoGraphX.

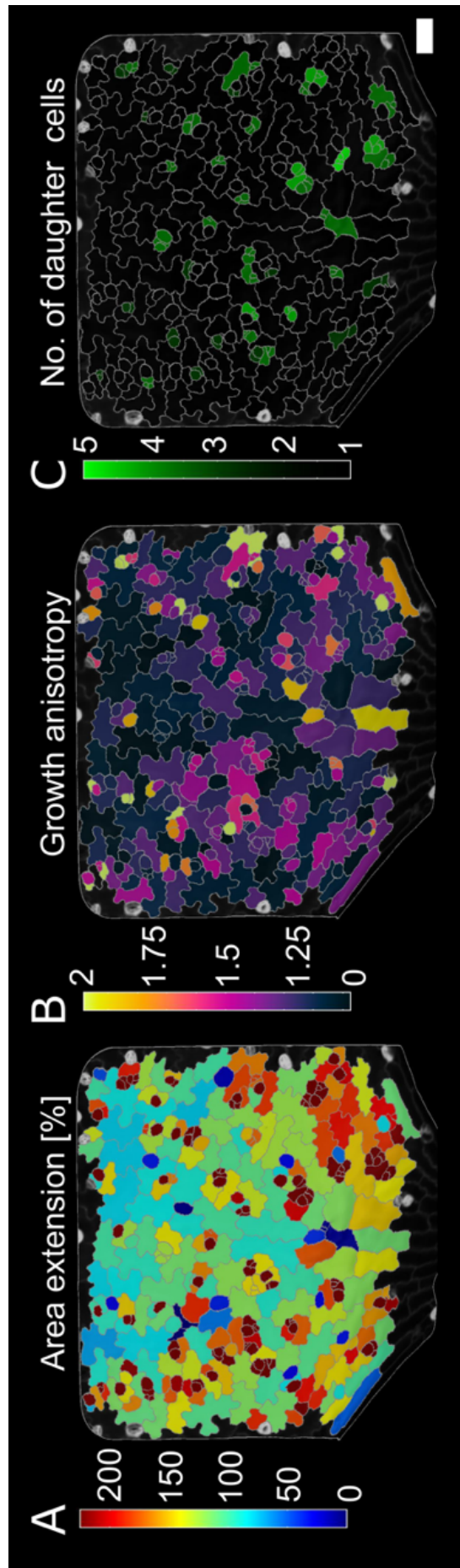


Figure 3.4. Growth tracking of an *Arabidopsis* cotyledon from 2 to 6 days after germination. Values displayed on the latest time point of the series (6 DAG). (A) Single cell growth rates. (B) Growth anisotropy (the ratio of expansion in the direction of maximal growth divided by expansion in the direction of minimal growth). (C) Map of cell divisions. Color scale represents the number of daughter cells in the final time point (6 DAG) that arose from one mother cell in the first time point (2 DAG). Scale bar, 50 μm .

3.2. An elliptical organ grows anisotropically: *A. thaliana* sepal

Sepals are the outermost floral organs and their function is to cover the reproductive organs (stamens and carpel) as they develop. Once these organs are mature, the sepals bend outwards, the flower opens and the reproductive organs are exposed to the environment (Fig. 3.5A).

A characteristic feature of the sepals is that their epidermis contains two distinct types of cells: very long, narrow, endoreduplicating cells called 'giant cells' and more uniformly shaped cells called 'small cells' (Fig. 3.B,C). It has been shown that apart from the obvious size criterion, small and giant cells have different (although not mutually exclusive) identities (Roeder et al., 2012). Apart from sepals, late giant cell identity has been reported in leaves and roots using enhancer trap lines. However, this marker does not represent cell ploidy since it is specific to the epidermis, but absent in trichomes which, like giant cells, are endoreduplicated (Eshed et al., 2004; Roeder et al., 2012). The emergence of trichomes is associated with increased turgor pressure caused by plasmodesmata gating (Ruan et al., 2001).

The appearance of giant cells in the sepal is controlled in two ways: (1) by cyclin-dependent kinase inhibitors (LGO, KRP) which drive endoreduplication or (2) by epidermal specification genes (DEK1, ATML1, ACR4, HDG11), which promote giant cell identity upstream of endoreduplication regulation (Roeder et al., 2010).

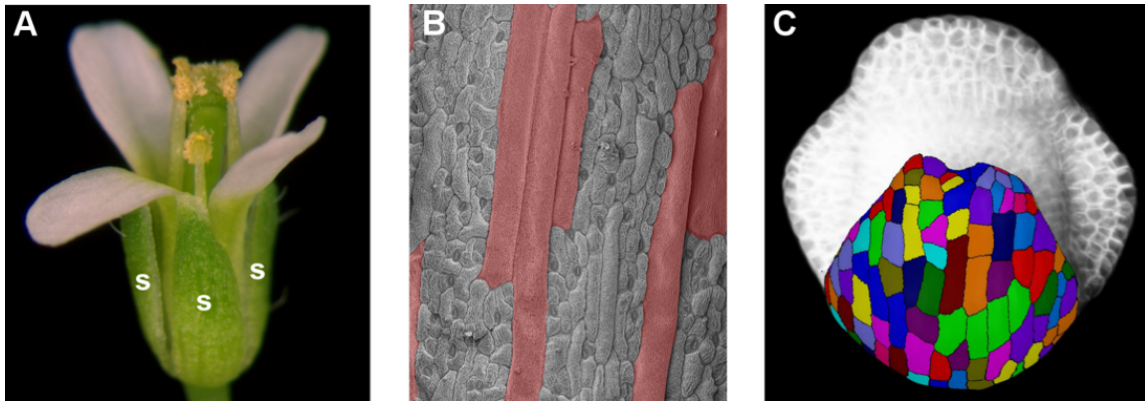


Figure 3.5. The schematic morphology of an *Arabidopsis thaliana* flower. (A) The flower with sepals (S), petals, and reproductive organs (stamens and carpels). (B) The epidermis of a mature sepal is composed of long cells called 'giant cells' (false-colored red) and smaller cubic cells referred to as 'small cells'. (C) A confocal microscope image of a young flower (white) with cell contours of a developing abaxial sepal segmented in MorphoGraphX. (A) and (B) reproduced from (Roeder et al., 2010).

It has been shown that in leaves, decreased number of cells (corresponding to lower division rates and, consequently, larger cells) is compensated by increase in their size, enabling them to reach a certain final shape of the organ. The exact nature of this phenomenon (whether or not cell division and growth are coordinated) is still debated (Hemerly et al., 1995; Hisanaga et al., 2015; Horiguchi et al., 2006). Strikingly, this diversity of cell shape results in a robustly shaped mature sepal, even though the distribution of the endoreduplicated giant cells among small cells in the sepal is stochastic (Hong et al., 2016; Roeder et al., 2010). In the following sections I compare cellular growth patterns in sepals of wild type and *lgo* mutant plants. Since LGO (Loss of Giant Cells in Organs) is a cyclin-dependent kinase inhibitor, *lgo* mutant plants do not form giant cells on sepals because entrance into endoreduplication is impaired (Roeder et al., 2012). The aim of my analysis is to check if the change of cell geometry (elongated to square) can change growth direction within the organ.

3.2.1 Growth patterns in wild type sepals

In order to study growth patterns in the abaxial sepal, Confocal Laser Scanning Microscopy was used to conduct time-lapse imaging experiments on wild type (Col-0 accession) containing a fluorescent marker in the plasma membrane (see Sec. 3.7). The sepals were

imaged every 24 hours for up to 8 days. I analysed deformation of single cells over time in the abaxial sepal using MorphoGraphX (Barbier de Reuille et al., 2015).

I used the canonical study of Smyth et al. (1990) as a reference to assign developmental stages of flowers in each time point of the imaging series. From stage 1 on, the flower primordium is created on the floral meristem, sepals are initiated followed by petal and stamen primordia. The stage when the flower bud is completely covered by sepals and four distinct stamens are created is called stage 6. In stages 7 to 12, petals initiate and elongate rapidly, the gynoecium forms and matures together with the stamens. Stage 13 begins when the flower opens (Table 3.1).

Table 3.1. Stages of flower development. Reproduced from (Smyth et al., 1990).

Stage	Landmark event
1	Flower buttress is created
2	Flower primordium is created
3	Sepal primordia are created
4	Abaxial sepal overlies the meristem dome
5	Stamen and petal primordia emerge
6	The meristem is fully covered by all 4 sepals
7	Long stamen primordia are stalked at base
8	Locules appear in long stamens
9	Petal primordia stalked at base
10	Petals level with short stamens
11	Stigmatic papillae appear
12	Petals level with long stamens
13	Bud opens, petals visible, anthesis

In this time lapse growth analysis, the abaxial sepals were imaged between stage 3 and 10 of flower development. Until stage 4 (as the abaxial sepal begins to cover the central zone of the flower), that is at the very beginning of sepal development, all the cells (still undifferentiated) appear to grow at the same rate. Around stage 6 (the sepal covers the whole central zone), a gradient in cell expansion forms – cells at the tip grow much faster than the cells at the bottom. Between stages 7 and 8, growth at the tip slows down and the area of maximal growth moves through the middle of the sepal towards its base (this

tendency is displayed until the end of the experiment). Stage 7 is also the moment where giant cells can first be observed as more elongated and more bulged out than the rest. By the time the flower reaches late stage 9, the fast-growing area is at the very base of the sepal. Afterwards, a decrease in growth can be observed, likely due to the experimental conditions and the decreasing vitality of the plant cultivated *in vitro* (Fig. 3.6A).

Division patterns between each time point (in 24-hour intervals) resemble the growth patterns, with the sepal tip having more divisions at the beginning of the time-course and the base having more divisions later on (stage 7-8), finally slowing down together with cellular growth (stage 10) (Fig. 3.6C). I projected the division rates from each time point on the initial point of the time course (stage 3) and observed that the epidermis of the whole sepal is created from a small file of cells located in a line at the sepal primordium. All the other cells constituting the sepal epidermis are just clones of these few cells (Fig. 3.7).

Using MorphoGraphX (Barbier de Reuille et al., 2015), I calculated principal directions of growth (PDG) for all time points of the time lapse. This revealed that growth of the sepal is highly anisotropic and the dominant direction of expansion of this organ is along its longitudinal axis. The highest values can be observed at stage 6, when growth rates are still uniform. Later on, anisotropy values decrease but the gradient of growth anisotropy follows the pattern of growth rates (Fig. 3.6B). The epidermal cells of the sepal rarely grow fast and isotropically. Contrary to the cotyledon, in the sepal I could only observe fast anisotropic growth or slow isotropic growth (Fig. 3.6A, B). The reason for the anisotropic growth can be geometry of single cells (Bassel et al., 2014) and the organ as a whole as well as elastic properties of the cells.

3.2.2. Growth patterns in *lgo* sepals

Next, I wanted to check if the presence of giant cells plays a role in growth patterns of the sepal. Therefore, I performed time lapse imaging on sepals of the *lgo* mutant which is known not to produce giant cells (Roeder et al., 2012). I suspected that the absence of these large cells which elongate along the axis of the highest growth in wild type (the apico-basal axis) might change the principal directions of growth in the epidermis.

Even though the *lgo* sepal does not have giant cells, its growth patterns are similar: up to developmental stage 6 it is the tip of the sepal that grows faster, and later (since stage 7) the growth maximum relocates to the base. The *lgo* flower appears to grow slower than wild type because when they are at the same developmental stage (such as stage 6), the wild type sepal is wider than *lgo* sepal and the tip growth last longer than in the case of wild type (compare Fig. 3.8 and Fig. 3.6A).

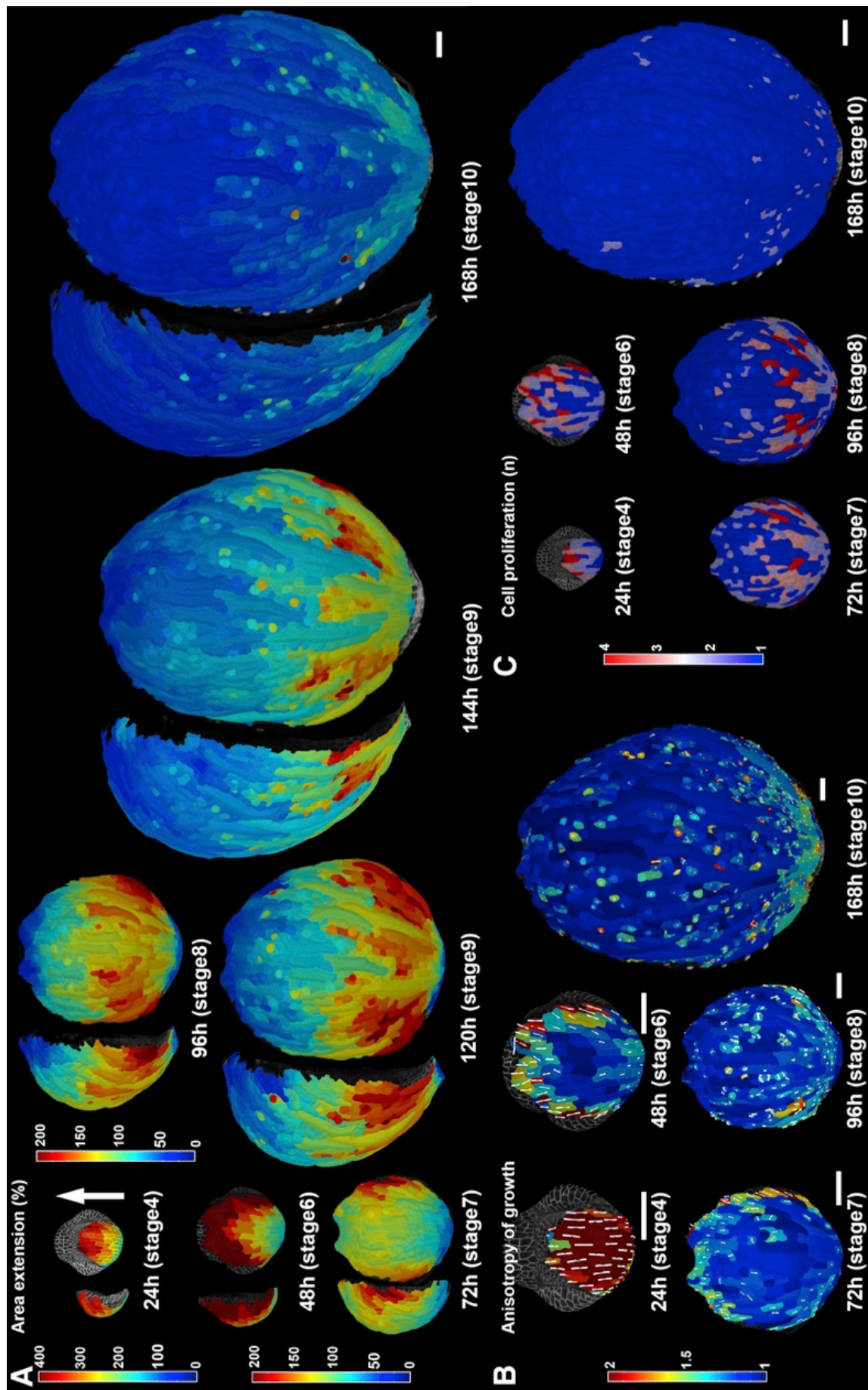


Figure 3.6. Growth patterns in a developing abaxial sepal of *Arabidopsis thaliana* (continued from p. 38). The white arrow shows the apico-basal axis of the flower (with base of the sepal at the bottom and tip of the sepal at the top). Each time point is displayed from the side (left) and from the top (right). Note that the same magnification is used for all stages. For each image, time from the start of the experiment and developmental stage of the flower based on (Smyth et al., 1990) is indicated. Color scale corresponds to increase of cell area over 24 hours, projected on the later time point. In this representation, value for each cell was averaged with respect to its immediate neighbors. (A) Heat maps of a growing wild type sepal. (B-C) Images of selected time points from the image sequence of wild type sepal displayed in panel A.

(B) Anisotropy of growth calculated as deformation in maximal growth direction (Principal Growth Direction, PDG_{max}) divided by deformation in minimal growth direction (PDG_{min}). White bars represent direction of maximal growth for cells displaying growth anisotropy above 20%. (C) Cell proliferation over 24 hours displayed for selected time points. Color scale: number of daughter cells that had arisen from a single cell within the previous 24 hours. Scale bars 50, μm . Adapted from (Hervieux et al., 2016).

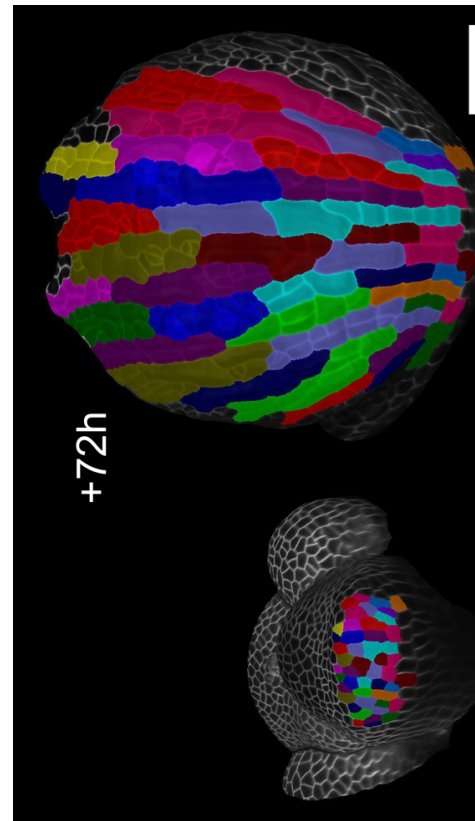


Figure 3.7. The abaxial sepal is created from a small band of cells. Left: a young flower with the sepal primordium (stage 3). Right: the same flower 72 hours later (stage 7). The sepal epidermis is created due to multiple divisions of a band of few cells at the bottom. The divisions are coupled with highly anisotropic growth (compare the elongated shape of the cell clones with Fig. 3.6B). Scale bar, 50 μm .

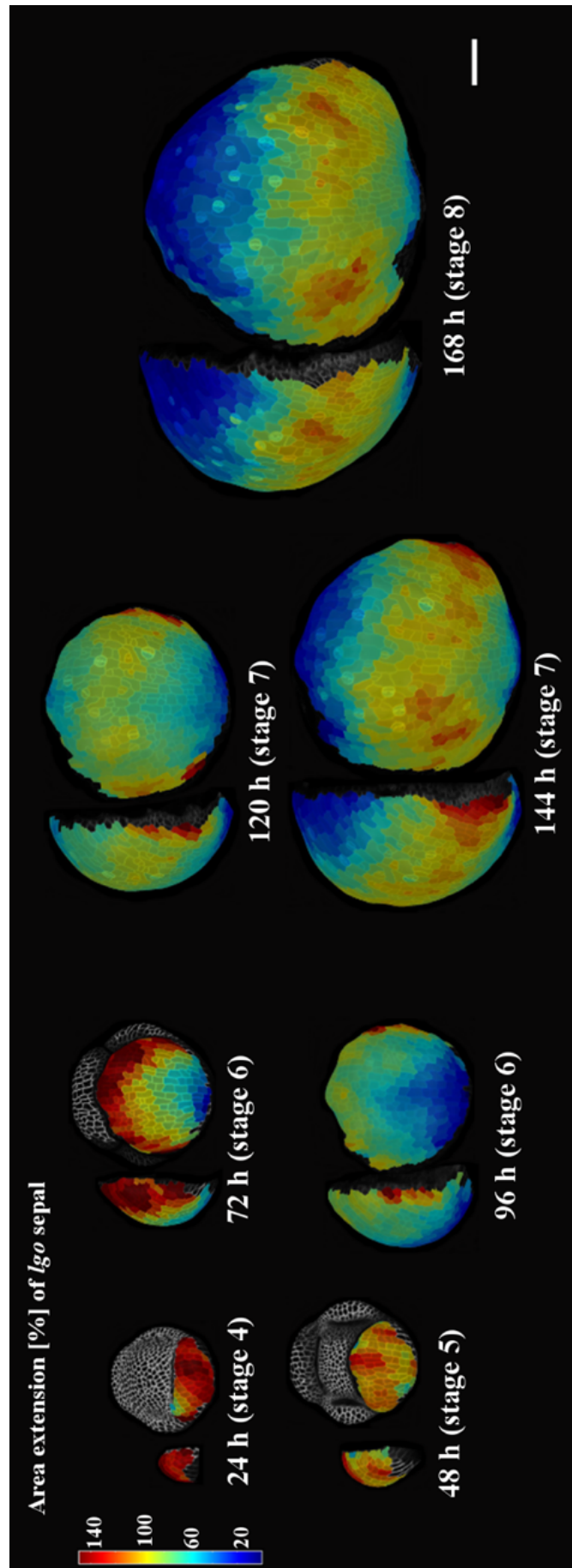


Figure 3.8. Heat maps of a growing *lgo* sepal. Note the lack of giant cells on the sepals. Scale bar, 50 μm .

3.2.3.A mechanical feedback restricts sepal growth and shape in *A. thaliana*

In the work of Hervieux et al. (2016), we combined the growth pattern information with high-resolution imaging of cortical microtubules (CMT). CMTs are hypothesized to align according to mechanical stress in the cell wall in order to potentially reinforce it. In the sepal, CMT organization followed the anisotropic growth until developmental stage 7, that is, as long as the growth of the sepal is largely anisotropic. Later (from stage 9 onwards), CMT organization followed the isotropic growth in the center of the sepal, but not at its tip. Even though the tip also grows isotropically at this point in development, the microtubules were aligned tangentially to the sepal tip, thereby not matching the growth regime. Since there is evidence that microtubule alignment is strongly connected to mechanical stress (Hamant et al., 2008; Hejnowicz et al., 2000; Sampathkumar et al., 2014), this observation prompted a search for another source of mechanical stress at the sepal tip.

In order to find out what can be the reason for the stress at the sepal tip, a mechanical model of a growing sepal was created. The modeled sepal had a gradient of elasticity along its apico-basal axis which corresponded to the growth for each stage observed in the time lapse series. It has demonstrated that several growth regimes within the same organ (corresponding to the migration of the zone of fast, anisotropic growth) can generate transverse tensile stress at the tip, to which the microtubules then align. Since the alignment of microtubules influences the deposition of cellulose microfibrils (Paredes et al., 2006), these results provide preliminary evidence of a self-shape-sensing mechanism.

This work puts forward a hypothesis that organs can sense their own shape via recognizing mechanical tension building up within them, and actively adjust their function (by changing microtubule alignment) to control the amount and direction of further growth. A lot of challenging experimental work needs to be done to confirm this hypothesis and decipher the shape sensing mechanism. However, the phenomenon of autonomous organ size control has been shown before, for instance in the case of salamander limbs. It has been shown in the 1920s that grafting embryonic tissue responsible for forming a leg between a large salamander species and a small salamander species does not cause the donor leg to adjust its size to the acceptor species. The leg of the large salamander was transplanted to the

small salamander (in a very early developmental stage). It grew to the size it would have had in its original species, resulting in a small salamander with an unusually large leg, and *vice versa* (Vogel, 2013). This experiment demonstrates that, despite the presence of growth stimulating agents acting throughout a whole living organism (hormones, transcription factors, signaling proteins etc.), there might be some size controlling processes happening on the organ level only.

This is an example of how a detailed description of organ growth on cellular level can be a starting point for exploring more complex questions. Such information can be used to make hypotheses to be tested by experiments or make assumptions used in the construction of mathematical models (as was the case in this study).

3.3. Summary of the results

A detailed analysis of cellular sepal growth revealed a gradient of growth rates along the apico-basal axis, with a fast-growing area gradually moving from the tip to the base of the organ. It is not known what the cause for different growth rates within one organ is. It is plausible that some mobile growth promoting or restricting agent is present there, especially since all the sepal epidermal cells are created from a horizontal few cells (Fig. 3.7). Previous studies have revealed growth repressors such as CUC2 or RCO that actively repress cellular growth in certain regions of leaf epidermis (Bilsborough et al., 2011; Vlad et al., 2014). In that case, the boundary between slow-growing cells and fast-growing cells is very sharp since there are no abnormally large cells crossing both zones. In the case of the sepal, the giant cells (randomly interspersed within the organ) cross the boundaries between the fast- and slow-growing regions and their growth rate values are intermediate between the fast and slow cells. This suggests a supra-cellular (organ level) growth controlling factor: either a mobile molecule or a mechanical factor. My growth tracking experiments clearly suggest a wave of growth promotion going from the tip to the bottom of the organ rather than a wave of growth restriction going from the bottom to the top. If the latter were the case, one could not have observed a situation where the middle of the sepal grows faster than both the tip and the base (Fig. 3.6A, stage 7).

A very striking feature of sepal growth is the strong anisotropy. The zones of high growth rates almost always are anisotropic (Fig. 3.6A, B). Previous reports on growth fields shaping plant organs have stated that an abstract ‘polarizing factor’ can be organized in a convergent field towards the organ tip (as in the *Arabidopsis thaliana* leaf reported by Kuchen et al., 2012) or in a divergent field facing away from the organ tip (as in the *Arabidopsis thaliana* petal reported by Sauret-Güeto et al., 2013). My data on the anisotropic growth of the sepal seems to suggest an intermediate, parallel growth field in which the abstract ‘polarizer’ is oriented along the apico-basal organ axis in the whole organ (Kuchen et al., 2012).

The difference between compensated growth of epidermal cells in leaf blade (or cotyledon) and appearance of non-dividing, elongated cells in sepal is that in the latter, cells of very different shapes placed among each other constitute the main surface of these organs. Conversely, the puzzle-shaped pavement cells in the leaf and cotyledon epidermis have similar shapes and comparable growth rates, as most likely they all undergo the same developmental program. Furthermore, since the puzzle shapes are irregular but the organ they constitute (cotyledon) has a consistent, round shape, there must be some organ-level mechanism coordinating the growth of each individual lobe and indentation. I do not take into consideration stomata (present throughout the whole epidermal surface) because even though each leaf has many of them, they constitute a small fraction of the whole leaf surface compared to the puzzle-shaped cells.

The small and giant cells in the sepal epidermis have distinct shapes. However, they most likely also undergo a similar developmental program since all the sepal epidermal cells originate from a small group of cells (Fig. 3.7). In addition, *lgo* mutant lacking giant cells has similar growth rates to wild type. It might mean that:

1. small and giant cells have the same identity, with only a small modification in entering endoreduplication,
2. there is a growth promoting signal which is globally distributed and probably acts in addition to cell-autonomous growing mechanisms and
3. cell growth and cell divisions are two separate processes which have different implications on the anatomy of the plant.

One can speculate that loss of giant cells in *lgo* sepals would impact their growth, for example by making it less anisotropic. It is known that a large cell expands more due to turgor pressure than a small cell, which can affect its growth (Bassel et al., 2014), so some discrepancies in growth of differently sized cells located next to each other could be expected. However, in the wild type sepal giant and small cells are located next to each other and yet, organ shape is robust in both cases (Hong et al., 2016; Roeder et al., 2010). Furthermore, the stochastic distribution of giant cells in wild type sepals does not affect the shape of a whole sepal. Hence, even a dramatic shape change of some cells is not enough to change the shape of the whole organ (Hong et al., 2016). One cannot exclude the possibility that in this particular case, this organ shape change is not feasible because a general trend of growth direction is not changing (both giant and small cells grow rather anisotropically). In other words, this particular shape change (elongated to square) is not dramatic enough to cause organ shape change.

Even though local changes of cell shape are not enough to change organ shape (see wild type sepal vs. *lgo* sepal), I wanted to check if differently shaped organs have different growth patterns. I found that the elongated sepal with small or giant, elongated cells grows more anisotropically than the round cotyledon with its jigsaw-puzzle shaped epidermal cells. Since the irregular shapes of puzzle cells usually do not have any prevalent axis, I consider the cotyledons to grow isotropically on cell and tissue level. Therefore, I have found correlation of cell growth and cell shape (anisotropic in the sepal, isotropic in the cotyledon).

This data is, however, only correlative and not causative. The still unresolved question is: what is it exactly that drives organ shape in plants? There are two possible explanations: one, that shape is directed by a growth hormone or some other biochemical signal (such as a cascade of molecular interactions) and cell shape is just a consequence of that, or two, that there is a mechanical signal regulating the shape as cells grow. I have managed to gather some evidence concerning the plausibility of the second explanation: cell geometry is sufficient to shape single cells and coordinate growth of neighboring cells within a tissue. This concept bridges the subcellular level and tissue level of growth control based on mechanics only (not requiring any biochemical signal). In Chapter 5 I present my findings

on why isotropic jigsaw-puzzle-like shapes are created in the epidermis of round cotyledons.

3.4. Materials and methods

For imaging both cotyledons and sepals, a *pUBQ10::myrYFP* line, which expresses Yellow Fluorescence Protein (YFP) in the plasma membrane, was used (Hervieux et al., 2016). For the sepal experiment, a 3-4 - cm-long main inflorescence stems were cut from the plant. To access young buds, the first 10–15 flowers were dissected out and the stem was then kept in ½ MS medium supplemented with 0.1% solution of Plant Protective Medium PPM, Plant Cell Technology), as described in (Vlad et al., 2014). The young buds were imaged with an SP8 laser-scanning confocal microscope (Leica) using long working distance 25× (NA 0.95) or 40× (NA 0.8) water immersion objectives. Plants were imaged every 24 h for 8 days. Flowers were dissected at the end of the time-lapse series to determine their growth stage based on internal organs (Smyth et al., 1990).

For the cotyledon experiment, I removed one of the two cotyledons from a young seedling (2 days after germination) and inserted the root and part of the hypocotyl into the same medium as described above. For the whole duration of experiments (both for sepals and cotyledons) samples were kept in a long day condition growth chamber.

I analyzed growth rates and growth directions using confocal image quantification software MorphoGraphX (Barbier de Reuille et al., 2015).

3.5. Acknowledgement

Portions of this chapter were included in:

Hervieux, N., Dumond, M., **Sapala, A.**, Routier-Kierzkowska, A.-L., Kierzkowski, D., Roeder, A.H.K., Smith, R.S., and Hamant, O. (2016). A mechanical feedback restricts sepal growth and shape in Arabidopsis. *Current Biology* 26, 1019–1028.

Author contributions:

time lapse imaging of the wild type sepals was performed by Daniel Kierzkowski (Max Planck Institute for Plant Breeding Research). Growth quantification of wild type sepals was performed by Anne-Lise Routier Kierzkowska (Max Planck Institute for Plant Breeding Research) and myself. Time lapse imaging and growth quantification of *lgo* sepals as well as wild type cotyledons were performed by myself. Seeds of *lgo* mutant were provided by Adrienne Roeder (Cornell University). The analysis of cortical microtubule orientation was performed by Nathan Hervieux (ENS de Lyon) and the model of shape sensing was created by Mathilde Dumond (ENS de Lyon).

4. Mechanical properties of growing plant cells

Plant cells are encased in the cell wall which is a rigid scaffold partially accounting for their 3D architecture. This fact has two important implications:

1. the cells cannot move relative to each other,
2. material properties of the cell wall are a determining factor of cellular growth and shape, as the growth happens when the cell wall yields to turgor pressure exerted on it by the cytosol and vacuole.

Consequently, the physical aspect of morphogenesis cannot be ignored. A number of biomechanical experimental methods have been adapted from material sciences to biology of both animals and plants. I have employed two of them to gain information on the distribution of forces within the cell wall (in combination with Finite Element Method modeling) and answer broader biological questions. In this chapter I describe experiments done with these two biomechanical methods.

The first one is Cellular Force Microscopy which is a micro-indentation method. A micro-electro-mechanical system (MEMS) force sensor (Felekis et al., 2011) probes the tissue until a given depth. Then, an in-house software MorphoRobotX (embedded in MorphoGraphX) computes the force required for the sensor to indent the tissue as a function of indentation depth. Stiffness [N/m] is then calculated for each measurement point as linear fit of this function. The output of CFM stiffness measurements is considered to indirectly indicate turgor pressure inside cells (the stiffer the cell, the higher the turgor pressure) (Routier-Kierzkowska et al., 2012). My results obtained with this technology were determinant in theoretical work studying the impact of cell geometry on tissue mechanics (Mosca et al., 2017).

The second method described and used in this chapter is osmotic treatment. It is based on calculating how much the cell wall shrinks upon rapid reduction of turgor pressure caused by immersing the tissue in a solution of osmolarity higher than that of the cytosol. This experiment informs on the elasticity of the cell wall which is regulated by many molecular factors. It has been used to hypothesize about the role of Reactive Oxygen Species (ROS) in the cell wall structure and organ maturation (Hong et al., 2016).

4.1. Cellular Force Microscope

To familiarize myself with the CFM method, I started with obtaining topography and stiffness measurements on onion (*Allium cepa*) epidermis according to the protocol established by Routier-Kierzkowska et al. (2012). The robot with the sensor was attached to an inverted optical microscope. I was able to produce surface maps of the onion epidermis that very closely matched the geometry of the cells, which bulge out substantially due to high turgor pressure (Fig. 4.1A). Even though the readout of the indentation measurements performed by CFM cannot be directly interpreted as turgor pressure (Mosca et al., 2017; Weber et al., 2015), I assume it can be its approximation used to compare turgor pressure in different cells during one measurement.

Next, I performed single cell ablation by puncturing one epidermal cell in a place precisely chosen on a CFM topography grid. The aim of this experiment was to check the ability of the setup to successfully perform cell ablation (for future experiments) and to ensure that

the decrease in turgor pressure after ablation is detectable by the setup. The consequences of the ablation were quickly visible on the cell: leakage of protoplast including the nucleus was visible already 2 minutes after ablation (notice the gradual accumulation of protoplast around the nucleus). This time was as fast as the experimental setup allowed to record a picture. However, the leakage went on for at least two hours (Fig. 4.1B).

In order to confirm the decrease of turgor pressure in the ablated cell, I measured stiffness of the ablated cell and its neighbors. In the ablated cell stiffness (as detected by CFM) decreased by over 50%, while stiffness of neighboring cells remained similar (roughly 10 measurement points per cell, only on flat areas, Fig. 4.1C).

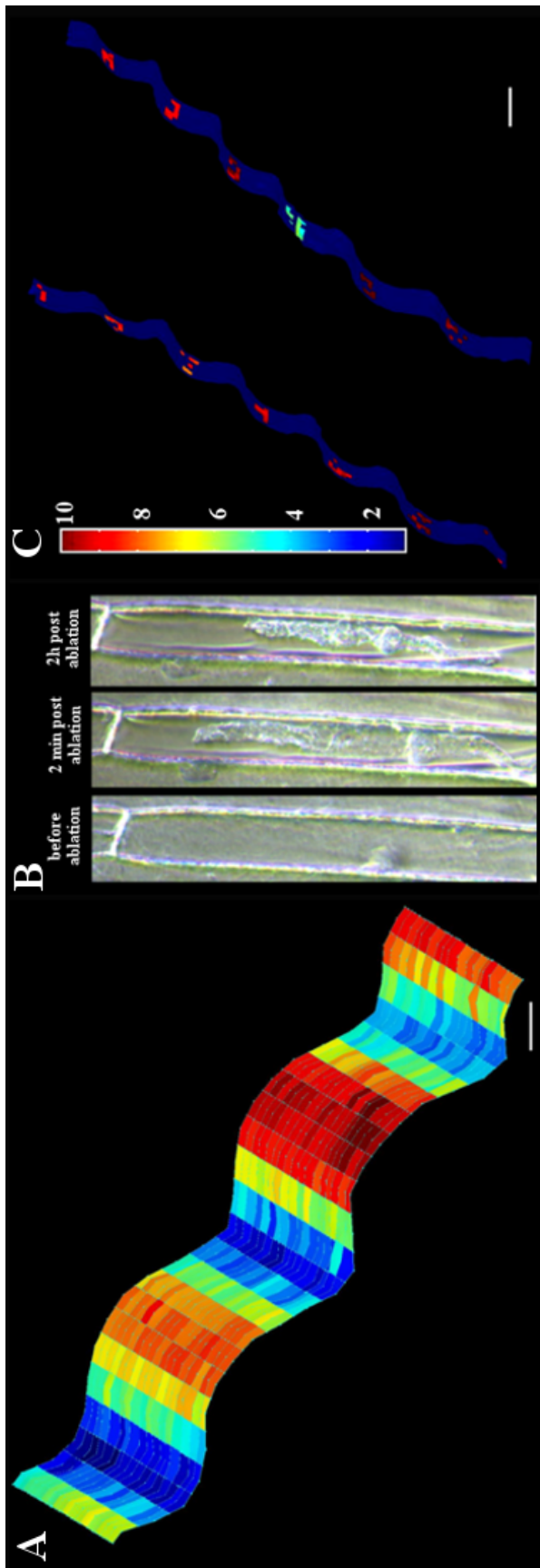


Figure 4.1. Results of Cellular Force Microscopy experiments on turgid onion epidermis. (A) Surface map of onion epidermis viewed from the side. Color scale corresponds to height within the tissue (red regions are more bulged out than blue regions). The red areas correspond to the surface of the cells (bulging out due to turgor pressure) and the blue corresponds to borders between cells. Scale bar, 5 μm . (B) Time-lapse imaging of a cell before ablation (left), 2 minutes after ablation (middle) and 2 hours after ablation (right). Shrinking and leakage of protoplasm can be observed. (C) Stiffness of 6 neighboring cells (a fragment of each cell images) before ablation (left) and after ablation (right), measured only on flat parts of each cell. Color scale: measured stiffness [N/m]. The stiffness of the ablated cell dropped while in its neighbors' stiffness remained unchanged. Scale bar, 20 μm .

4.2. Combining the Cellular Force Microscope technology with a confocal laser scanning microscope

Since optimizing the CFM system for onion epidermis studies mentioned above, the Smith Lab extended the applicability of the setup to a smaller scale by mounting the force sensor-navigating robot on a confocal microscope (Fig. 4.2). The key advantage of the CFM-confocal setup is that the area of CFM scans can be very precisely chosen based on an image obtained with the confocal microscope (Fig. 4.3A). Therefore, much smaller cells can be imaged than in the case of a normal light microscope. I have scanned an area of the sepal which resulted in surface maps (Fig. 4.3B) and stiffness measurements on single cells (Fig. 4.3D).

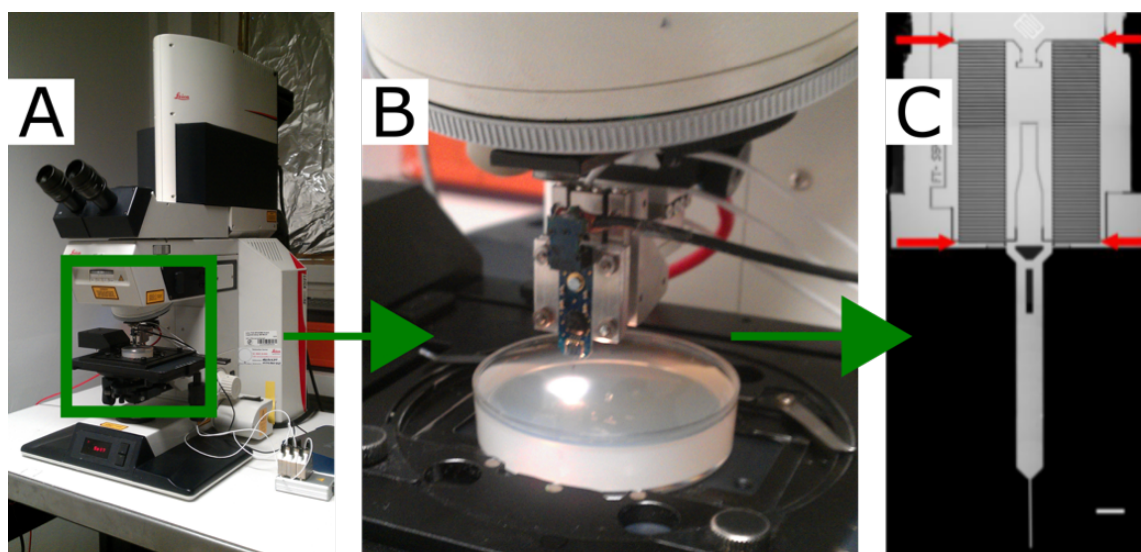


Figure 4.2. A scheme of the CFM-confocal setup. (A) A Leica SP2 confocal laser scanning microscope. The CFM hardware is marked by the green box. (B) The nanorobot and CFM sensor are attached to the microscope as a lens. The user can flip between the CFM setup and any other lens whenever a confocal image of the sample is needed. The sample is immersed in low melting point agarose in a plastic Petri dish. All measurements are performed in water. (C) The MEMS force sensor with a tungsten needle attached at the bottom. Red arrows indicate capacitors which transduce force into an electric signal. Scale bar, 300 μm .

Image in (C) adapted from (Routier-Kierzkowska et al., 2012).

The surface map (output of CFM measurements) comprises of squares sized between $1 \times 1 \mu\text{m}$ and $3 \times 3 \mu\text{m}$, each representing one measurement point. This resolution makes it possible to distinguish separate cells from each other (compare fig. 4.3C and D). Stiffness measurements (force/indentation curves, F/x) are performed on flat parts of each cell, as values obtained from inclined areas appear softer due to the slope of the surface (Routier-Kierzkowska et al., 2012).

I was able to record multiple stiffness measurements on one cell and stiffness values were considerably uniform within single cells (see measurement points within each cell in Fig. 4.3D). Another valuable observation from these experiments is that apparent stiffness values from the F/x curves are comparable within each cell type. In those results, apparent stiffness values are higher for giant cells than for small cells (Fig. 4.3D). However, this does not necessarily mean that giant cells have higher pressure – raw stiffness measurements are biased by the geometry of the cells (Weber et al., 2015), making large cells appear stiffer for the same turgor and wall stiffness.

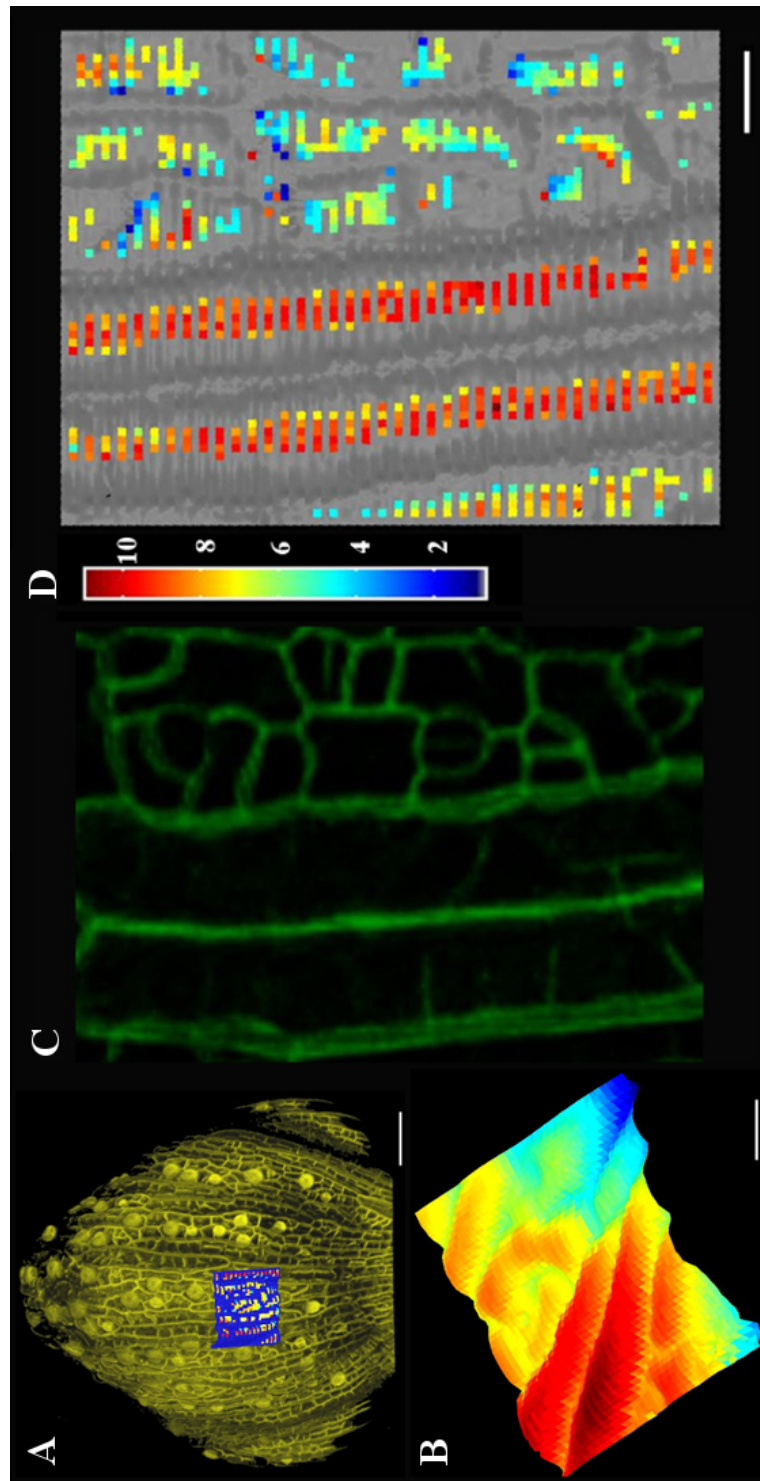


Figure 4.3. CFM measurements on sepal epidermis performed using the CFM-confocal setup. (A) Stiffness map can be precisely aligned to the confocal stack of the whole organ. Scale bar, 50 μm . (B) Surface map of a sepal (color scale from blue – low to red – high). Single cells can be easily distinguished from each other. Scale bar, 20 μm . (C) A confocal stack of CFM-scanned area and (D) stiffness map of exactly the same area. Stiffness values within 1 cell are fairly consistent. Scale bar, 10 μm .

4.3.Osmotic treatment for quantifying cell wall elasticity in the sepal of *Arabidopsis thaliana*

Mechanical simulations have shown that CFM is not suitable for directly measuring cell wall elasticity because the method is mainly sensitive to turgor pressure and cell geometry (Weber et al., 2015). Cell wall elasticity is important for developmental studies since plastic (irreversible) expansion of cells (growth) depends on the cell wall's ability to yield under turgor pressure. Softer cell wall and elevated growth rates have been shown to correlate (Kierzkowski et al., 2012; Peaucelle et al., 2011; Pien et al., 2001), which suggests that cell wall stiffness plays an important role in growth regulation.

Osmotic treatment is an experimental method that entails changing turgor pressure of a cell/a group of cells by submerging them in a solution of different osmotic potential than that inside a cell. As a result of that, water moves between the inside and outside of the cells due to the phenomenon of osmosis. If the solution has lower concentration of ions than the cell (higher osmotic potential), water will move into the cell causing it to swell up. If, in turn, the solution has higher concentration of ions than the cell (lower osmotic potential), water will move out of the cell and into its surroundings and thereby release the turgor pressure of the cell (Fig. 4.4). Consequently, the interior of the cell will not exert force on the wall any more, and the cell will shrink.

The amount by which the cell changes its size (deformation) is calculated, in my case using MorphoGraphX. In order to have a full range of cell wall shrinking, it is important that the sample is incubated in pure water for some time (takes up as much water as it can, in other words: reaches full turgor). Comparing cell size in full turgor to size after plasmolysis gives an estimate of the elasticity of the cell wall. The Young's modulus (E) is a measure of cell wall stiffness and is defined as the ratio of mechanical stress over strain (deformation of a material induced by the stress divided by the material's initial length). Therefore, the larger the shrinkage of the cell surface observed in the experiment, the lower the Young's modulus and the softer the material.

Inferring the exact E values is not trivial, as strains can be different along different directions and can depend on other material parameters such as the Poisson's ratio (measure of compressibility). Nevertheless, comparisons of cell wall elasticity within an organ or between different genotypes of the same species in the same tissue type can give a qualitative measure of differences in stiffness (Hong et al., 2016). The more a cell shrinks upon osmotic treatment, the more elastic it is.

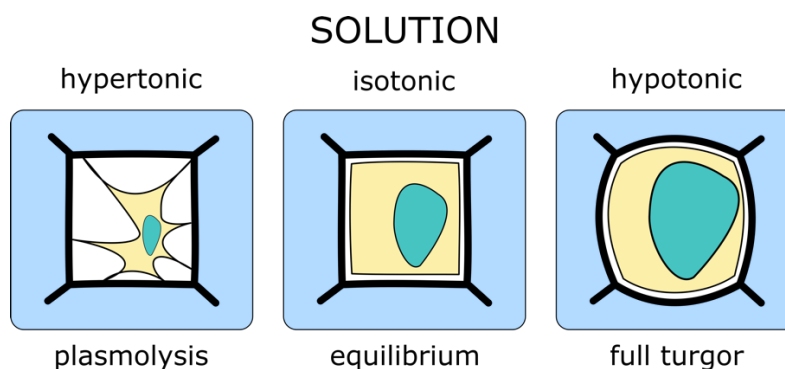


Figure 4.4. The principle of an osmotic treatment experiment. Water goes out of the cell in a hyperosmotic solution and goes into the cell in a hyperosmotic solution.

The method of osmotic treatment needs to be optimized for the tissue it is performed on. Therefore, before measuring shrinkage of sepal epidermal cells, I needed to answer the following technical questions:

1. How long does it take for cells to become fully turgid?
2. What is the optimal concentration of the osmotic agent (NaCl)?
3. What is the optimal time of incubating the tissue in the osmotic agent, after which I can observe cell shrinkage but the cell wall stain (PI) has not been fully washed out yet?

To address the first question, I submerged a flower in pure water and took a confocal image right after, 1 hour after and 2 hours after submergence. Then, I calculated sepal cell area expansion at those timepoints. I observed that during the 1st hour the sepal epidermis takes up water (cells expand up to 10%), while in the 2nd hour the water uptake is almost negligible (Fig. 4.5). Therefore, I decided to always start the osmotic treatment experiment with 1 hour incubation in pure water in order to assure full turgor of cells. This step can be

useful in any imaging experiment where cell area or volume is calculated (for example, time lapse imaging).

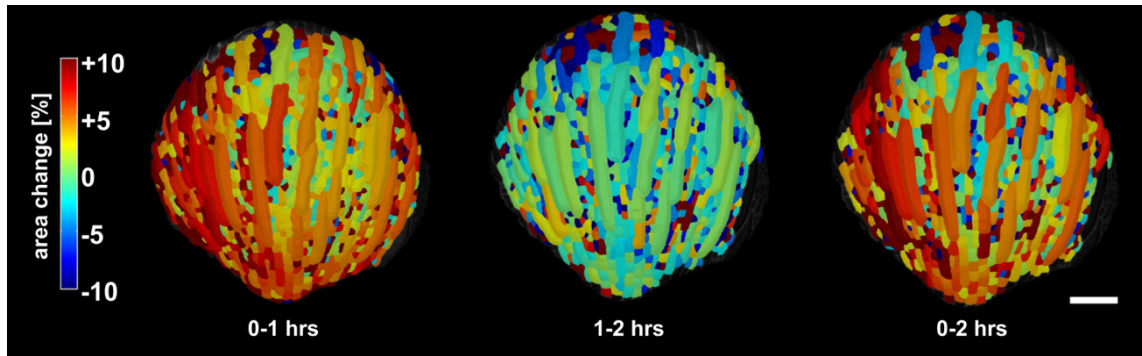


Figure 4.5. Submergence of the sepal in pure water in order to achieve full turgidity of the cells (starting point for osmotic treatment experiments). Color scale represents the change in cell area between time points (above 0 – the cell expands, below 0 – the cell shrinks). Water uptake happens mostly in the first hour of incubation. Scale bar, 50 μm .

In order to choose the optimal concentration of NaCl, I imaged wild type sepals containing the YFP marker in the plasma membrane (Hervieux et al., 2016) stained with propidium iodide. Since detachment of the plasma membrane from the cell wall is one of signs of cell plasmolysis, I needed to find a concentration of the osmotic agent (NaCl) which would be sufficient to plasmolyze the cells but not compromise the viability of the cells and the visibility of the propidium iodide. After checking concentrations of 0.1M, 0.2M, 0.4M, 0.6M and 1.0M I set the optimal NaCl concentration for this experiment was 0.4 M (Fig. 4.6, Sapala and Smith 2018, sec. 4.7.3 for numbers of replicates for all osmotic treatment experiments).

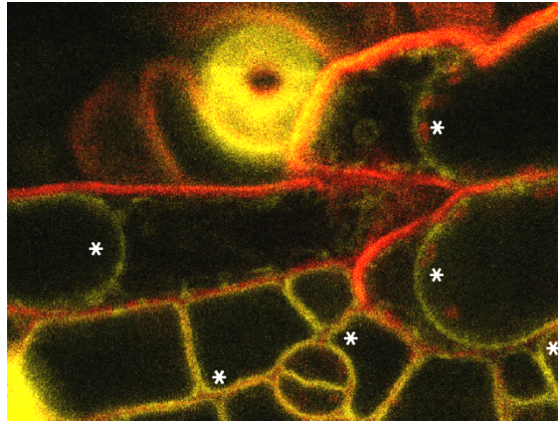


Figure 4.6. Plasma membrane (marked by YFP, yellow) and cell wall (stained with PI, red). Imaged at the same time in order to determine the optimal NaCl concentration for osmotic treatment. In concentrations 0.4M and higher, the plasma membrane is detaching from the cell wall which means plasmolysis has occurred.

The optimal time of incubation in the osmotic agent was 30 minutes. It was long enough for plasmolysis to occur (shrinkage of cells was detectable), but not long enough to wash off the cell wall stain (which would make it impossible to process the data in MorphoGraphX). To measure shrinkage of cells, quantified as the area decrease after osmotic treatment, I processed confocal pictures taken before and after treatment with MorphoGraphX. Interestingly, the areal deformation was slightly lower for giant cells than for small cells (Fig. 4.7A). In some cases, the difference in deformation between neighboring small cells was high, which might have been an artefact resulting from MorphoGraphX segmentation error. Therefore, I fused groups of small cells together (Fig. 4.7B). It should be kept in mind that the merging of small cells might lead to a bias of the shrinkage values, but for my study this type of bias is acceptable since I am interested in how single cell properties influence tissue or organ level effects. The difference of shrinkage between giant cells and groups of small cells was less pronounced (Fig. 4.7C). Another explanation for the differences of shrinkage ratio between small and giant cells could be that they have different turgor pressure. In the following subsection I will describe mechanical simulations performed in order to explore this and other possibilities.

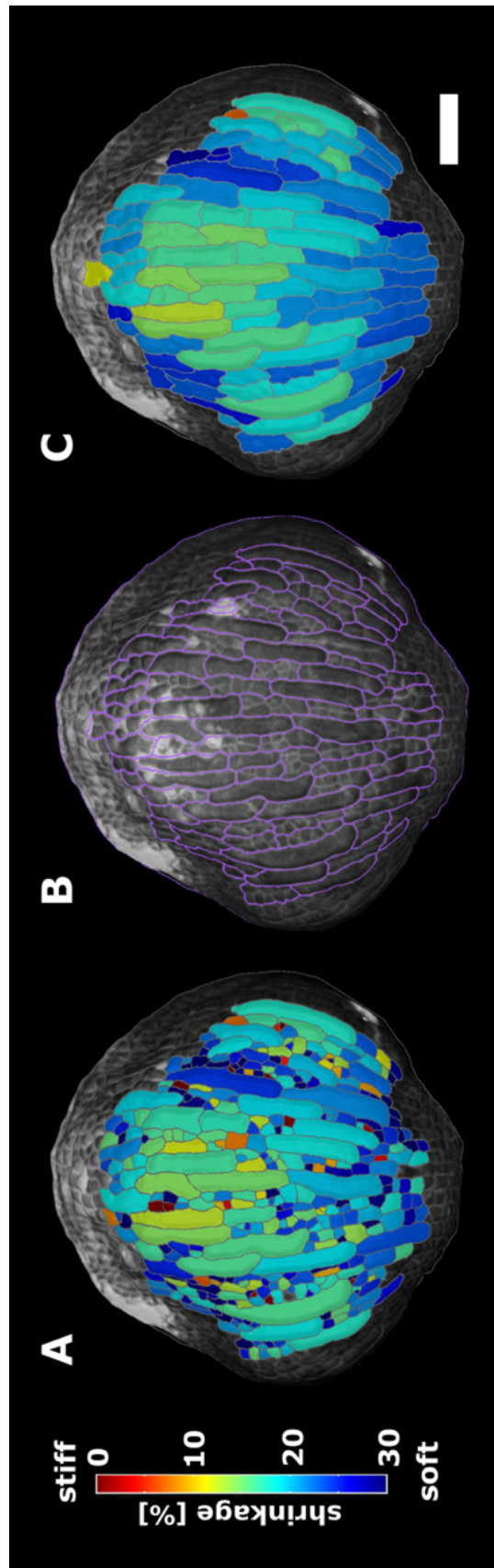


Figure 4.7. Cell wall shrinkage upon osmotic treatment in wild type sepal. (A) Map of cell shrinkage displayed on the post-treatment time point. Note the variability in neighbouring small cells. (B) Since post-treatment image quality is not good enough, I merged the small cells into groups which resembled giant cells in shape and are convex. (C) Map of shrinkage for giant cells and averaged groups of small cells. Using this method, I have demonstrated that the stiffer zones of the sepal (here: the tip and center) overlap with the zones that grow slower at that particular stage of flower development, as described in Chapter 3. Scale bar, 50 μm .

4.4. On the micro-indentation of plant cells in a tissue context

In the previous section I mentioned that obtaining exact values of Young's modulus is not trivial because it can vary in different directions and can be influenced by other properties (see Sec. 4.3). Hence, to achieve quantitative values, a reverse engineering approach based on mechanical simulations can be used, with the finite element method (FEM) as a commonly employed technique (Mosca et al., 2017; Weber et al., 2015). This means simulating a complete system (or experiment) and capturing features that influence it the most. An example of this approach is a computer model of a CFM indentation, where we wanted to explore how the output values of an indentation experiment are affected by other features of the cells and the setup. In other words, we wanted to know how to relate the numbers achieved by CFM measurements to the actual turgor pressure inside the cell (Mosca et al., 2017).

An FEM model was used to simulate an experiment performed in the lab: measuring force in an indentation experiment on three dimensional cells. This model depended on several properties: cell size (geometry), material properties, indenter size, turgor pressure and wall thickness. Since the results of these indentations on sepal epidermal cells were known from my CFM experiments, and the Poisson's ratios could be estimated based on osmotic treatment experiments, the importance of the other properties could be explored.

Similar work on single cells has revealed that indentations within the range of a few microns in depth are mostly sensitive to turgor pressure, indentation depth and cell geometry, and less sensitive to Young's modulus (or elasticity, deduced from osmotic treatments), Poisson's ratio (compressibility) or shear modulus (Weber et al., 2015). This type of sensitivity analysis is crucial in mechanical experiments in order to correctly refer measurement values to a real biological phenomenon.

Stiffness measurements on sepal cells have shown that on average, giant cells have higher stiffness than small cells (Fig. 4.3D). This may have the following reasons:

- A) different cell size,
- B) different material properties (such as stiffness),

C) different turgor pressure.

A three-dimensional tissue comprised of pressurized cells was simulated using in-house FEM code (Bassel et al., 2014). Cell walls were modeled as an isotropic, linearly elastic, large deformation (Saint Venant-Kirchhoff) material, which conveniently depends only on Young's modulus and Poisson's ratio. Then, an indentation experiment was simulated to calculate stiffness values of the cells. The initial simulations were performed on cells which had 5 μm diameter so that they resembled meristematic cells in real plants. It was demonstrated on these hypothetical cells that if the cell size is doubled in one direction, stiffness values increase by 11-17%; if two dimensions are doubled, stiffness increases by 25-33% and if all three dimensions are doubled, stiffness increases by over 45% (Mosca et al., 2017). This was the first indication that cell geometry is a crucial parameter when interpreting stiffness measurements.

In order to test if cell size alone can explain the stiffness readout differences between small and giant sepal cells, the indentation results from real tissue were compared with a simulation of an indentation experiment. This time, the indented simulated tissue was created by extruding a 2D MorphoGraphX mesh which originally came from a confocal image of the same tissue scanned by CFM in the real experiment (Fig. 4.8). Thereby, we had experimental and simulated stiffness values from cells of exactly the same geometry. Other parameters (cell wall thickness, elasticity, compressibility and turgor pressure) were set as equal for all cells

We found a good agreement between real and simulated stiffness values (only points on flat parts of cells were considered, Table 4.1). Firstly, this experimentally validates the FEM model. Secondly, it suggests that geometry (or cell size) is enough to explain the difference in stiffness results obtained from CFM, which was at 64% for real cells (Table. 4.2). Difference in turgor pressure or material properties were not required in the simulation to get higher stiffness in giant cells than in small cells. However, this is not proof that there is no difference in material properties between these two cell types, however the most parsimonious explanation is that geometry accounts for the difference in stiffness.

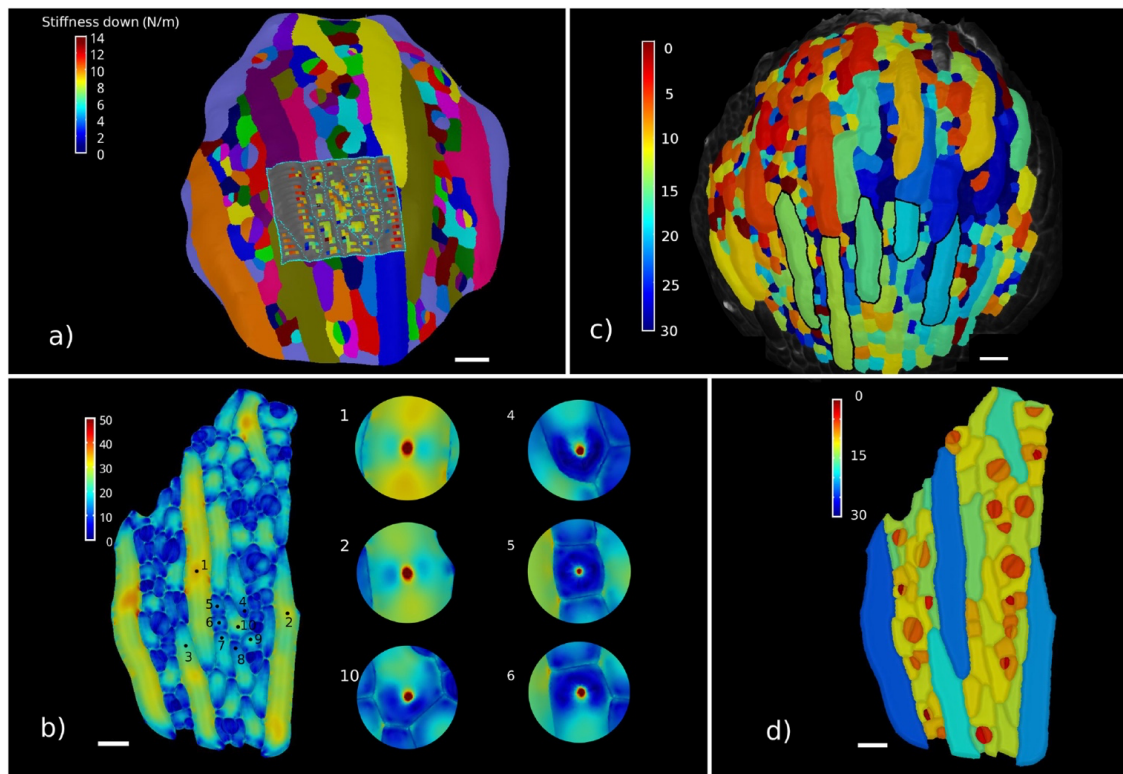


Figure 4.8. CFM indentation and osmotic treatments on an *A. thaliana* sepal implemented in the FEM model. (a) CFM indentation experimental data superimposed on the 2D cell surface mesh generated in MorphoGraphX from confocal microscopy images of the sepal. Heat map color represents the linear stiffness [N/m]. (b) FEM simulation results obtained on a template derived from the image in (a). Material parameters used were Young's modulus $E = 200$ MPa, pressure $P = 0.5$ MPa, and Poisson's ratio $\nu = 0.3$. Heat map color indicates the trace of Cauchy stress capped at 50 MPa. The left panel shows the template after inflation and prior to indentation, while the right panel shows a magnification of the area around some of the indentation points. (c) Experimental surface shrinkage data in percentage $(100 * \frac{\text{InflatedSurface} - \text{PlasmolyzedSurface}}{\text{InflatedSurface}})$ from a sepal at a comparable developmental stage as the one in (a). The cells in a position comparable to the indented ones are outlined in black. (d) Volume shrinkage ratio in percentage $(100 * \frac{\text{InflatedVolume} - \text{PlasmolyzedVolume}}{\text{InflatedVolume}})$ from the same simulation as in (b). Scale bar, 20 μm . Adapted from (Mosca et al., 2017).

Table 4.1. Experimental and simulated indentation stiffness results fitted between 2–1.5 μm indentation depth for the points in figure 4.8. Adapted from (Mosca et al., 2017).

	Stiffness [N/m]									
	Giant cells			Small cells						Point 10
	Point 1	Point 2	Point 3	Point 4	Point 5	Point 6	Point 7	Point 8	Point 9	
Experimental data	13.7	14.0	12.0	8.6	7.2	7.4	7.4	9.3	9.1	10.7
Simulation	12.6	12.6	11.4	7.4	7.9	6.68	8.46	10.2	8.58	10.6

Table 4.2. Average stiffness values for small and giant cells (Table 4.1) and relative stiffness variation between them. Adapted from (Mosca et al., 2017).

	Avg. stiffness giant cells [N/m]	Avg. stiffness small cells [N/m]	Relative stiffness variation [%]
Experimental data	13.3	8.1	64
Simulation	12.3	8.2	50

4.5 The correlation between cell wall elasticity, ROS levels and cell maturation

Given my findings that patterns of cell wall elasticity overlap with patterns of growth rates, I used osmotic treatments to study local (sub-organ) mechanical properties of sepal cells in wild type and *vos1* mutant (Hong et al., 2016). This allowed me to speculate about the functionality of reactive oxygen species (ROS) in the process of cell maturation and maintaining robustness of organ shape (Hong et al., 2016).

There have been some studies on robustness of organ size (reviewed by Powell and Lenhard, 2012). However, there is little data on robustness of organ shape. In order to investigate how plant organs (in this case – sepals) maintain their shape, mutants with defects in these mechanisms, that is mutants with variable organ shapes are needed. The sepal is a particularly good system to focus on for this question, since one plant produces hundreds of them, and they are very uniform in shape. In this work, a mutant with variable sepal shapes *vos1* (*variable organ size and shape 1*) was identified in the Roeder Lab (Cornell University). In this mutant, different sepals within an individual flower can have variable shapes, as opposed to wild type flowers where sepal shape is not variable (Hong et al., 2016). It has been demonstrated that this effect (higher shape variability compared to wild type) is not a side effect of smaller sepal size, and that this phenotype is created after the sepals are already established, not when sepal primordia are formed.

Genetic analyses have shown that *vos1* carries a mutation causing a premature stop codon in FtsH4 protein, and therefore the mutant of interest will be referred to as *ftsH4-5*. The FtsH4 protein resides in the inner membrane of the mitochondrion, facing the intermembrane space and promoting the assembly of oxidative phosphorylation complexes

(Ito and Akiyama, 2005). Inactivating this protein causes mitochondrial defects and leads to increased ROS levels, which was also demonstrated in *A.thaliana* sepals using 3,3'-diaminobenzidine (DAB) and nitroblue tetrazolium (NBT) staining to visualize levels of two abundant ROS molecules: H_2O_2 and O_2^- , respectively. Furthermore, it was shown that elevated ROS levels cause increased shape variability and decreased size of *ftsh4* sepals, and that epidermal cells in *ftsh4* mature faster than in wild type. Cell maturation in this context is understood as the slowing down of growth and cessation of cell divisions (Ito and Akiyama, 2005).

The elevated ROS levels and early maturation of *ftsh4* compared to wild type sepals led us to suspect that cell wall properties are also affected in this mutant. Previous studies have provided data suggesting that ROS affect cell wall structure in two contradictory ways:

1. stiffening the cell wall by promoting the creation of polysaccharide-glycoprotein cross-links, thereby limiting growth (Fry, 2004), or inhibiting enzymatic hydrolysis of the cell wall via creation of polysaccharide-polysaccharide or polysaccharide – lignin cross-links (Ralph et al., 2004);
2. loosening the cell wall by enzymatic or non-enzymatic scission of polysaccharides (Fry, 1998; Schopfer, 2006).

However, it is rather challenging to confirm the real role of the oxidative enzymes and the events leading to formation/cleavage of chemical bonds between the cell wall fibrils, since most of the biochemical studies required for this are only applicable *in vitro*, and not *in vivo* in real plant cells (Fry, 2004). Assessing the mechanical properties of plant cells might be a good way to evaluate these *in vitro* results by measuring the potential effects of this enzymatic activity (change in cell wall stiffness).

I used osmotic treatment experiments to check if cell wall stiffness of *ftsh4* is different than in wild type, and thereby decide which of the two possibilities is the way ROS influence cell wall mechanics. I observed that cell wall stiffness in wild type sepals of developmental stage 8-9 was higher at the tip of the sepal compared to its base (Fig. 4.9A). This matches the growth rate patterns discussed in Chapter 3: in that developmental stage, at the tip cells grow slower. *ftsh4* sepals displayed a similar trend, although overall, their growth pattern distribution is similarly spaced but slightly delayed compared to a wild type sepal. The

overall shrinkage of wild type sepals (all cells pooled together) was at $17\% \pm 2.6\%$, while the overall shrinkage for *ftsh4* sepals was at $11\% \pm 1.7\%$ (mean \pm SD, $n = 3$ sepals of each genotype) (Fig. 4.9B). This data shows that epidermal cell walls in *ftsh4* sepals are stiffer than cell walls in epidermal cells in wild type sepals.

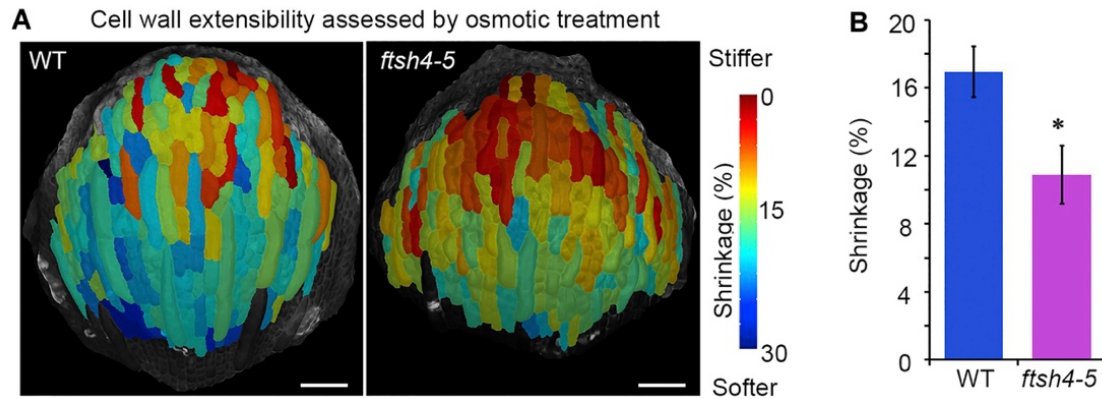


Figure 4.9. Comparison of cell wall elasticity between wild type and *ftsh4-5* at developmental stages 8–9. (A) Heatmaps of cell shrinkage, with small cells grouped. The cells in red have low shrinkage and are stiffer than cells in blue with high shrinkage. (B) Plots of area shrinkage for the whole sepal. * $p < 0.1$, significant difference from wild type (t-test). Cell walls are stiffer (had a lower percent shrinkage in osmotic treatments) in *ftsh4* sepals than in wild type. Data are mean \pm SD. $n = 3$ for WT and *ftsh4*. Scale bar, 50 μ m.

Figure adapted from (Hong et al., 2016).

4.6. Summary of the results

I have modified and improved protocols of two biomechanical measurement methods which allowed me to bring new input into cell wall elasticity and turgor pressure of sepal epidermal cells: osmotic treatment and Cellular Force Microscopy (CFM) coupled with a confocal microscope.

My CFM measurements on sepal epidermis have shown higher stiffness in giant cells than in small cells. Since it has been known before that these measurements are mostly sensitive to turgor pressure, these results presented a possibility that turgor pressure is different in those two kinds of cells. These data together with osmotic data were then fed into an FEM model of an indentation experiment. Parameter exploration of the model showed that the discrepancy of stiffness values can be explained exclusively by different geometry of these

cells (Mosca et al., 2017). Therefore, the possibility of the two cell types having different turgor pressure is not likely (even though there is not enough experimental data to exclude it completely).

The sepal osmotic treatment results were not precise enough to address the difference in cell wall stiffness between giant cells and small cells, as in some places the cell contours were not sharp enough for small cells due to washing off of the stain. They had to be fused into groups in order to calculate shrinkage ratios. Even in the regions where the cell contours were visible, I did not detect a striking difference between the shrinkage of small cells and stomatal guard cells. This difference could be expected as guard cells are known to have much higher turgor pressure than other cells (Franks et al., 1995, 2001). On the other hand, this might be balanced by a stiffer cell wall in which case difference in shrinkage would not be observable.

While it has been reported using AFM that cell wall properties are inhomogenous on a very small, sub-cellular scale (Hong et al., 2016; Majda et al., 2017; Sampathkumar et al., 2014), AFM measures elastic wall properties in a plane perpendicular to the cell/organ surface, not parallel to it. Therefore, my results using osmotic treatment are the first study done on the sepal considering elasticity in the plane in which the cell actually grows, and along which the deposited cellulose reinforces the cell from stress. The shrinkage ratios detected using osmotic treatments overlap with growth patterns of the sepal in corresponding stages of flower development – the slower-growing zone is stiffer than the faster-growing zone. This observation is one of the most straightforward demonstrations of the correlation between cell wall loosening and increased growth rates available so far (Hayot et al., 2012; Kierzkowski et al. 2012; Peaucelle et al. 2011; Pien et al., 2001).

Finally, I used osmotic treatment to compare cell wall stiffness of sepals in wild type and *ftsh4* mutant, shown to have elevated levels of reactive oxygen species (Hong et al., 2016). The cells of the mutant had stiffer cell walls than wild type cells. These results indicate that ROS increase stiffness of the cell wall and therefore they are in line with the observation that *ftsh4* cells mature faster (and therefore they may seem to have lower growth rates, as rapid growth is attributed to young cells; Hong et al., 2016). Therefore, ROS may control

organ growth by speeding up cell maturation *via* stiffening the cell wall in certain areas of the organ (here: sepal tip). Since ROS are short-lived compounds, it is an attractive scenario that they serve as very site-specific growth regulators (Fry, 1998). In that case, the required 'reaction time' of the cell wall is shorter than time required by a cell wall degrading enzyme, activated for example via auxin (Schopfer, 2001). As a result, decreased cellular growth rates compared to wild type were observed (Hong et al., 2016). Even though my results suggest that in the context of the *ftsh4* mutation ROS act as cell wall stiffeners and slow down growth, it is important to keep in mind the possibility that other ROS may participate in some processes loosening the cell wall, just in a different context.

4.7. Materials and methods

4.7.1. Onion CFM

The experimental setup was as described in (Routier-Kierzkowska et al., 2012). I used a spherical indenter with 0.7 μm radius. Stiffness was measured on flat parts of the tissue by indenting the cell around 2 μm in depth and the force/indentation (F/x) curves were recorded for each point. For the stiffness measurement, the indentation was performed in very smooth steps in order not to damage the sample. In order to compute the stiffness for one point, a linear equation was fit to the F/x curve, in the range where the relation was linear (on average, between 1.5 and 2 μm indentation depth after contact. For the single cell ablation, I punctured the cell with one abrupt step of 1.5 μm below the cell surface. Afterwards, I performed a normal stiffness scan (as described above) in order to assess the differences in turgor pressure between the punctured cell and other cells in its proximity.

4.7.2. CFM setup mounted on the confocal microscope

For measuring the apparent stiffness of sepal epidermal cells I used the Cellular Force Microscope (Routier-Kierzkowska et al., 2012) attached to Leica SP2 confocal laser scanning microscope. Since the CFM robot was attached to the microscope as a normal lens, it was possible to collect microscope pictures (20x long working distance water immersion lens) and CFM scans of exactly the same region of the sample. I used a *pUBQ10:myrYFP* line in which the cell borders are visible because the plasma membrane is tagged with yellow fluorescent protein (Hervieux et al., 2016). The flower was

immobilized by partial submergence in 1.5% low melting point agarose solution (Roth) in such a way that the CFM scanned region was not covered by agarose. Both confocal images and CFM scans were performed in water.

4.7.3. Osmotic treatment

I dissected a young flower of stage 8-9 and immobilized it in $\frac{1}{2}$ MS medium in the same way as described for time lapse imaging of sepals (Chapter 3). Next steps are described below (Sapala and Smith, 2018):

1. Fill an Eppendorf tube with 0.1% PPM water. Insert the dissected stem, taking care that the flower is under water. Incubate for 1 hour.
2. Transfer the sample into another Eppendorf tube filled with 0.1% propidium iodide (PI) solution. Incubate for 15 minutes.
3. Put the sample into the $\frac{1}{2}$ MS solid medium (stem in the medium, flower sticking out, with the abaxial flower as parallel to the medium surface as possible).
4. Determine the optimal concentration of osmotic agent for your study. It should be enough to plasmolyse the cells but not so high as to stress them.
5. Fill the Petri dish with water or the osmotic agent solution and take the first image. This will be time point 0 (T0).
6. Incubate for 30 minutes.
7. Take another confocal image with the same settings as in pt. 5. This will be time point 1 (T1).
8. Calculate cell shrinkage using the growth tracking methodology of MorphoGraphX. In case the T1 image quality is poor, small cells can be grouped together (Fig. 4.6).

Imaging conditions for propidium iodide (visualizing the cell wall): 605-644 nm emission spectrum, 488 nm laser for excitation. Imaging conditions for YFP (visualizing the plasma membrane): 519-550 nm emission spectrum, 514 nm laser for excitation. Each experiment (osmotic treatment for each genotype and water treatment) was performed in 3 independent biological replicates.

4.7.4. Integrating the CFM and osmotic treatment data into a mechanical model

In-house FEM software (Bassel et al., 2014) was used to simulate an indentation experiment. The area around the indentation point is refined in order to better approximate the deformation and the reaction force in this location. Indentations were performed at the center of the periclinal wall of the central cell of the template. The area of contact between the cell wall and the indenter was modeled as a point load.

The template had an average triangle side length of about 0.8 μm and was refined near the indentation points so that the element side length was approximately 0.3–0.5 μm . The sepal was assigned a Saint Venant–Kirchhoff isotropic material law with Young’s modulus $E = 200$ MPa, Poisson’s ratio $\nu = 0.3$, turgor pressure of 0.5 MPa and a uniform cell wall thickness of 0.25 μm .

Next, the indentation simulation was performed. A spherical indenter of 0.7 μm radius was used (as in experiment). Linear stiffness was computed by subtracting the reaction force at 2.0 μm and 1.5 μm indentation depth (as used in the experimental procedure). In order for the fitting to be accurate, the data from simulated indentation points have to be compared with experimental data belonging to points in similar locations within the cells. Only points on relatively flat portions of the cell surface (i.e. perpendicular to the indentation direction), where the stiffness data showed good consistency, were considered.

4.7.5. Comparing stiffness in sepal epidermal cells between wild type and *ftsh4-5* mutant

I performed osmotic treatments as described above were performed on wild type (Col-0 accession) flowers and *ftsh4-5* flowers (Hong et al., 2016), in 3 separate repetitions per genotype. Mutant seeds were provided by the Roeder Lab (Cornell University). Average stiffness values were compared using Student t-test.

4.7.6. Acknowledgement

Portions of this chapter were included in:

Sapala, A. and Smith, R.S. (2018). Osmotic treatment for quantifying cell wall elasticity in the sepal of *Arabidopsis thaliana*. *Methods in Molecular Biology*. Submitted.

Mosca, G., **Sapala, A.**, Strauss, S., Routier-Kierzkowska A.L., Smith, R.S. (2017). On the micro-indentation of plant cells in a tissue context. *Physical Biology* 14.

Hong, L., Dumond, M., Tsugawa, S., **Sapala, A.**, Routier-Kierzkowska, A.-L., Zhou, Y., Chen, C., Kiss, A., Zhu, M., Hamant, O., et al. (2016). Variable Cell Growth Yields Reproducible Organ Development through Spatiotemporal Averaging. *Developmental Cell* 38, 15–32.

Author contributions:

I have performed all CFM experiments both on onion and sepal epidermis. The setup adjustments necessary to attach the CFM robot to the confocal microscope were designed and made by Anne-Lise Routier-Kierzkowska (Max Planck Institute for Plant Breeding Research). The FEM model of indentations was created by Gabriella Mosca (Max Planck Institute for Plant Breeding Research, University of Bern), but the experimental data fed to the model were performed exclusively by myself. The *ftsh4* mutant was identified and described by Lilan Hong and Adrienne Roeder (Cornell University).

5. Why plants make puzzle cells and how their shape emerges

The shape and function of plant cells are often highly interdependent. The puzzle-shaped cells that appear in the epidermis of many plant species, including *Arabidopsis thaliana*, are a striking example of a complex cell shape (Fig. 5.1). However, it has remained elusive what functional benefit for the plant they provide (Bidhendi and Geitmann, 2018). It has been hypothesized that the interdigitation of the lobes and indentations may strengthen the leaf surface (Glover, 2000; Jacques and Vissenberg, 2014; Sotiriou et al., 2018), with material sciences studies supporting the plausibility of this idea (Lee, 2000). Alternatively, puzzle-shaped cells may allow for the correct spacing of the other epidermal cell types, such as guard cells and stomata (Glover, 2000). However, there is little experimental support for these hypotheses at present.

Based on the combination of computational modeling, genetic engineering, growth tracking and cell shape quantification, we propose that these intricate forms provide an effective strategy to reduce mechanical stress in the cell wall of the epidermis.

When tissue-level growth is isotropic, I hypothesize that lobes emerge at the cellular level to prevent formation of large isodiametric cells that would bulge under the stress produced by turgor pressure. Simulation models have shown that a mechanism actively regulating cellular stress plausibly reproduces the development of epidermal cell shape (Sapala et al., 2018). Our model relies on a few physical assumptions regarding growth restricting connections inserted across the cell during growth. These assumptions are in line with molecular studies which suggest a co-repression network of proteins involved in growth restriction (ROP6) and growth enhancement (ROP2), interchangeably located along the cell borders in indentations and lobes, respectively (Fu et al., 2002, 2009).

Lowering cell wall stress is important for the plant as it most likely decreases the amount of energy and resources (e.g. cellulose) needed to reinforce the cell wall against turgor pressure. It has been proposed that the cell shape feeds back on growth by sensing mechanical stress and puzzle shapes are created as a result of this feedback (Sampathkumar et al., 2014). However, this idea was not supported by a dynamic model of growing cells.

In this Chapter, data from various plant organs and species support the relationship between lobes and growth isotropy, which I tested with mutants where growth direction is perturbed. Together, these results suggest that mechanical stress is one of the key drivers of cell shape morphogenesis.

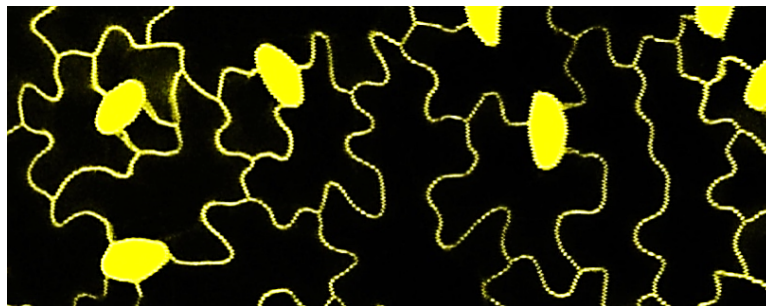


Figure 5.1. Epidermis of a mature leaf of *Arabidopsis thaliana*. The three main types of epidermal cells are: circular stomata (yellow spots), puzzle-shaped cells and trichomes (defensive structures, not shown in the image).

5.1. Cell shape predicts mechanical stress magnitude

In order to explore the effect of cell shape on turgor-induced mechanical stresses in the cell wall (Bassel et al., 2014), we performed simulations on single cells with idealized shapes using the Finite Element Method (FEM). The theoretical cells were assigned equal, uniform material properties and turgor pressure (see sec. 5.9 – Materials and methods). Starting with a small cube-shaped cell ($10 \times 10 \times 10 \mu\text{m}$) we increased the initial cell size in different dimensions. We observed that an increase of cell length in one direction ($50 \times 10 \times 10 \mu\text{m}$) does not significantly increase maximal stress in the cell wall. Next, we simulated a cell expanded in two directions ($50 \times 50 \times 10 \mu\text{m}$) and observed that the maximal stress was much higher. Enlarging the cell in two directions created a large open surface area, causing the cell wall to bulge out in response to turgor pressure, greatly increasing the stress. When the third dimension is enlarged to form a cube ($50 \times 50 \times 50 \mu\text{m}$), only a small increase in maximal stress is observed compared to the $50 \times 50 \times 10 \mu\text{m}$ case (Fig. 5.2).

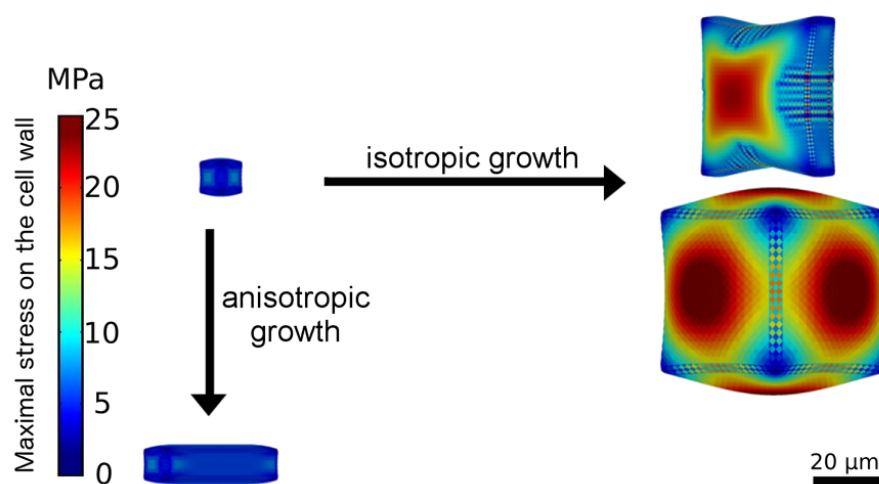


Figure 5.2. Cellular stress patterns in finite element method (FEM) simulations. Cell walls have uniform, isotropic material properties. Enlargement in two or more dimensions (isotropic growth) substantially increases stress in the center of the cell walls, while enlargement in one direction (anisotropic growth) does not cause a significant increase in maximal stress. Adapted from (Sapala et al., 2018).

This suggests that anisotropic growth that results in long thin cells is a mechanically advantageous strategy to limit stress magnitude, limiting the wall thickness required to maintain the cell's integrity. Plant organs such as roots, hypocotyls, sepals, many grass

leaves and stems grow primarily in one direction (Fig. 3.1) and have elongated cells, which would maintain low stress during growth. But how do cells avoid excessive stress if they are part of a tissue that grows in two directions, such as the surface of broad leaves?

We propose that the puzzle cell shape, with lobes and indentations, provides a solution to this problem. To test this hypothesis, we analyzed the stress in a mechanical model of the cotyledon epidermis of *Arabidopsis thaliana*. A cellular surface mesh was extracted from confocal images using the image analysis software MorphoGraphX (Barbier de Reuille et al., 2015). The mesh was then extruded to form a layer of 3D cells of uniform thickness representing the cotyledon epidermis (Mosca, et al., 2017). Next, the cells were pressurized, and the stresses visualized (Fig. 5.3A). In order to examine the effect of lobes on the stress, we created a second template with simplified cell shapes using only the junctions (points shared by three different cells) of the original cells (Fig. 5.3B). While the average cell area in the original and simplified tissue is the same, the overall stress is much lower in the original (puzzle-shaped) tissue, especially for large cells.

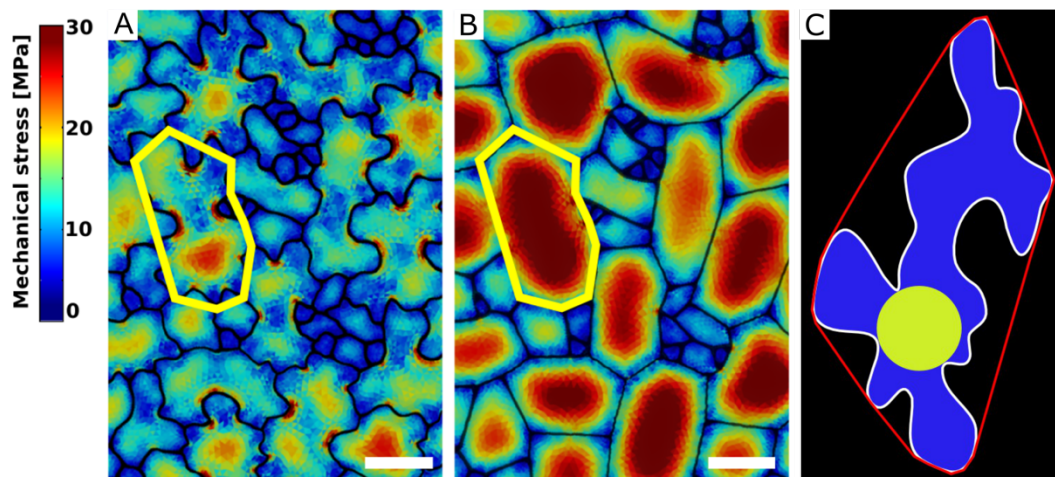


Figure 5.3. Principal stresses generated by turgor *in vivo* simulated in an FEM model. (A) Pressurized template extracted from confocal data. (B) A simplified tissue template using the junctions of the cells in (A). The yellow outline marks a corresponding cell in (A) and (B). Total area and number of cells is the same, however the maximal stress is much lower in the puzzle-shaped cells compared to the more isodiametrically-shaped cells. Scale bars, 50 μm . (C) Measures used to quantify puzzle cell shape and stress. The largest empty circle (LEC, yellow) that fits inside the cell is a proxy for the maximal stress in the cell wall. The convex hull (red) is the smallest convex shape that contains the cell. The ratio of cell perimeter (white) to the convex hull perimeter (red) gives a measure of how lobed the cell is (termed “lobeyness”). Adapted from (Sapala et al., 2018).

High stress values appear in open areas and in the indentions between protrusions, consistent with previous observations (Sampathkumar et al., 2014). In the absence of lobes, the load acting in the middle of the cell is transmitted approximately evenly to the cell contour, whereas in puzzle-shaped cells, the central load is transferred to the area between the lobes, creating stress hot spots in the indentations. The magnitude of stress in the indentations is therefore a direct reflection of the large open areas of the cell that they support, and is thus higher when cells bulge more. Despite the stress hot spots between protrusions, overall stress at both the cell and tissue level is much lower in puzzle shaped cells than in the simplified cell shape template (Fig. 5.3A,B).

Following these observations, I propose that mechanical stress in both puzzle-shaped and non-lobed cells is approximated by the size of the largest empty circle (LEC) that can fit into the cell contour (Fig. 5.3C, yellow). For long thin cells, such as in roots or stems, the size of the empty circle is the cell diameter, which is known to predict stress for cylindrical cells (Geitmann and Ortega, 2009). In a strongly anisotropically growing organ the plant would make long thin cells, whereas in more isotropic organs puzzle cells would be produced.

5.2. Cell shape measures

In order to discuss the role of puzzle cells, a method to quantify the puzzle shape of cells is required. A common measure to estimate the complexity of a contour is circularity, indicating how closely a given object resembles a circle. Circularity is calculated using the ratio of the perimeter to the square root of area (Majda, 2017; Zhang et al., 2011). However, it is not suitable for my purposes as both simple, elongated cells and lobed puzzle cells have increased circularity values. Consequently, it cannot be used to reliably distinguish between these cell shapes. Another common approach is to calculate a skeleton based on the cell contour and count its branches (Le et al., 2006). Unfortunately, these methods can be very sensitive to small changes in shape (such as the error produced by discretization) making it difficult to robustly quantify the geometric features of cells.

Here we use a method based on the convex hull (Wu et al., 2016), the smallest convex shape containing the cell (think of a rubber band surrounding the cell). We define cell *lobeyness* as the perimeter of the cell divided by the perimeter of its convex hull (Fig. 5.3C, white and red, respectively). The higher this value, the more lobed the cell is expected to be. The ratio of the cell's convex hull area to that of the cell is another possibility, however we found that for important special cases, such as worm-shaped or boomerang-shaped cells, using the area may produce high ratios even when cells do not have significant lobes.

5.3. A mechanistic model for puzzle shape emergence

In section 5.1 I hypothesized that due to a growth-restricting mechanism shaping the cells, the plant would make long, thin cells upon anisotropic growth and puzzle cells upon isotropic growth. We decided to check the plausibility of this hypothesis by creating a computational model of growing cells, which would account for this restriction (keeping LEC low), to see if the resulting shapes match our predictions.

A dynamic simulation model of puzzle cell patterning based on the idea that cells can respond to mechanical signals generated by cell geometry was created. The basic principle behind the model is that as cells grow, stresses gradually increase, and when they reach a threshold level the cell wall is reinforced to resist these stresses. The biological justification for this idea is that cortical microtubules orient along the maximal direction of tensile stresses (Hamant et al., 2008; Hejnowicz et al., 2000) and then guide the deposition of cellulose microfibrils (Green, 1962; Paredez et al., 2006). Therefore, growth happens mostly in the direction perpendicular to these reinforcements (Suslov and Verbelen, 2006).

Cells are represented as polygons (Fig. 5.4A), with wall segments between nodes acting like linear springs (Prusinkiewicz and Lindenmayer, 2012), and nodes having resistance to bending between adjoining segments (Matthews, 2002). A simulation step consists of 3 phases (Fig. 5.4B,C). During the first phase, springs are inserted across cells in addition to those defining the cell polygon. These additional springs account for the presence of oriented cell wall stiffening components, such as cellulose microfibrils whose deposition is guided by cortical microtubules (Paredez et al., 2006) that are thought to respond to stress

(Hamant et al., 2008; Hejnowicz et al., 2000). These connections across the cells introduce growth restrictions into the model and are placed according to two criteria. First, these springs connect each node to the closest node across the cell falling within a given angle from the normals of the two nodes. Second, connections are inhibited if the the cell wall is convex. In the second phase, growth is simulated by displacing the wall segments, based on the specified tissue growth (e.g. isotropically or anisotropically), and relaxing cell wall springs. The connections across the cells do not grow. In the third and final phase, a new resting state is found by updating cell shapes to achieve mechanical equilibrium. The next simulation step commences by reassigning microtubule/cellulose connections based on the new cell shape and updating the rest length of cell wall segments.

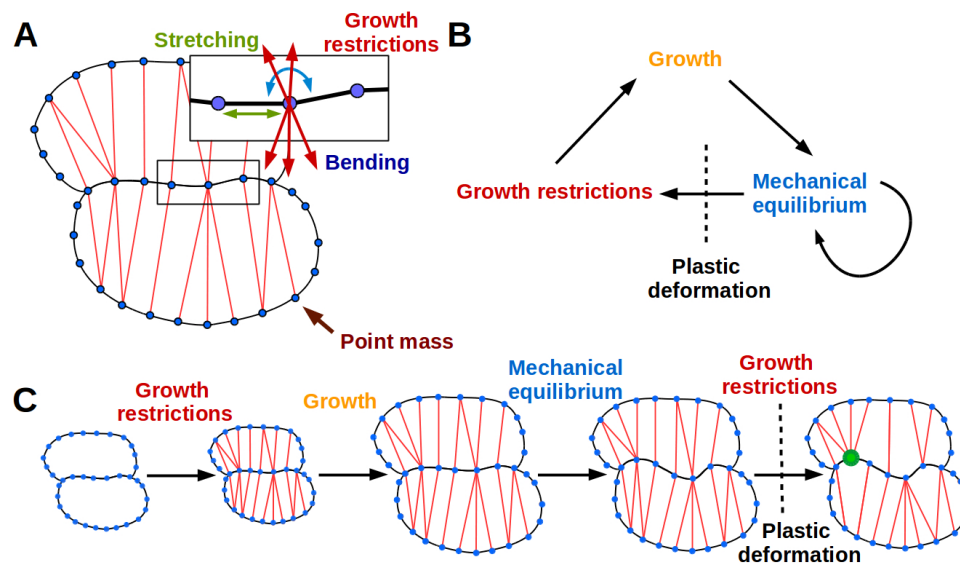


Figure 5.4. The 2D puzzle cell model. (A) Mechanical representation of cells. Cell walls are discretized into a sequence of point masses (blue circles) connected by linear wall-segments (black lines). Growth restricting connections (red lines) join point masses across the cell. The forces acting on the point mass are produced by stretching of wall segments and growth restricting connections as well as bending of the cell wall at the mass. (B-C) The simulation loop consists of 3 steps (B), as depicted for a diagrammatic example in (C). Step 1: additional transversal springs (red) are added to the model to represent oriented cell wall stiffening components guided by microtubules connecting opposing sides of the cell. They act like one-sided springs in that they exert a force when under tension (i.e. stretched beyond their rest length) but are inactive when compressed. This is consistent with the high tensile strength of cellulose. Step 2: the tissue is scaled to simulate growth, which can have a preferred direction (i.e. is anisotropic). Step 3: the network of springs reaches mechanical equilibrium. Transversal springs restrict cell expansion in width, causing cell walls to bend. Before the next iteration, wall springs are relaxed and transversal springs are rearranged to

reflect the new shape of cells. Cell shapes emerging in the model are determined by the nature of the assumed tissue growth direction. Note that in (C) the deformation of the cell causes the placement of growth restrictions to change during the subsequent iteration, where the green mass at the lobe tip attracts more connections on the convex side and loses connections on the concave side. Adapted from (Sapala et al., 2018).

Cell geometry at one growth step feeds back on growth in the next steps. This is achieved through conditions for the placement of the growth restricting connections. Connections are prevented in concave regions (lobes) and attracted in regions where opposite walls of the same cell are close to each other (indentations). Thereby, when a small lobe is created, it will be enhanced in the following simulation steps. Using simulations on idealized cell templates, we tested whether these principles are sufficient to generate different cell shapes, depending on the anisotropy of tissue growth. The emerging cell shapes primarily arise from the growth direction imposed at the tissue level that is locally modulated by stress-based growth restriction.

If tissue growth is isotropic, cells quickly approach their target LEC, and connections representing the cellulose and microtubules begin to stretch. Lobes emerge as the indentations (concave regions) attract more connections and protrusions (convex regions) lose connections, creating shapes similar to ones which I observed in the *Arabidopsis* leaf blade (Fig. 5.5A,D).

If the simulation is performed with anisotropic growth, the cellulose-microtubule connections are never stretched significantly beyond the LEC, and cells simply elongate, and lobes do not emerge, as I observed in the *Arabidopsis thaliana* petiole (Fig. 5.5B,E). In other words, stress-based activation of connections induces indentations, coinciding with locations of ROP6 activity, which necessarily generate incipient lobes in adjacent portions of the cell-wall where ROP2 is localized, accentuating their outgrowth. Thus, although phrased in geometric terms, our model is consistent with both the antagonistic local molecular interactions of ROP2-ROP6 and the stress-based feedbacks proposed by Sampathkumar (2014).

If the growth specified has a gradient of anisotropy at tissue scale, a gradient of cell shapes from elongated to lobed is produced. Similar gradients in cell shape are seen in *Arabidopsis* leaves, where elongated cells cover the anisotropically growing midrib, whereas lobed cells adorn the adjacent isotropically growing leaf blade (Fig. 5.5C).

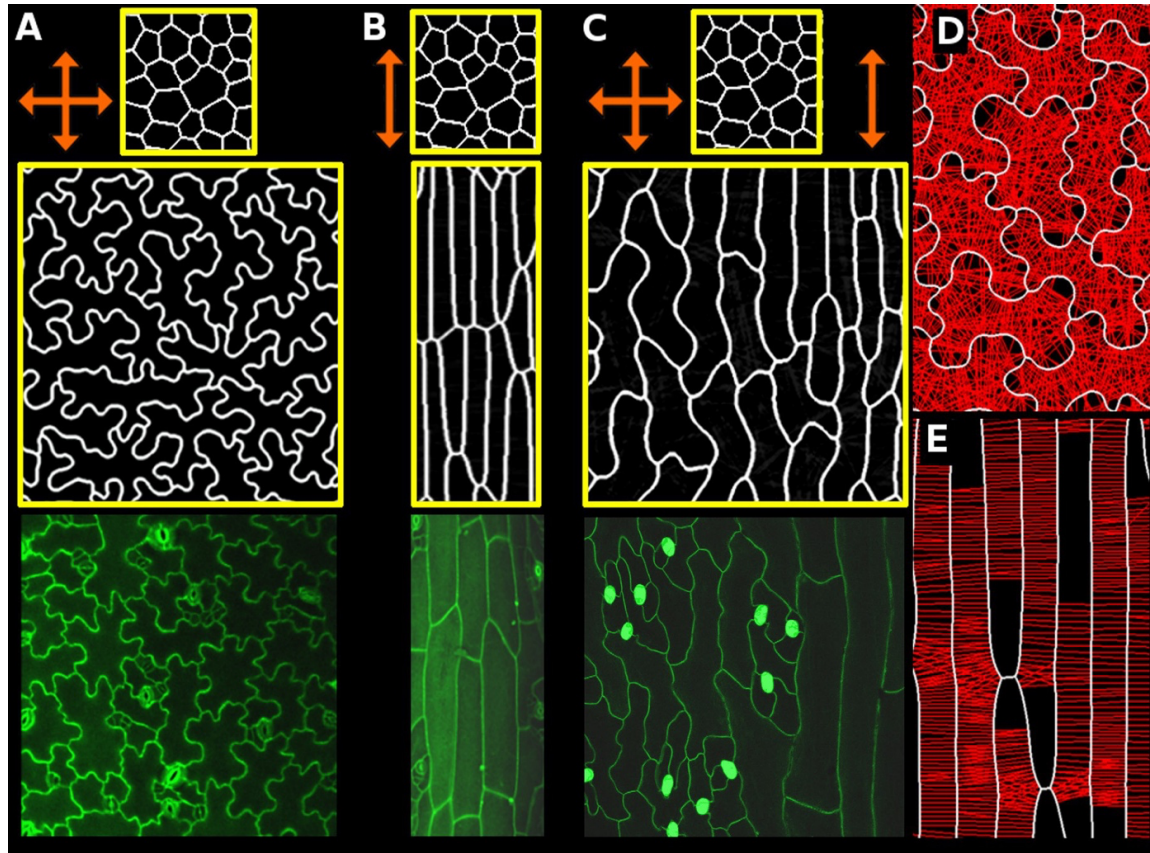


Figure 5.5. Geometric-mechanical model of puzzle cell emergence. (A) Starting with meristematic-like cells (top), growing the tissue isotropically, i.e. equally in all directions (arrows), produces puzzle-shaped cells (middle) that resemble cotyledon epidermal cells (bottom). (B) Growing the tissue frame primarily in one direction (anisotropically) results in elongated cells (middle) as observed, for example, in the petiole (bottom). (C) A gradient of growth anisotropy (increasing left to right) produces a spatial gradient of cell shapes (middle), as observed between the blade and midrib of a leaf (bottom). (D-E) Connections of transversal springs (red) restricting growth in each simulation step in tissues with isotropic (D) and anisotropic (E) growth. To make connections more apparent, only 50% are visualized. Adapted from (Sapala et al., 2018)

To validate the model, we confirmed in a FEM analysis that limiting the size of the LEC by creating lobes during growth reduces the cellular stress (Fig. 5.6). The model thus

illustrates how a mechanism actively limiting the mechanical stress of cells by restricting large open areas (LECs), including feedback coming from cell geometry, can lead to the formation of puzzle-shape cells in the context of isotropic growth.

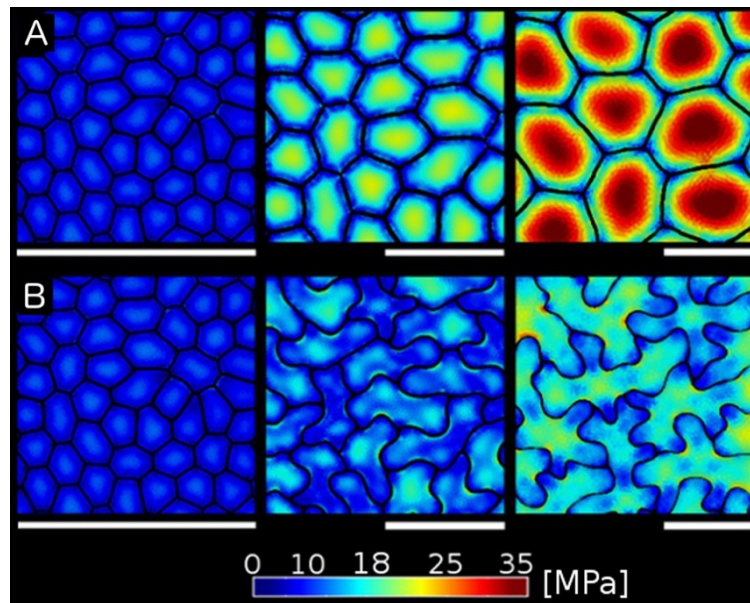


Figure 5.6. Stresses in modeled cell shapes. Cell outlines from 2D models with isotropic growth were used to generate 3D templates for FEM models (growth progresses from left to right, scale bars: 80 μm). (A) As the tissue grows, cells lacking transversal springs conserve their original shape. In pressurized cells, mechanical stress increases with the cell size. (B) When transversal springs are added, tissue expansion generates lobed cells. Color scale: trace of Cauchy stress tensor in MPa. Adapted from (Sapala et al., 2018).

5.4. Isotropic tissue growth is correlated with puzzle-shaped cell formation

Our model predicts that puzzle cells should appear when cells stop dividing and tissue growth is primarily isotropic. To test this prediction experimentally, I performed time-lapse confocal imaging on cotyledons ($n=3$ time-lapse series), which have a blade of roughly isodiametric shape, growing from 2 to 6 days after germination (DAG). Epidermal cells of *Arabidopsis thaliana* cotyledons begin to acquire a puzzle-shaped morphology roughly 2 DAG, whereas the organ achieves its characteristic round shape at approximately 3 DAG, long before reaching its final size (Zhang et al., 2011). I used MorphoGraphX (Barbier de Reuille et al., 2015) to extract growth rates and directions, and these results confirm that

the overall growth of cotyledon is isotropic as suggested by its round shape (Fig. 5.7A). To examine the correlation between growth anisotropy and lobeyness I pooled the data from the final time-point of our time-lapse series. I then extracted the largest 100 cells from this set (i.e. those most likely to be affected by the stress-minimizing mechanism) and found a significant correlation between growth anisotropy and lobeyness (Pearson correlation coefficient $r = -0.46$, $p = 0.6 \times 10^{-6}$). This supports my hypothesis that growth anisotropy and lobeyness are inversely related in the isotropically growing cotyledons of *Arabidopsis thaliana* (Fig. 5.7A).

In contrast to cotyledons, the *Arabidopsis thaliana* sepal is an elongated organ with epidermal cells that are either small and relatively isodiametric in shape, or large and elongated. Sepals initiate from a band of cells in the floral meristem (Fig. 3.7), undergoing strongly anisotropic growth (Hervieux et al., 2016) which produces giant cells that are far less lobed than those of the cotyledon (Fig. 3.5B, Fig. 3.6). Thus, growth isotropy and final organ shape correlate with lobeyness in these two organs.

Next, I examined a case where genetic modifications changed growth anisotropy and overall organ shape. This can be seen in plants overexpressing the *LONGIFOLIA1* (*TRM2*) gene. It causes an elongated cell and organ phenotype in *A. thaliana* cotyledons and leaves (Drevensek et al., 2012; Lee et al., 2006), consistent with effects of a related protein in rice grains (Wang et al., 2015). I created transgenic plants where *LNG1* is overexpressed under the *35S* promoter (*p35S::LNG1*). My T₁ lines had phenotypes ranging from highly elongated cotyledons and leaves to wild type (Fig. 5.7C-E). Plants with the elongated phenotype grew more anisotropically than wild type and had epidermal cells with reduced lobeyness ($n=3$ time-lapse series for each genotype, Fig. 5.7A-B and F-I). Thus, the change in growth and organ shape from isodiametric to elongated correlated with a decrease in cell lobeyness.

To further test the generality of the correlation between organ shape and cell shape, I examined fruit epidermal cells in a sample of 21 species from the Brassicaceae family (full dataset shown in Hofhuis and Hay, 2017). These fruit pods were either elongated siliques or short, rounded silicles and we only observed puzzle-shaped cells in silicles, not in

siliques (Fig. 5.7J, K). This strict correspondence between fruit shape and puzzle-shaped epidermal cells fits the prediction of our model that puzzle shapes are required to allow cells to enlarge in isotropically growing tissues, but are not required in elongated organs.

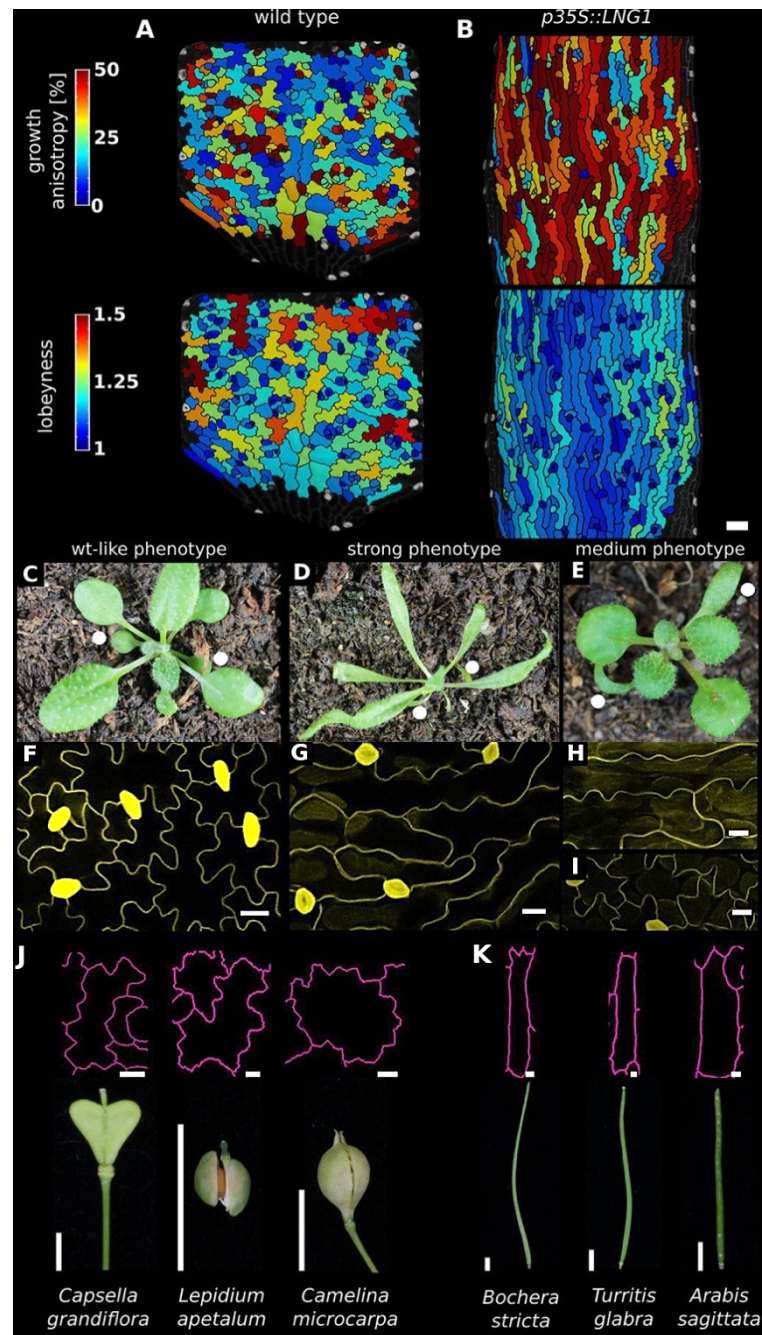


Figure 5.7. Correlation between growth direction and shape on the cell and organ level. (A-B) Time-lapse confocal imaging. Pictures were taken every 48 hours and analyzed using MorphoGraphX. The last time point of each series is shown. Growth anisotropy between 2 and 6 days after germination (DAG), calculated as the expansion rate in the direction of maximal growth divided by expansion rate in the direction of minimal growth, and cell lobeyness in wildtype (A) and *p35S::LNG1* (B) cotyledons. The *p35S::LNG1* cotyledon displays more anisotropic growth and less lobed epidermal cells. Scale bars: 50 μm. (C-E) *p35S::LNG1* T₁ plants with wild type-like phenotype (C, 61/98 plants), strong phenotype with dramatically elongated cotyledons and leaves (D, 16/98 plants) and intermediate phenotype with elongated cotyledons (Hofhuis et al., 2016) but wt-like leaves (E, 12/98 plants). Cotyledons are marked by white dots.

The remaining 9 obtained plants displayed elongated cotyledons and mildly elongated leaves (not shown). (F-I) Confocal images of epidermal cells. Scale bars: 20 μm . (F) shows cells from a leaf in (C), (G) shows cells from a leaf in (D), (H) shows cells from a cotyledon in (E), and (I) shows cells from a leaf in (E). (J-K) Epidermal cell outlines from fruit with more isotropic shapes (silicles, J) and more anisotropic shapes (siliques, K). Fruit images reproduced from (Hofhuis et al., 2016). Cell outlines reproduced from (Hofhuis and Hay, 2017). Scale bars: 10 μm for cell outlines, 1 mm for fruit. Adapted from (Sapala et al., 2018).

5.5. Lobeyness allows cells to increase their size while avoiding excessive stress

I have been able to experimentally prove a correlation between growth anisotropy and cell shape. Puzzle cells are formed upon isotropic growth and long, thin cells are formed upon anisotropic growth. These observations strongly resemble the results of our model in which cells are subject to local growth restrictions preventing LEC from becoming too high.

Next, I wanted to check if there really is a mechanism controlling LEC. If such mechanism was not present in the cells, the ratio between cell size and LEC size would be linear independently of cell size. This scenario would be observed if cells were circles or squares, not changing their shape while growing, or if cells were creating lobes in an uncoordinated manner. If, instead, there was a mechanism controlling LEC (and thereby stress on the cell wall), there should be a target threshold LEC which a cell would not exceed while growing (Fig. 5.8).

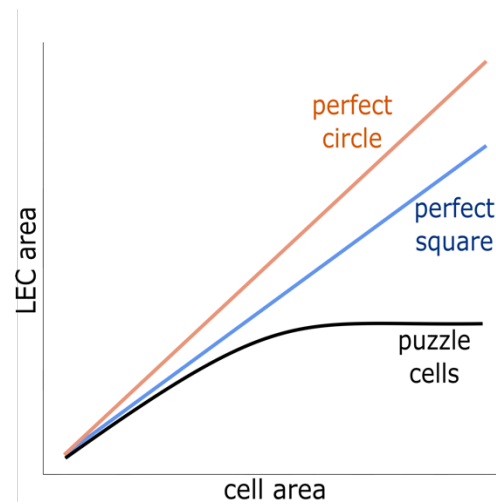


Figure 5.8. The predicted relationship between cell size and LEC size. If there was no stress controlling mechanism, growing cells would be perfect circles (orange) or perfect squares (blue), and the ratio of LEC area and cell area would always be linear. If there was a stress controlling mechanism *via* creating puzzle shapes (black), the LEC area would plateau after reaching a threshold value and cell area would increase without increasing LEC size.

In order to assess whether or not the stress minimization is present in real epidermal cells, it is necessary to compare cells of different shapes. Therefore, I used transgenic lines overexpressing two different IQD (IQ67-domain) proteins under 35S promoter. This family of proteins has been reported to interact with calmodulin in different cellular compartments. They are platform proteins that integrate calmodulin-dependent calcium signaling for multiple purposes (Bürstenbinder et al., 2017; Mitra et al., 2018). I imaged mature leaves of *p35S::IQD16* and *p35S::IQD8* which had long, thin cells and isotropic, non-lobed cells, respectively, and compared their geometric properties to Col-0 wild type leaves (Fig. 5.9). Then, I segmented cells from each genotype (7-9 plants per genotype) using MorphoGraphX and quantified their lobeyness, aspect ratio, cell area and LEC area. For the statistical comparison I decided to use only the largest cells in the datasets (over 10000 μm^2), under the assumption that this mechanism is only necessary for large cells. In small cells, cell wall stress is likely too low to trigger the potential minimization mechanism (Fig. 5.8).

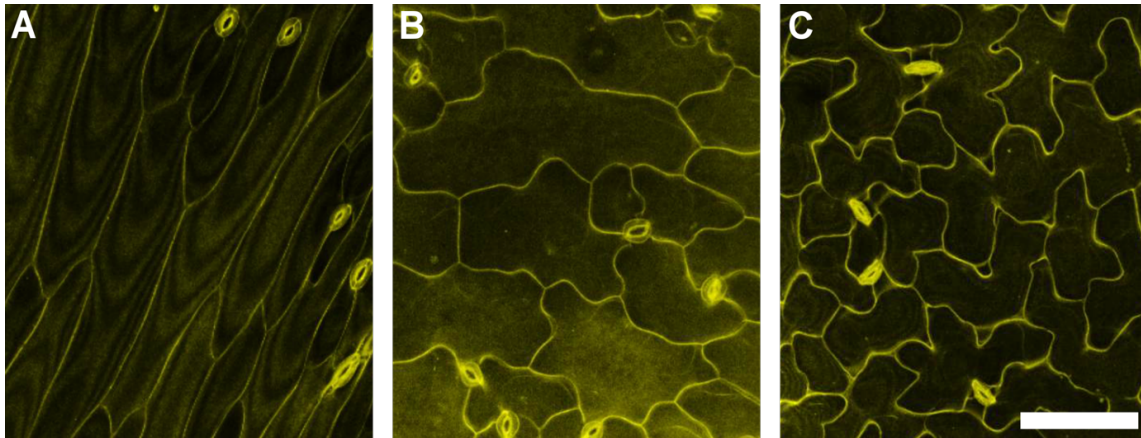


Figure 5.9. Different epidermal cell shapes in adult leaves of transgenic lines (Bürstenbinder et al., 2017). (A) Long, thin cells of *p35S::IQD16*. (B) Non-lobed, isotropic cells of *p35S::IQD8*. (C) Puzzle-shaped cells of wild type.

The cells of *p35S::IQD16*, *p35S::IQD8* and wild type display a statistically significant increase in lobeyness, which can also be observed qualitatively (Fig. 5.9, Fig. 5.10A). The cell aspect ratio (the ratio of length to width) is significantly higher for *p35S::IQD16* than for *p35S::IQD8* and wild type, while there is no statistically significant difference between the latter two genotypes (Fig. 5.10B). Therefore, the cell shapes of *p35S::IQD8* and wild type can be considered isotropic, at least relatively compared to IQD16 for the purpose of this study.

I detected no statistically significant difference in cell area between these three genotypes (Fig. 5.10C). The isotropically shaped, but non-lobed cells of *p35S::IQD8* displayed higher LEC area than the long, thin cells of *p35S::IQD16* and puzzle-shaped cells of wild type (Fig. 5.10D). This is an indication that LEC control is disrupted in *p35S::IQD8* cells together with impaired ability to create lobes.

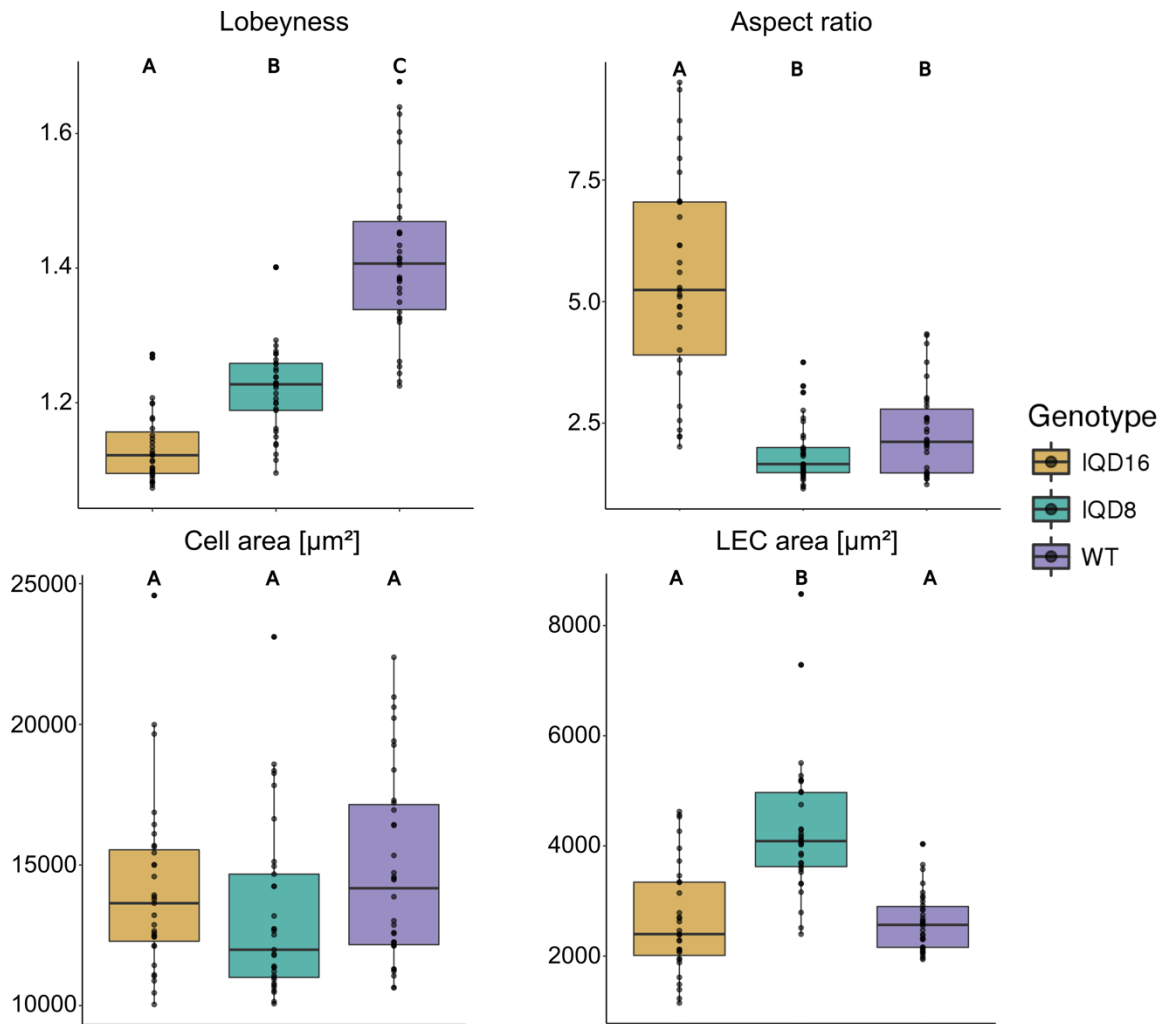


Figure 5.10. Geometric features of cell populations. Only cells of area above $10000 \mu\text{m}^2$ were analyzed (IQD16: $n=31$ cells pooled from 9 plants; IQD8: $n=33$ cells pooled from 7 plants; WT: $n=34$ cells pooled from 8 plants, $p\text{-value} \leq 0.05$).

In summary, these results indicate that in the case of isotropically shaped cells which make fewer lobes ($p35S::IQD8$), LEC size (or, indirectly, mechanical stress) is elevated. This means that the presence of lobes and indentations in the puzzle-shaped cells of wild type leaves, or the highly elongated shape of cells in $p35S::IQD16$ leaves, is very likely to follow the theoretical stress control mechanism in which at some point of cell expansion a target LEC is achieved (Fig. 5.8).

Distribution of cell size and LEC size for the whole cell population confirms that wild type and $p35S::IQD16$ follow my theoretical mechanism while $p35S::IQD8$ does not (Fig.

5.11). These results, taken together, strongly suggest that plant cells indeed have an active tendency to avoid too high stress on the cell wall. In this scenario, two ways of doing it are:

1. creating long, thin cells for anisotropic structures or
2. creating lobes and indentations (puzzle shapes) for isotropic structures.

If the mechanism of lobe creation is disrupted, the isotropic shapes that are created have higher stresses on the cell wall due to the fact that their LEC values is higher, as is the case for *p35S::IQD8*.

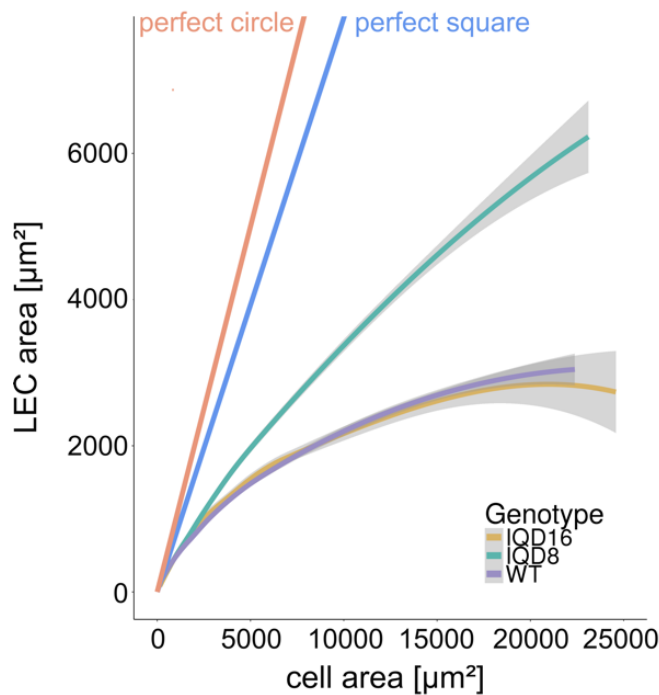


Figure 5. 11. Distribution of LEC area vs. cell area for all cells. Local polynomial regression fitting was performed for 3 studied genotypes (*p35S::IQD16*, *p35S::IQD8* and WT). The grey ribbon corresponds to 95% confidence interval (IQD16: n=564 cells pooled from 9 plants; IQD8: n=799 cells pooled from 7 plants; WT: n=745 cells pooled from 8 plants. 'Perfect circle' and 'perfect square' are hypothetical distributions (see Fig. 5.7).

A natural question to ask is: if in *p35S::IQD8* cells the stress management mechanism is disrupted, how do these plants manage to create cells and tissues that are fully functional (although the leaves are smaller than in wild type)? In this case, it cannot be excluded that the high stress on the cell wall is offset by the thickness or subcellular composition of the

cell wall. This means that in a larger time frame the plant might find an alternative way of managing stress, even if it is not the most convenient one. However, in the next section I am going to present a case in which a pharmacologically induced rapid, isotropic cell expansion might lead to bursting of the periclinal cell wall due to too high mechanical stress.

5.6. Experimental evidence that stress needs to be managed

Our model and experiments show that a mechanism, likely cortical microtubule-dependent, generates puzzle shapes to limit stress in large cells when tissue growth is isotropic. It is commonly observed that the periclinal cell walls slightly bulge out in healthy, turgid cells. However, if stress is indeed a developmental constraint, then when cells grow isotropically without this mechanism, they should bulge excessively, reach their rupture point and burst. The shoot apex of *Arabidopsis thaliana* grows isotropically in areas without lateral organs (Kierzkowski et al., 2012; Kwiatkowska and Dumais, 2003), with the cells presumably managing their mechanical stress by employing cell division to remain small. In plants grown with auxin transport inhibitor 1-N-naphtylphtalamic acid (NPA), the shoot apex is unable to produce lateral organs, and is uniformly covered in small rapidly dividing cells of isodiametric shape (Reinhardt et al., 2000). Treating these meristems with oryzalin, a chemical compound that depolymerizes cortical microtubules, blocks cell division and anisotropic growth restriction, preventing the formation of puzzle shapes. It has been shown in *Arabidopsis thaliana* hypocotyls that oryzalin treatment changes the trajectory of cellulose microfibril-producing molecules (CESA), as there is no organized cortical microtubule array to follow, but does not appear to change the rate of cellulose production (Chan et al., 2010). As such, although oryzalin makes cell walls isotropic by preventing the directionally organized deposition of cellulose, it does not necessarily reduce the overall deposition of cellulose, although this cannot be precluded. Cells of shoot apices in these conditions do not divide, but continue to grow developing large, isodiametric shapes that tend to balloon out (Corson et al., 2009; Hamant et al., 2008).

After treating naked meristems of NPA-grown seedlings with oryzalin (5 biological replicates), 20 displayed full microtubule depolymerization following oryzalin treatment (as assessed by the absence of cell division). In those 20 samples, we could see cell bursting

in the latest time points of 13 samples, out of which 10 displayed bursting cells were located in the flank of the meristem, where cell size increased substantially (Fig. 5.12). Although it cannot be completely excluded that these lateral cells, under these experimental conditions, have different wall properties, the most parsimonious explanation is that their cell walls could not withstand the increasing mechanical stress induced by the isotropic expansion. This provides direct experimental support for the proposition that large isodiametrically shaped cells are not viable due to the high stresses on their walls.

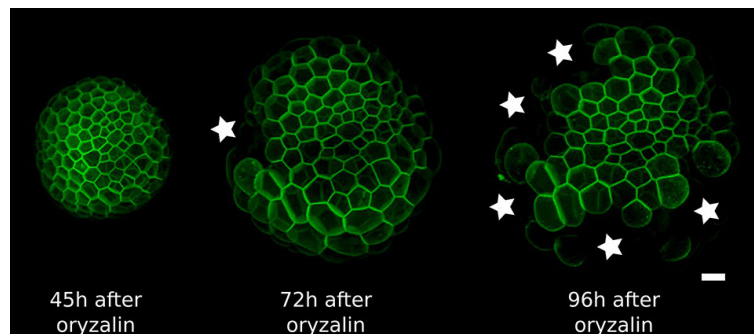


Figure 5.12. Depolymerization of cortical microtubules by oryzalin treatment causes cells of NPA-treated meristems to expand without division, ultimately leading to the rupture of the cell wall due to increased mechanical stress. Regions where cells have ruptured (white stars) are primarily located on the flanks of the meristems, where cells are larger. Scale bar: 20 μm . Adapted from (Sapala et al., 2018).

5.7. Cell shape and size across species

Our data indicates that the stress control mechanism we propose is conserved between various organs in *A. thaliana*, and within the fruit of Brassicaceae (Fig. 5.7J, K). This raises the question as to how broadly this mechanism is conserved, with large cell size and isotropic growth correlating with puzzle-shaped cells. Under this assumption, two geometric strategies are possible for cell expansion in isotropically growing organs without requiring excessively thick walls: (1) keeping cell size small by frequent divisions or (2) creating larger, puzzle-shaped cells. We measured cell area, LEC area and lobeyness in the adaxial epidermis of 19 unrelated plant species including trees, shrubs and herbs. A statistical analysis revealed that there was a positive correlation between cell size and lobeyness for each species (Fig. 5.13, Fig. 5.14A,B). Species with the largest average lobeyness also tended to have the largest cells (and vice-versa, Fig. 5.13). For average

values of lobeyness and cell area of each species (including sample size). Pearson correlation coefficients ranged from 0.23 for *Catharantus roseus* to 0.94 for *Solanum nigrum* (Fig. 5.8B). When pooling cells of all species together, the Pearson correlation coefficient was 0.64. Lobe formation is therefore more likely to be observed in big cells rather than small cells, which is intuitive if one considers cell division (where cell size remains low) as an alternative strategy to limit LEC size and cell wall stress. This suggests our hypothesis, that plants create puzzle-shaped cells in order to reduce stress in large isotropically growing cells, may be conserved among many plant species.

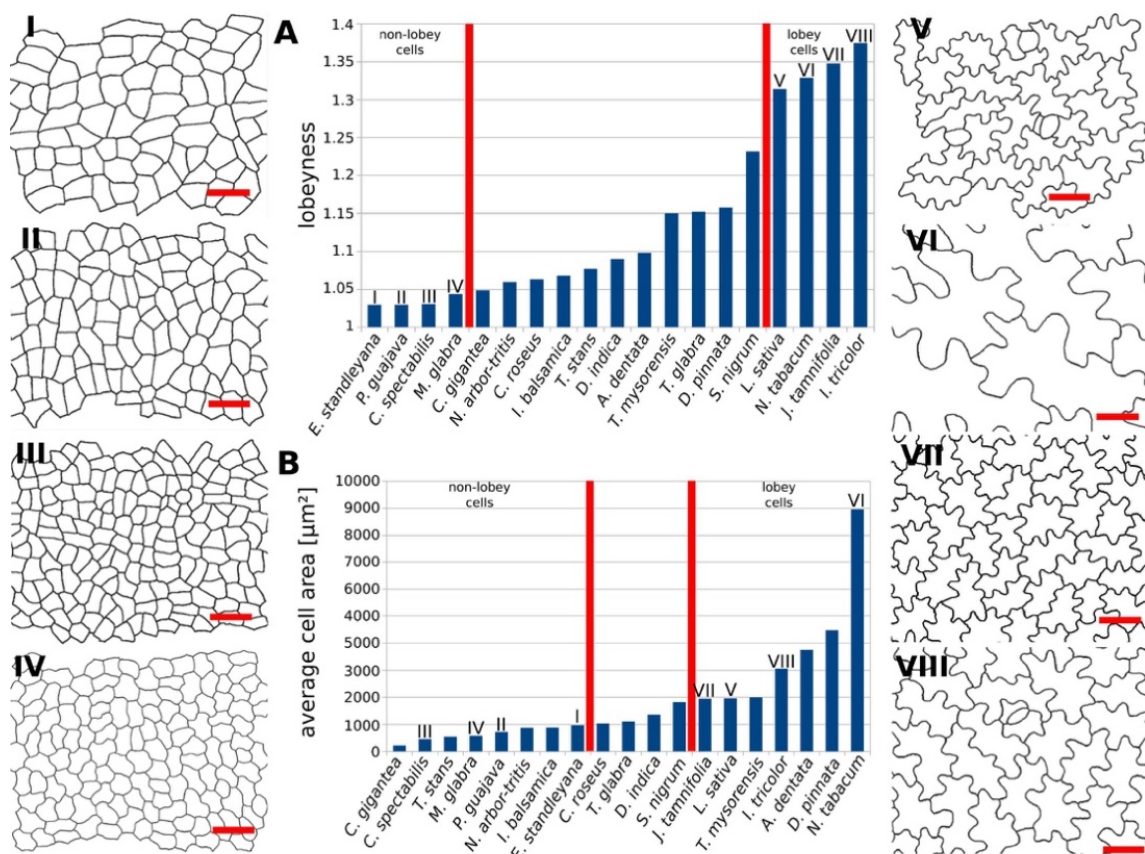


Figure 5.13. Multi-species cell shape analysis. (A) Average cell lobeyness. (B) Average cell area. (I-VIII)

Pictures of leaf epidermal cells of species corresponding to numbering in (A) and (B), numbered by the order of appearance in (A). Scale bars, 50 μm . Adapted from (Sapala et al., 2018).

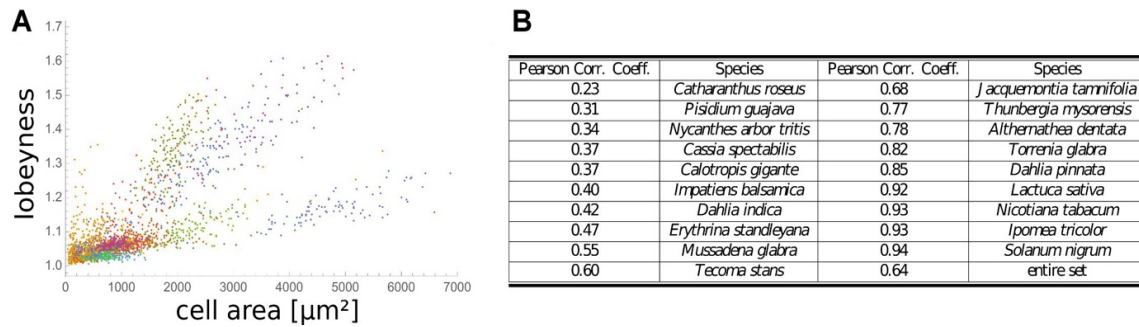


Figure 5.14 Correlation of lobeyness and cell area. (A) A plot of lobeyness vs. area for cells of all species pooled together. Each color symbolizes one species. (B) Pearson correlation coefficients between lobeyness and cell area for each species and for all cells pooled together (entire set). Note that in all cases a positive correlation between lobeyness and cell area is observed (correlation coefficient is greater than 0).

Adapted from (Sapala et al., 2018).

5.8 Summary of the results

In this chapter I have explored the phenomenon of jigsaw puzzle-like shapes being created in the epidermis of leaves and cotyledons of many plant species, including the model species *Arabidopsis thaliana*. In the past there have been a few hypotheses as to why these shapes are created. Some of them involved correct spacing of stomata and thereby optimizing transpiration (Glover, 2000) or providing mechanical integrity to the epidermis (Glover, 2000; Jacques and Vissenberg, 2014; Sotiriou et al., 2018). The creation of these shapes has been attributed to a co-repression network of proteins distributed along the cell walls which form interchangeable zones of growth repression and enhancement (Fu et al., 2002, 2005, 2009; Lin et al., 2013; Xu et al., 2010).

Here I propose an alternative scenario, in which the puzzle cells are created based on a growth-restricting mechanical feedback in order to minimize mechanical stress exerted on the periclinal cell walls by the turgor pressure coming from inside the cell (Sapala et al., 2018).

Finite Element Method simulations on tissue templates coming from original microscopy data revealed that walls of puzzle-shaped cells are under much less mechanical stress than walls of cells which have similar area but are shaped like polygons. This implied that cells

might have an active mechanism of minimizing this stress, approximated by the largest empty circle that can fit inside a cell (LEC). A 2D growing mass-spring model of cell development predicted that indeed, if a few subcellular growth-restricting assumptions are introduced, isotropic tissue growth will result in puzzle cell shapes, while anisotropic cell growth will result in long, thin cells. In order to examine cell shape in more detail, we established a simple but reliable cell shape measure called lobeyness (perimeter of the cell divided by the perimeter of its convex hull).

I demonstrated that the growth restriction-based model reproduces cell shapes observable in mature leaves of *Arabidopsis thaliana*. Moreover, when the tissue growth direction is altered due to genetic manipulations (for example anisotropically growing cotyledons and leaves of *p35S::LNG1*), the cell shape follows according to the predictions of our LEC-limiting computational model.

In order to check if plant epidermal cells really have an active LEC-minimizing mechanism, I used transgenic lines overexpressing proteins from the IQD family which have altered cell shapes (anisotropic *p35S::IQD16* and isotropic *p35S::IQD8*). I quantified cell size and shape in lines with long, thin cells as well as isotropic cells (less lobey than wild type) and compared them with the intricate puzzle shapes of wild type leaves. Firstly, I observed that large, isotropic cells that do not make lobes have larger LEC (proxy for mechanical stress). Secondly, by analyzing a broad distribution of cell sizes for these 3 cell shapes, I was able to demonstrate this stress-controlling mechanism in isotropic cells creating puzzle shapes as well as anisotropic cells. Taken together, this very strongly supports the hypothesis about cells actively minimizing cell wall stress, which, in turn, justifies my proposed hypothesis about the purpose of puzzle cells. Another piece of evidence is that pharmacological treatments on shoot apical meristems which stop cell division but not cell expansion showed that the isotropic meristematic cells can burst if they become too large and the cell wall cannot withstand high stress.

The cell shapes in the IDQ transgenic lines demonstrate features supporting my hypothesis, but this is a single, artificially enforced case. In order to validate this hypothesis on a more diverse dataset, I compared cell size and lobeyness in leaves of 19 different species of trees

and bushes, taking advantage of the wide range of final cell sizes among those species. It turned out that cells which ranked as averagely small tended to be non-lobey, while the relatively large cells were among the most lobey ones. This demonstrates that small cells, in which LEC must be low anyway, do not need to produce lobes, while the large ones do.

In this work I combined predictions of computational modeling with observations of real plants to propose a novel purpose for the intricate cell type that are the jigsaw puzzle-shaped pavement cells in leaf and cotyledon of epidermis (Sapala et al., 2018). So far, this has been the most elaborate explanation of the creation of these shapes because it explains the full spectrum of shape change and does not require any cell-cell signaling. While this molecular factor cannot be excluded, it most likely works upstream of the mechanical cues.

5.9. Materials and methods

5.9.1 FEM modelling of mechanical stress

FEM simulations were performed using 2D membrane elements embedded in 3D space. To access basic relations between cell shape and stress uniform, isotropic elastic properties were used for cell walls. All the cellular templates were pressurized to 0.5 MPa. The same parameters were used for all simulations: Young's modulus: 300 MPa, Poisson's ratio: 0.3, Cell wall thickness: 2 μm for walls shared between two cells (vertical walls), 1 μm for the remainder. The stress measures displayed in the main text figures are the sum of the principal in-plane Cauchy stresses (the out-of plane principal stress is zero by hypothesis). A detailed description of the FEM code implementation can be found in (Mosca et al., 2017).

5.9.2 2D mass-spring model of cell growth

Models of pavement cell morphogenesis were implemented in C++ using the VVe simulation framework (Smith et al., 2003). VVe provides a framework for simulating growing 2D cellular-tissues. Cell walls were represented as a series of point-masses connected by springs. Each point-mass stored its position, and each spring a length representing its unstressed or *rest length*. Masses and springs residing on the tissue boundary were marked, and constrained to move with the boundary as it grew, inducing tension throughout the cellular network. Additional springs, representing mechanical

constraints resulting from the deposition of cellulose and microtubules in response to stress, were dynamically introduced and updated during simulation. Parameter values for all simulations reported in the main text, as well as a detailed description of the model, are described in (Sapala et al., 2018).

5.9.3 Live imaging of cotyledons

I grew seedlings on 1/2 MS medium in long day conditions as previously described in (Vlad et al., 2014). I imaged young cotyledons (2-6 days after germination, DAG) using the Leica SP8 microscope with 20x (HCX APO, numerical aperture 0.8) and 40x (HCX APO, n.a. 0.5) long working distance, water immersion objectives. Col-0 and *p35S::LNG1* plants contained a plasma membrane-localized fluorescent marker *pUBQ10::myrYFP* previously described in (Hervieux et al., 2016) and I collected fluorescent signal from 519-550 nm emission spectrum using 514 nm laser for excitation.

5.9.4 Creating transgenic lines

The *LNG1* gene full-length CDS was PCR amplified and cloned into the pENTR/D-TOPO vector (Invitrogen) as described in the manual, using primer pair 5'-CACCATGTCGGCGAAGCTTTTGT ATA ACT-3' and 5'-GAACATAAGAAAGGGGTTTCAGAGA-3'. The resultant vector was LR recombined into the gateway vector pK7WG2 (Karimi et al., 2002) to generate the final construct *p35S::LNG1*. The intermediate and final constructs were verified by sequencing. I transformed the *p35S::LNG1* construct into Col-0 plants by *Agrobacterium*-mediated floral dipping. I sowed T₁ seeds on Kanamycin-containing medium and transferred them into soil approximately 2 weeks after germination.

5.9.5 Analysis of fruit and exocarp cell shape

Fruit shape was classified as an elongated silique or a silicle (if the length was less than three times the width of the fruit) for 21 species in the Brassicaceae family. Exocarp cells were stained with propidium iodide, imaged with a confocal laser scanning microscope (as described in section 'Live imaging of cotyledons') and cell outlines extracted using MorphoGraphX.

5.9.6 Imaging cell shapes in mature leaves of IQD lines

I grew seeds of Col-0 wild type, *p35S::IQD8* and *p35S::IQD16* in long day conditions until the plants were flowering. Then, I imaged epidermis of mature leaf 6 (7-9 plants per genotype) with the confocal laser scanning microscope (Leica SP8). I stained the cell walls with propidium iodide and collected fluorescent signal from 605-644 nm emission spectrum using 488 nm laser for excitation.

Next, I segmented the images in MorphoGraphX and calculated lobeyness, aspect ratio, cell area and LEC area for each cell in each sample. For the statistical analysis, I only considered cells larger than 10000 μm^2 since I expected the LEC-minimizing mechanism to occur only in relatively largest cells. I performed statistical analyses using R. I used the Shapiro-Wilk test to check if the data distributions were normal. For each compared feature the data was non-normally distributed, therefore I used Man-Whitney pairwise test to compare distributions for each genotype within each feature (lobeyness, cell aspect ratio, cell area, LEC area).

5.9.7 Pharmacological treatment

The *p35S::LTI6b-GFP Arabidopsis thaliana* lines have been described previously (Cutler et al., 2000) and were grown in tall petri dishes on a solid custom-made Duchefa “Arabidopsis” medium (DU0742.0025, Duchefa Biochemie) supplemented with 10 μM of NPA (N-(1-naphthyl) phthalamic acid) as described in Hamant et al. (2008). As soon as naked inflorescences had formed, the plants were transferred to a medium without inhibitor. First images (T=0h) were taken 1 day after the plants were taken off the drug. The samples were then immersed for 3h in 20 $\mu\text{g/ml}$ oryzalin at T0h, T24h and T48h, as described in Hamant et al. (2008). Images were acquired using a Leica SP8 confocal microscope. GFP excitation was performed using a 488 nm solid-state laser and fluorescence was detected at 495-535 nm.

5.9.8 Multi-species leaf cell shape analysis

Leaf surface impressions were taken from the adaxial side using transparent nail enamel (Revlon). The impressions were viewed under the differential interference contrast (DIC) mode of an Olympus BX52a upright microscope (Olympus, Japan) and imaged using a

CapturePro CCD camera (Jenoptik, Germany). I loaded the images into MorphoGraphX and projected cell outlines on a flat (2D) mesh. I segmented the mesh and calculated cell area, lobeyness and LEC radius for all segmented cells.

5.10. Acknowledgement

Portions of this chapter were published in:

Sapala, A., Runions, A., Routier-Kierzkowska, A.L., Gupta, M.D., Hong, L., Hofhuis, H., Verger, S., Mosca, G., Li, C.B., Hay, A., Hamant, O., Roeder, A.H.K., Tsiantis, M., Prusinkiewicz, P., Smith, R.S. (2018). Why plants make puzzle cells, and how their shape emerges. *eLife* 7:e32794.

Author contributions:

the framework for FEM simulations was created by Gabriella Mosca (University of Bern, Max Planck Institute for Plant Breeding Research). The FEM simulations on single cells were performed by Anne-Lise Routier-Kierzkowska (Max Planck Institute for Plant Breeding Research). The 2D mass-spring model was created by Adam Runions (Max Planck Institute for Plant Breeding Research). The *p35S::LNG1* plasmid was provided by Lilan Hong (Cornell University). The images of entire fruit and epidermal cells were provided by Hugo Hofhuis and Angela Hay (Max Planck Institute for Plant Breeding Research). The IQD lines were provided by Katharina Buerstenbinder (Leibniz Institute for Plant Biochemistry). The pharmacological treatment of meristems was performed by Stephane Verger and Olivier Hamant. The images of epidermal cells of multiple species (multi-species analysis) were collected by Mainak Das Gupta (Indian Institute of Science, Max Planck Institute for Plant Breeding Research). The calculation of the Pearson correlation coefficient for the multi-species analysis was done by Chun-Biu Li (Stockholm University). The rest of the experiments, image analysis and statistical analyses were performed by myself. Puzzle cell templates for FEM simulations were created based on confocal images created by myself.

6. Conclusion

6.1. Summary of the findings

- I related cell shapes to different growth regimes in the plant epidermis (Chapter 3).
- I showed a strong correlation between growth rates and elastic properties of the cell wall in the sepal epidermis. I then compared these results for wild type with a mutant of altered growth patterns (*fish4*, in which cells mature faster), thereby linking changes in cell wall mechanics with an organ growth phenotype (Chapter 4).
- My Cellular Force Microscopy experiments contributed to creating a continuum mechanics model of plant tissue micro-indentation, necessary for proper interpretation of the physical aspects of cell and tissue growth (Chapter 4).
- I managed to change the growth regime in young cotyledons and thereby validate the results of a dynamic tissue growth model which assumes that cell shape depends on local growth restrictions (Chapter 5).
- I proposed an evidence-based, novel function for the intricate jigsaw puzzle shapes appearing in the epidermis of many plant species: the minimization of mechanical stress on the cell wall, thereby optimizing resources necessary to withstand this stress (Chapter 5).

6.2. Discussion of research contributions

6.2.1. Mechanical properties of the cell wall reflect cellular growth rates in wild type and *ftsh4* sepals

One of the objectives of my thesis work was to validate a mechanical model of micro-indentation in plant tissue. Therefore, I performed two biomechanical experiments: Cellular Force Microscopy coupled with confocal microscopy and osmotic treatments. It required implementing the existing protocols for these two experiments in a new system – the sepal of *A. thaliana*. With this I obtained indirect measurements of turgor pressure and cell wall elasticity, respectively.

My experiments on wild type sepals were ones of the first addressing cell wall stiffness specifically in this organ. AFM data is also available, but it shows heterogeneity on subcellular scale rather than whole organ scale patterns of cell wall stiffness (Hong et al., 2016). For me, the latter was more interesting since I wanted to compare cell wall stiffness (inferred from the amount of shrinkage) with growth patterns of the sepal (presented in Chapter 3).

My results showed that the sepal (flower stage 8-9) was stiffer (expanded less under turgor pressure) in the upper part (between the tip and the middle) than in the lower part (between the middle and the bottom of the sepal). This observation is in line with the growth tracking results (Chapter 3), where I detected that at a corresponding developmental stage, the upper part of the sepal grows slower than the lower part of the sepal (Fig. 3.6A). The correlation of elevated growth and softening of the cell wall has been vaguely demonstrated in the shoot apical meristem (SAM) (Kierzkowski et al., 2012; Peaucelle et al., 2011; Pien et al., 2001). For instance, Kierzkowski et al. (2012) showed in the tomato SAM that the slow-growing apex of the meristem is stiffer than the fast-growing periphery zone (where leaf primordia are created). However, this cannot be considered a direct information about the cell wall. The authors claim that this difference might not only result from difference in cell wall properties but also from the amount of stretching the meristem zones are under due to its dome-like geometry (an elastic material has different abilities to expand in different ranges of stretching). Peaucelle et al. (2011) used AFM to find that pectin

demethylesterification makes the SAM cells more elastic, but they also claimed that it is triggered by inner tissues which, again, makes these finding more complicated than just measuring epidermal cell wall elasticity. Hayot et al. (2012) combined nanoindentations with FEM modeling to detect differences in viscoelastic properties of the cell wall between leaves of two natural accessions: *A. thaliana* Col-0 and Ws-2. However, they struggled to link these differences to any growth measurements, speculating more about the cell wall structure (and thereby thickness) as the reason for the differences between natural accessions. They also showed aberrations in viscoelasticity between Ws-2 and *atx1* mutant. ATX1 is a protein known to regulate over 80 genes encoding cell wall-related proteins (Ndamukong et al. 2009), and since there are cases when the same factor can have opposite effects on the cell wall stiffness (Chanliaud et al., 2004; Saladié et al., 2006), this case is too complex to make concrete conclusions. Therefore, although the studies mentioned above have attempted to demonstrate experimentally that fast-growing cells have softer cell wall, they have struggled to do it in a convincing way. The most direct experiment remains the one where creation of a new organ was recorded upon application of a wall-loosening enzyme expansin, although it was purely qualitative (Pien et al., 2001). In the light of this, my combination of detailed growth tracking and an estimation of cell wall elasticity in wild type sepal emerges as a straightforward and informative experiment.

Osmotic treatments helped decipher the role of ROS in cell maturation within the studies on *ftsh4* mutant in which cell maturation is faster and ROS levels are elevated compared to wild type (Hong et al., 2016). This is also reflected in stiffer cell walls (in *ftsh4* mutants cells were shrinking less than in wild type). These observations taken together allow for a speculation that ROS act as organ growth controlling factors in that they speed up cell maturation by stiffening the cell walls in a very local manner (Fry, 1998). Furthermore, it is a good example of a case when cell wall stiffness is connected to a growth phenotype – apart from having stiffer cell walls, the cells of this mutant also display lower and more variable growth rates as well as more isotropic shapes compared to wild type (Hong et al., 2016; Sapala et al., 2018). Finally, this study is a good demonstration of how the osmotic treatment can be used to help validate related biological hypotheses.

6.2.2. Cellular Force Microscopy coupled with confocal microscopy and computational modeling as a good method to measure turgor pressure *in vivo*

My CFM and osmotic treatment results on the sepal were also used to validate a reverse-engineering mechanical model of an indentation experiment (Mosca et al., 2017). The sepal has two kinds of cells (small cells and giant cells), and the CFM stiffness measurements (obtained by coupling the force measurement setup with a confocal microscope) showed different values for the two cell types. Stiffness was consistently higher for the giant cells than for the small cells. Since it is unlikely that these two cell types have different turgor pressure (they are connected by plasmodesmata, and pressure should equilibrate between connected vessels), this brought about the possibility that cell geometry influences the readout of CFM (and possibly also AFM) measurements (Bassel et al., 2014). Therefore, Finite Element Method (FEM) model of an indentation experiment was needed to address this issue.

The stiffness values (obtained with CFM) and cell wall elasticity values (obtained by osmotic treatments) were fed into the FEM model of plant tissue indentation. It showed that these differences in stiffness can be explained by different geometries of those cells (small cells are closer to cuboids and giant cells are much more elongated and bulged out). In other words, the stiffness readout alone is not sufficient to assess the turgor pressure. At a first glance the CFM result can lead to a conclusion that turgor pressure is different in those two cell types. However, computer simulations showed that even if small and giant cells have equal turgor pressure and cell wall elasticity, stiffness values obtained by indentation experiments can still be higher for giant cells. That being said, it is important to keep in mind that based on these simulations, neither cell wall stiffness differences nor turgor pressure differences can be completely ruled out.

Our model is in agreement with another model proposed by Beauzamy et al. (2015b), where they measured cell wall elasticity with AFM under different turgor pressure values (manipulated with osmotic treatments) and modeled cells as thin elastic shells (Vella et al.,

2012). Even though they used different methodologies both experimentally and computationally, their pressure values correlate with our FEM model. The most important difference between our model and the model of Beauzamy et al. is that our model works in the tissue context (as opposed to single cells modeled by Beauzamy et al.), which we show to be an important factor influencing stiffness values as well (Mosca et al., 2017).

It appears that the plant biomechanics community is still struggling to find an optimal framework for measuring cellular properties with indentation experiments (there are many different setups and mathematical models involved – as reviewed by Routier-Kierzkowska and Smith, 2013). Our results on the accountability of cell geometry on differences in stiffness readouts is therefore a benchmark that should be kept in mind while choosing data interpretation methods in the future. This type of work will hopefully help avoid misleading interpretation of these challenging experiments in the future.

6.2.3. The relationship between cell and organ shape

In Chapter 3 I measured cellular growth in two organs of different shapes: the round cotyledon and the elliptical sepal. While the cotyledon epidermis is comprised of isodiametric, puzzle-shaped cells, epidermal cells of the sepal are either small and square or long and thin. Genetic modifications are able to alter growth directions which changes the shape of epidermal cells as well as, in some cases, the overall shape of the organ. I demonstrated this on two different transgenic lines: *p35S::LNG1* and *p35S::IQD16*, where cotyledon epidermal cells change their shape from puzzle-like (wild type) to highly elongated and non-lobed (Chapter 5). I was able to show change in cellular growth direction (from isotropic to anisotropic) on one of those lines (*p35S::LNG1*). An opposite example in which cell growth direction changes from anisotropic to isotropic is more difficult to come by, but very slight differences can be detected for example in *rotundifolia3* mutant (Kim et al., 1998) or *fish4* mutant (Hong et al., 2016; Sapala et al., 2018).

On the other hand, there are cases in which a change in cell shape does not cause a change in organ shape or growth directions. For instance, the wild type sepal of *Arabidopsis thaliana* is considered to be an elliptical organ. Its epidermal cells are either square (small cells) or large but shaped like cylinders (giant cells). Using confocal microscopy and

MorphoGraphX I demonstrated that the growth of the wild type sepal is highly anisotropic. I also analyzed sepal growth of the *lgo* mutant which does not form giant cells, and therefore all its epidermal cells are isodiametric (square). However, growth anisotropy of the *lgo* sepal is very similar to wild type. In the *lgo* mutant, endoreduplication of the giant cells is impaired (Roeder et al., 2012) and therefore they undergo more rounds of divisions. If, in this case, growth directions are similar to the case where giant cells are present, it is very likely that there is a completely separate signal regulating the direction of cell (and thereby also organ) growth. In other words, this result speaks for the presence of a supra-cellular factor controlling cellular growth.

I also demonstrated that in the wild type sepal there is a wave of high growth which moves from the tip of the organ to its base throughout the development (Fig. 3.6). Interestingly, the giant cells are often straddled between the zones of fast and slow growth. This provokes the question about the nature of this global growth signal – is it a wave of gene expression, an extracellular factor (growth hormone) or a mechanical feedback resulting from tissue architecture? While there is some work supporting the plausibility of all those scenarios (Heisler et al., 2010; Hervieux et al., 2016; Jönsson et al., 2006; Smith et al., 2006; Vlad et al., 2014), the plant developmental biology community still struggles to precisely describe which of those factors (or a combination of factors) that drives growth. One also needs to consider a possibility that it is not a wave of growth enhancement moving from the tip to the base of the organ, but rather a wave of growth restriction moving from the base to the tip. In this scenario, tissue-level mechanical stress might cause the growth arrest (Hervieux et al., 2016). It will be interesting to observe future work on this subject trying to decipher the global nature of tissue growth.

6.2.4. Puzzle cells minimize mechanical stress on the cell wall

Jigsaw puzzle-shaped cells can be spotted within a large number of plant species. Because of that, and because of the fact that creating them probably requires high-level coordination, it is natural to wonder what their purpose is. A few hypotheses have been put forward in recent years. Some of them are related to providing physical strength to the leaf. For instance, Jacques and Vissenberg (2014) have proposed that the wavy, interlocking cell walls can increase the adhesion between cells, thereby making the epidermis more likely

to maintain its integrity. This idea is in line with material science studies (Lee, 2000). Similarly, Sotiriou et al. (2018) proposed that puzzle shapes allow the leaves to make large-scale deformations such as stretching or bending. Another possibility is that these irregular shapes play a role in the physiology of the plant, for instance by spreading stomata and trichomes (other types of epidermal cells) around the leaf (Glover, 2000) or helping the leaf remain flat and thereby optimizing light capture (Galletti and Ingram, 2015). Unfortunately, none of those hypotheses were properly tested experimentally. One reason for this may be that the mentioned processes (light capture, leaf bending, trichome spacing) are very complex and it is difficult to address them with a simple experiment. In addition, they would have to be coupled with computer models. Finally, not many genetic lines with convincing puzzle cell formation phenotypes are available (Bürstenbinder et al., 2017; Fu et al., 2002, 2005, 2009; Liang et al., 2018; Qiu et al., 2002). My study on the puzzle cell formation managed to address at least some of these concerns because it couples obvious phenotypes (long, thin cells or isotropic, non-lobey cells) with computer modeling of cell growth. The result of that (discussed below) is a simple, yet insightful and exhaustive explanation for the purpose of puzzle shapes of epidermal cells.

I propose that the puzzle shaped cells emerge from a mechanism that evolved to limit mechanical stress in tissues that grow isotropically, such as epidermis of leaves and cotyledons. The base for this observation is an FEM analysis of 3D pressurized cells of simple, polygonal shapes and puzzle shapes. When comparing two cells of the same surface area, the puzzle-shaped one will have much less mechanical stress on the cell wall than the polygonal one (Fig. 5.3). The feature that greatly elevates the stress is when a cell becomes large in two directions (i.e. creates a large open area). Based on this, I have introduced an indirect measure of cell wall stress that is the size of the largest empty circle that can fit inside a cell, also called LEC (Largest Empty Circle).

In stems, roots and siliques, growth is strongly anisotropic, and cells can simply elongate. This is, however, not possible for isodiametric organs such as broad leaves, cotyledons and silicle fruit pods (Fig. 5.7J, K). I propose that puzzle-shaped cells in the epidermis of more isodiametric plant organs provide a means to avoid large open areas in the cell and the high stresses that they induce. Since turgor pressure inside cells is high, minimizing mechanical

stress by shape regulation may be a way of reducing the resources required to reinforce the cell wall and at the same time maintaining its structural integrity during growth (Fig. 6.1).

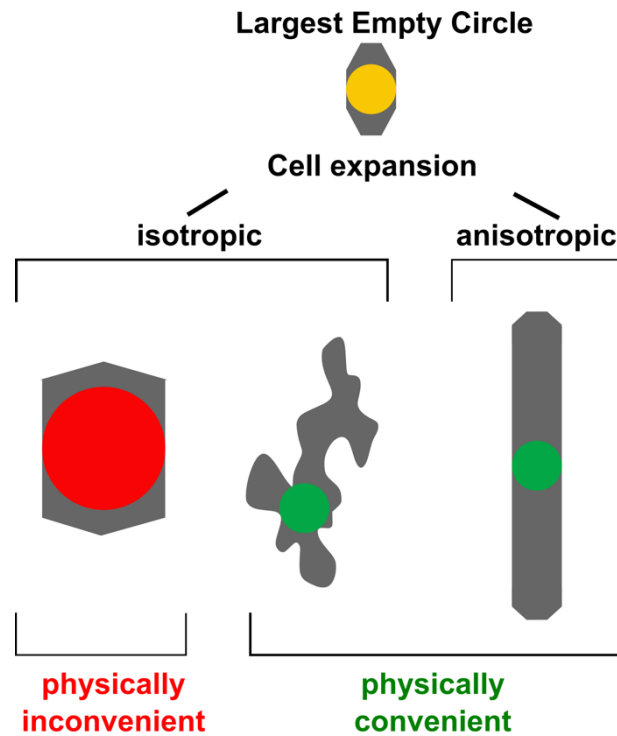


Figure 6.1. Cell shape as a means of minimizing mechanical stress on the cell wall. I use the size of the largest empty circle that can fit into a cell (LEC) as a proxy for mechanical stress on the cell wall. If a cell grows anisotropically into a long, thin shape, or if it grows isotropically into a puzzle shape, the stress is low (green). If a cell expands isotropically without adjusting its shape, stress on the cell wall increases drastically (red). Compare Fig. 5.2 and 5.3.

6.2.5. Local growth restrictions and curvature sensing reproduce puzzle cell shapes

My hypothesis regarding the role of puzzle cell shapes, although purely physical, does not preclude the existence of molecular factors facilitating the creation of these shapes. In fact, the processes underlying the formation of puzzle cells have been studied on the sub-cellular level. It has been proposed that they emerge from either the localized outgrowth of lobes (also called protrusions) (Fu et al., 2002; Mathur, 2006; Xu et al., 2010; Zhang et al., 2011), localized restriction of indentations (Fu et al., 2009; Lin et al., 2013; Sampathkumar et al.,

2014), or a combination of both (Abley et al., 2013; Armour et al., 2015; Fu et al., 2005; Higaki et al., 2016; Majda, 2017).

Specific members of the Rho GTPase of plants (ROP) family of proteins play a key role in shaping these cells. ROP2 and ROP6 mutually inhibit each other's accumulation at the plasma membrane, creating a co-repression network that divides the plasma membrane into alternating expression domains. ROP2 and ROP6 are thought to locally regulate growth by interacting with RIC4 and RIC1, respectively (Fig. 6.2). Disruptions in the ROP/RIC pathways lead to defects in puzzle cell formation (Fu et al., 2002, 2005, 2009; Lin et al., 2013; Xu et al., 2010).

Since a lobe in one cell must be matched by an indentation in its neighbor, some manner of extracellular communication is required. The plant hormone auxin has been proposed to act as this signal (Fu et al., 2005; Li et al., 2011; Xu et al., 2010, Fig. 6.2), although recent data call for a re-evaluation of this hypothesis (Belteton et al., 2017; Gao et al., 2015). In the light of these findings, the ‘supracellular’ regulator of puzzle cell formation remains unknown.

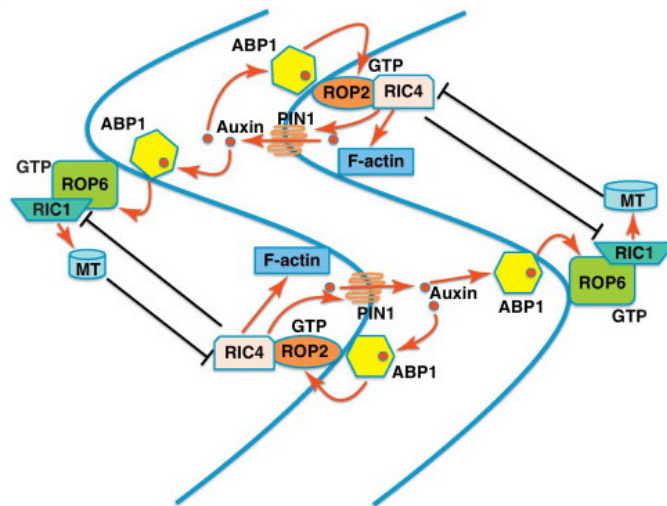


Figure 6.2. The proposed molecular network driving puzzle cell formation. ROP6 acts locally at an indentation by attracting growth restricting microtubules (MT) via RIC1. ROP2, in turn, acts locally in a protrusion by attracting growth enhancing actin filaments via RIC4. ROP6 and ROP2 locally exclude each other creating an interchanging localization pattern. These two proteins were proposed to be activated by auxin-dependent ABP1 and PIN1 (Xu et al., 2010), thereby introducing auxin as an extracellular signaling

factor regulating puzzle cell shape formation. However, with the function of ABP1 recently undermined (Belteton et al., 2017; Gao et al., 2015), it remains unclear whether an extracellular factor is involved and what it is. Adapted from (Craddock et al., 2012).

My hypothesis suggests that isotropic growth at the tissue level is a primary driver of puzzle cell shape. As a tissue grows, the stress increases and microtubules align to direct cellulose deposition to resist the stress (Hejnowicz et al., 2000). This causes small indentations in the cell, which transfers more stress to them, further recruiting microtubules and more cellulose deposition. The process generates a local activation feedback of cell shape on growth *via* the mechanical stresses that are induced by that shape (sec. 5.3).

The geometric-mechanical simulation model of cell growth confirms that my stress-minimizing hypothesis is plausible, and the model is able to produce puzzle-shaped cells from a few simple assumptions. The model explains the gradual emergence of lobed cells from polygons resembling meristematic cells, providing an explanation for the till now enigmatic morphogenesis of these distinctive cells. It suggests that the main driver of the complex puzzle shape comes from the restriction of growth in the indentations, rather than the promotion of growth in the protrusions (compare with sec.6.4). This is supported by a recent study of Liang et al. (2018) where they demonstrated that cells of the *iqd5* mutant, defective in microtubule stabilization, fail to produce puzzle-shaped cells. Our model also predicts that the puzzle cell shape is triggered by isotropic growth, and that puzzle cell morphogenesis may not require any signaling molecules to coordinate a protrusion in one cell with the corresponding indentation of its neighbor (Sapala et al., 2019). Nonetheless, the model does not preclude a role for inter-cellular signaling, which could reinforce patterns produced by geometry sensing or facilitate the initial steps of lobing.

The model is consistent with the functions attributed to the main molecular players that have been reported to influence puzzle cell formation, the ROP family of GTP-ases. The growth-restricting connections inserted in a way that enhances the creation of indentations and lobes are equivalent to the placement of microtubules by ROP6 and RIC1. The model is also consistent with the idea that ROP6 is a part of the stress sensing mechanism, and that stress is the trigger for localized ROP6 accumulation. Currently, the molecular mechanism for how stress could be sensed and its relationship to the ROPs is unknown, although microtubules have been proposed to respond to stress *in planta* (Hamant et al.,

2008; Hejnowicz et al., 2000). Since stress is closely related to shape in pressurized plant cells, a curvature sensing mechanism could be involved (Higaki et al., 2016), similar to that proposed for villi patterning during gut morphogenesis (Shyer et al., 2015). Simulations have shown that a ROP2-ROP6 co-repression network can indeed partition a cell in discrete domains of ROP2 and ROP6 expression (Abley et al., 2013).

6.2.6. Experimental evidence of the stress minimizing mechanism in plant epidermis

In the previous section I described a computational model which confirms that upon the assumption that LEC (or, indirectly, stress) is kept low in growing cells, puzzle-shaped cells will emerge as a result of isotropic growth. As a result of anisotropic growth, long, thin cells will emerge. In addition to this theoretical work, it was my aim to provide experimental evidence of the accuracy and of the versatility of our models:

1. In young cotyledons, genetically changing growth direction from isotropic to anisotropic (*p35S::LNG1*) results in a switch of cell shape from puzzle-like to elongated. Moreover, it is followed by a change in organ shape (Fig. 5.7).
2. In adult leaves, puzzle cells (wild type) and elongated cells (*p35S::IQD16*) appear to have a target maximal LEC area, after which cells keep growing but LEC area does not increase any more. Conversely, when the lobe-creating mechanism is disrupted (*p35S::IQD8*), the relation of LEC to cell area is much more linear (Fig. 5.11).
3. A cell shape analysis of adult leaves of 19 different plant species (with a broad range of final cell area) has revealed a positive correlation between cell size and lobeyness. While larger cells are highly lobey, the small cells do not display puzzle shapes (Fig. 5.13).
4. In shoot apical meristems, if cell divisions (another way of lowering cell area and mechanical stress) are pharmacologically impaired, the largest cells may burst, presumably due to too much stress on the cell wall (Fig. 5.12).

The experiments mentioned above provide a solid justification for the hypothesis that plants avoid high stress on the cell wall. The question that naturally follows is: how do cells actually sense this stress? Previous studies have given solid evidence that cortical

microtubules orient according to stress directions (Hamant et al., 2008; Hejnowicz et al., 2000). However, it still remains unclear how this stress sensing happens.

6.2.7. A role for mechanical or geometric cues in cell shape formation

It has been proposed that cell geometry itself may account for microtubule orientations (Chakraborty et al., 2018; Gomez et al., 2016). In other words, microtubules may be able to directly sense cell shape and/or local curvature. Based on simple rules derived from observation of microtubule behavior, Chakraborty et al. (2018) simulated the interaction of microtubules with each other and the curvature of the cell wall. They were able to reproduce patterns resembling those observed *in planta* (Chakraborty et al., 2018). Similar simulations by Mirabet et al. (2018) indicate that highly curved cell shapes (i.e. with sharp edges) have more anisotropic microtubule distribution than those with smooth edges, which may lead to more focused cell wall reinforcement by CESA. The alignment of microtubules perpendicular to sharp-edged corners can be overcome by CLASP (cytoplasmic linker-associated proteins) which accumulate in corners and create microtubule bundles (Ambrose et al., 2011). The tendency for microtubules to bundle when they interact may provide an additional mechanism for the accumulation of microtubules in indentations. This, in turn, may cause cellulose reinforcements there (Fig. 6.3A). This could work in concert with the self-enhancing behavior of the membrane bound form of ROP6 proposed in molecular models of pavement cell patterning (Abley et al., 2013b; Fu et al., 2009) with ROP2 in the lobes promoting enhanced growth rates (Armour et al., 2015).

I have proposed that jigsaw puzzle cell shapes are an outcome of self-enhancing growth restriction in the lobes that helps the cells mitigate excessive stress from large, isodiametric shapes. When cells (and stresses) become too large, microtubules orient to direct growth restrictions. Small indentations attract microtubules and are enhanced, whereas lobes become enhanced by the loss of microtubules. In this model, the coordination of a lobe in one cell with the indentation in its neighbor is transmitted through cell geometry. The model is able to reproduce a wide variety of pavement cell patterns similar to those observed in different plant species (Sapala et al., 2018).

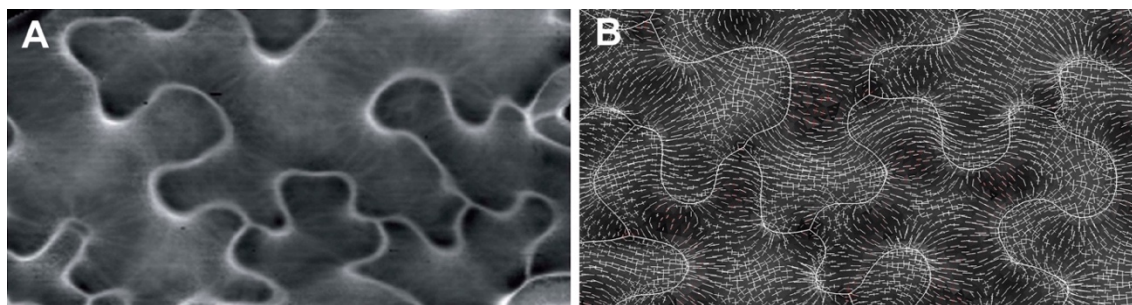


Figure 6.3. Cell wall reinforcements follow stress directions in the periclinal cell walls. (A) Surface of pavement cells in *Arabidopsis thaliana*. Image obtained with an Atomic Force Microscope, darker regions are soft and lighter regions are stiffer. Note the orientated pattern, thought to reflect that of cellulose fibrils which are the stiffest component of the cell wall. Their deposition is guided by cortical microtubules. Adapted from (Sampathkumar et al., 2014). (B) A finite element method (FEM) simulation of pressurized 3D puzzle cells with stress directions are visualized as white lines. Stress orientations are similar to the cellulose fibrils in (A), radiating out from the high stress indentations, and oriented across the lobes.

Adapted from (Sapala et al., 2019).

6.2.8. Could cells sense stress through geometry?

Since plants are pressurized cellular structures, there is a close correlation between cell shape and stress (Beauzamy et al., 2015b; Mosca et al., 2017), where curvature and cell pressure are the primary determinants of cell wall stress. The idea of curvature sensing controlling shape through gene expression has been proposed in rod-like elongated bacterial cells (Hussain et al., 2018), animal intestinal stem cell niches (Shyer et al., 2015), and other systems (recently reviewed by (Haupt and Minc, 2018)). Self-organization of microtubules may be central to curvature sensing (Haupt and Minc, 2018) as indicated by simulation studies in plants (Chakraborty et al., 2018; Mirabet et al., 2018), as well as experiments in *Drosophila melanogaster* embryos where cell shape aligns microtubules (Gomez et al., 2016). In the case of plant puzzle cells, creating intricate forms *via* a mechanism of shape or curvature sensing may be the outcome of optimizing mechanical stress in cell walls (Fig. 6.3B). While there is increasing evidence that stress is a central factor in morphogenesis and signal transduction, it has remained elusive how, or even if, it is possible for the cell to measure stress in the cell wall. Most stress measurement methods ultimately rely on measuring strains, yet strain-based feedbacks on growth do not seem to be sufficient (Bozorg et al., 2014). The pressurized nature of plant cells offers an exception. Plant cells could be using geometry (i.e. curvature) sensing to sense and counteract stress.

6.2.9. Acknowledgement

Portions of section 6.2. were included in:

Sapala, A., Runions, A. and Smith, R.S. (2019). Mechanics, geometry and genetics of epidermal cell shape regulation: different pieces of the same puzzle. *Current Opinion in Plant Biology* 47, 1-8. Published online on 28.08.2018.

6.3. Directions for future work

6.3.1. Biomechanics

The work described in Chapter 3 has significantly contributed to the advancement of the CFM technology, especially when it comes to coupling it with the confocal microscope. However, in order to make it more user friendly, it needs to be more automatized and gain more compatibility with MorphoGraphX. Measuring turgor pressure in very small cells is physically possible and we have information on what influences these measurements (Mosca et al., 2017; Weber et al., 2015), which will hopefully open the possibility to utilize the CFM in cells smaller than the onion epidermis. A particularly promising experiment is single cell ablation, which can be used to study mechanical properties of growing tissue by locally releasing turgor pressure and observing how the rest of the tissue relaxes as a consequence. Ablating a cell with the CFM sensor could potentially be more precise than laser ablation, because it would not cause heating up of neighboring cells.

6.3.2. Regulation of growth directions on cell, tissue and organ level

Using genetic engineering (*p35S::LNG1*), I have been able to demonstrate how a change in growth direction from isotropic to anisotropic affects cell shape. Even though this correlation seemed intuitive, so far it has not been shown as a confirmation of a dynamic growing model based on growth restrictions. As the next step, it would be interesting to find a counter-example which would change growth from anisotropic to isotropic and see which set of model parameters it resembles. A good candidate is *p35S::IQD8* which has isotropic cell shape in the leaves.

Furthermore, studying the relationship between cell shape and organ shape is an attractive direction, especially given the fact that it is still not clear how the growth direction is regulated on a global scale. It is, however, known that epidermis controls organ growth (Savaldi-Goldstein et al., 2007).

6.3.3. The stress minimization mechanism in plants

It cannot be excluded that, apart from adjusting the cell shape to keep LEC low, cells have other ways to protect their walls from bursting. These could include making the cell wall thicker or more elastic, or dividing it. Therefore, these three properties are likely correlated.

In order to assess this, an interesting direction to follow would be to check if cells of (relatively) high LEC have thicker cell walls than cells of relatively small LEC. Apart from creating puzzle shapes or thickening the cell wall, high cell wall stress could be compensated by making the cell wall more elastic. Osmotic treatments could be used to assess whether cells of higher LEC have more elastic cell walls. These studies could provide a comprehensive idea of how crucial this shape-adjusting mechanism is for maintaining the balance between resource allocation and maintaining cell wall integrity.

One should keep in mind that the relationship between cell wall thickness, cell wall elasticity and cell size might be very complex. It is likely that a mechanical model would be necessary to assess this issue. The recent advances in applying FEM models to plant tissues (partially described in this thesis) should be sufficient to provide a computational environment to study these relationships.

Finally, *p35S::IQD8* is one of a few genotypes in which cells do not form lobes as extensively as wild type cells but plants still survive and reproduce. It could be exploited as a system for deciphering the molecular control of puzzle cell formation.

6.4. Closing remarks

„We should not be discouraged by the difficulty of interpreting life by the ordinary laws of physics.”

Erwin Schrödinger, ‘What is life? The physical aspect of a living cell’, 1948

The growth of plant cells is a very complicated, dynamic process. From the small, polygonal, meristematic cells to the fully functional tissue, cells need to expand even a few hundred times. To regulate this genetically is a very complex task, especially considering the constraints provided by the cell walls (not present in animal systems).

For that reason, studying developmental biology without physical experiments, mathematical models and computer simulations is not possible. Molecular biology, powerful as it is, cannot suffice to speculate about growth factors steering a complex hydraulic system such as a plant tissue. Image acquisition and analysis technologies can describe morphogenesis qualitatively, biomechanical experimental methods adapted from other fields can help uncover the physical aspects of it (such as AFM described in the previous section), and finally computer models can bring this information together with molecular data (such as gene expression patterns). I personally believe that this interdisciplinary mindset is the best approach to study morphogenesis.

Some of the questions asked in this thesis may appear very basic: how do plant cells grow? Why do they create jigsaw puzzle-like shapes? However, behind these ideas lie the complex ways plants regulate their own forms, spanning genetic information, intracellular interactions of biomolecules and organ-wide signaling. It is only by understanding the synergy of those levels, and the variety of disciplines required to study them, that we can think of fully controlling plant growth and using this control to our advantage.

Bibliography

- Abley, K., Reuille, P.B.D., Strutt, D., Bangham, A., Prusinkiewicz, P., Marée, A.F.M., Grieneisen, V.A., and Coen, E. (2013). An intracellular partitioning-based framework for tissue cell polarity in plants and animals. *2074*, 2061–2074.
- Allen, M.J., Kanteti, R., Riehm, J.J., El-hashani, E., and Salgia, R. (2015). Whole-animal mounts of *Caenorhabditis elegans* for 3D imaging using atomic force microscopy. *Nanomedicine: Nanotechnology, Biology, and Medicine 11*, 1971–1974.
- Ambrose, C., Allard, J.F., Cytrynbaum, E.N., and Wasteneys, G.O. (2011). A CLASP-modulated cell edge barrier mechanism drives cell-wide cortical microtubule organization in *Arabidopsis*. *Nature Communications 2*, 430.
- Armour, W.J., Barton, D. a., Law, A.M.K., and Overall, R.L. (2015). Differential Growth in Periclinal and Anticlinal Walls during Lobe Formation in *Arabidopsis* Cotyledon Pavement Cells. *The Plant Cell 27*, 2484–2500.
- Avery, G.S. (1933). Structure and development of the tobacco leaf. *American Journal of Botany 20*, 565–592.
- Ballmann, C.W., Thompson, J.V., Traverso, A.J., Meng, Z., Scully, M.O., and Yakovlev, V.V. (2015). Stimulated Brillouin Scattering Microscopic Imaging. *Scientific Reports 5*, 18139.
- Barbier de Reuille, P., Routier-Kierzkowska, A.-L., Kierzkowski, D., Bassel, G.W., Schüpbach, T., Tauriello, G., Bajpai, N., Strauss, S., Weber, A., Kiss, A., et al. (2015). MorphoGraphX: A platform for quantifying morphogenesis in 4D. *eLife 4*, e05864.
- Bassel, G.W., Stamm, P., Mosca, G., Barbier de Reuille, P., Gibbs, D.J., Winter, R., Janka, a., Holdsworth, M.J., and Smith, R.S. (2014). Mechanical constraints imposed by 3D cellular geometry and arrangement modulate growth patterns in the *Arabidopsis* embryo. *Proceedings of the National Academy of Sciences 111*: 8685-8690.
- Beauzamy, L., Derr, J., and Boudaoud, A. (2015a). Quantifying Hydrostatic Pressure in Plant Cells by Using Indentation with an Atomic Force Microscope. *Biophysical Journal 108*, 2448–2456.
- Beauzamy, L., Louveaux, M., Hamant, O., and Boudaoud, A. (2015b). Mechanically , the Shoot Apical Meristem of *Arabidopsis* Behaves like a Shell Inflated by a Pressure of About 1 MPa. *Frontiers in Plant Science 6*, 1–10.
- Belteton, S., Sawchuk, M.G., Donohoe, B.S., Scarpella, E., and Szymanski, D.B. (2017). Reassessing the roles of PIN proteins and anticlinal microtubules during pavement cell morphogenesis. *Plant Physiology* pp.01554.2017.
- Bidhendi, A.J., and Geitmann, A. (2018). Finite Element Modeling of Shape Changes in Plant Cells. *Plant Physiology 176*, 41–56.

Bilsborough, G.D., Runions, A., Barkoulas, M., Jenkins, H.W., Hasson, A., Galinha, C., Laufs, P., Hay, A., Prusinkiewicz, P., and Tsiantis, M. (2011). Model for the regulation of *Arabidopsis thaliana* leaf margin development. *Proceedings of the National Academy of Sciences of the United States of America* *108*, 3424–3429.

Bozorg, B., Krupinski, P., and Jönsson, H. (2014). Stress and Strain Provide Positional and Directional Cues in Development. *PLOS Computational Biology* *10*, e1003410.

Bringmann, M., and Bergmann, D.C. (2017). Tissue-wide mechanical forces influence the polarity of stomatal stem cells in *Arabidopsis*. *Current Biology* *27*, 877–883.

Brophy, J.A.N., LaRue, T., and Dinneny, J.R. (2018). Understanding and engineering plant form. *Seminars in Cell & Developmental Biology* *79*: 68-77.

Bürstenbinder, K., Möller, B., Plötner, R., Stamm, G., Hause, G., Mitra, D., and Abel, S. (2017). The IQD Family of Calmodulin-Binding Proteins Links Calmodulin Signaling to Microtubules, Membrane Microdomains, and the Nucleus. *Plant Physiology* pp.01743.2016.

Chakraborty, B., Blilou, I., Scheres, B., and Mulder, B.M. (2018). A computational framework for cortical microtubule dynamics in realistically shaped plant cells. *PLOS Computational Biology* *14*, 1–26.

Chan, J., Crowell, E., Eder, M., Calder, G., Bunnewell, S., Findlay, K., Vernhettes, S., Höfte, H., and Lloyd, C. (2010). The rotation of cellulose synthase trajectories is microtubule dependent and influences the texture of epidermal cell walls in *Arabidopsis* hypocotyls. 3490–3495.

Chandler, J.W. (2008). Cotyledon organogenesis. *J Exp Bot* *59*, 2917–2931.

Chanliaud, E., De Silva, J., Strongitharm, B., Jeronimidis, G., and Gidley, M.J. (2004). Mechanical effects of plant cell wall enzymes on cellulose/xyloglucan composites. *Plant J.* *38*, 27–37.

Chebli, Y., Kaneda, M., Zerzour, R., and Geitmann, A. (2012). The Cell Wall of the *Arabidopsis* Pollen Tube—Spatial Distribution, Recycling, and Network Formation of Polysaccharides. *Plant Physiology* *160*, 1940–1955.

Chen, J., Wang, F., Zheng, S., Xu, T., and Yang, Z. (2015). Pavement cells : a model system for non-transcriptional auxin signalling and crosstalks. *Journal of Experimental Botany* *66*, 4957–4970.

Coen, E., Rolland-Lagan, A.-G., Matthews, M., Bangham, J.A., and Prusinkiewicz, P. (2004). The genetics of geometry. *Proceedings of the National Academy of Sciences of the United States of America* *101*, 4728–4735.

Corson, F., Hamant, O., Bohn, S., Traas, J., Boudaoud, A., and Couder, Y. (2009). Turning a plant tissue into a living cell froth through isotropic growth. *Proceedings of the National Academy of Sciences of the United States of America* *106*, 8453–8458.

Cosgrove, D.J. (2005). Growth of the plant cell wall. *Nature Reviews. Molecular Cell Biology* *6*, 850–861.

- Cosgrove, D.J. (2014). Re-constructing our models of cellulose and primary cell wall assembly. *Current Opinion in Plant Biology* 22, 122–131.
- Craddock, C., Lavagi, I., and Yang, Z. (2012). New insights into Rho signaling from plant ROP / Rac GTPases. *Trends in Cell Biology* 22, 492–501.
- Dolan, L., and Poethig, R.S. (1998). Clonal analysis of leaf development in cotton. *American Journal of Botany* 85, 315–321.
- Drevensek, S., Goussot, M., Duroc, Y., Christodoulidou, A., Steyaert, S., Schaefer, E., Duvernois, E., Grandjean, O., Vantard, M., Bouchez, D., et al. (2012). The Arabidopsis TRM1–TON1 Interaction Reveals a Recruitment Network Common to Plant Cortical Microtubule Arrays and Eukaryotic Centrosomes. *Plant Cell* 24, 178–191.
- Elsayad, K., Werner, S., Gallemí, M., Kong, J., Guajardo, E.R.S., Zhang, L., Jaillais, Y., Greb, T., and Belkhadir, Y. (2016). Mapping the subcellular mechanical properties of live cells in tissues with fluorescence emission – Brillouin imaging. *Science Signaling* 9, 1–13.
- Elsner, J., Michalski, M., and Kwiatkowska, D. (2012). Spatiotemporal variation of leaf epidermal cell growth: a quantitative analysis of Arabidopsis thaliana wild-type and triple cyclinD3 mutant plants. *Annals of Botany* 109, 897–910.
- Elsner, J., Lipowczan, M., and Kwiatkowska, D. (2017). Differential growth of pavement cells of Arabidopsis thaliana leaf epidermis as revealed by microbead labeling. *American Journal of Botany* 105, 257–265.
- Eshed, Y., Izhaki, A., Baum, S.F., Floyd, S.K., and Bowman, J.L. (2004). Asymmetric leaf development and blade expansion in Arabidopsis are mediated by KANADI and YABBY activities. *Development* 131, 2997–3006.
- Essmann, C.L., Elmi, M., Shaw, M., Anand, G.M., Pawar, V.M., and Srinivasan, M.A. (2017). In-vivo high resolution AFM topographic imaging of Caenorhabditis elegans reveals previously unreported surface structures of cuticle mutants. *Nanomedicine* 13, 183–189.
- Felekis, D., Muntwyler, S., Vogler, H., Beyeler, F., Grossniklaus, U., and Nelson, B.J. (2011). Quantifying growth mechanics of living, growing plant cells in situ using microrobotics. *Micro & Nano Letters* 6, 311–311.
- Fernandes, A.N., Chen, X., Scotchford, C.A., Walker, J., Wells, D.M., Roberts, C.J., and Everitt, N.M. (2012). Mechanical properties of epidermal cells of whole living roots of Arabidopsis thaliana: An atomic force microscopy study. *Phys. Rev. E* 85, 021916.
- Forouzesh, E., Goel, A., Mackenzie, S.A., and Turner, J.A. (2013). In vivo extraction of Arabidopsis cell turgor pressure using nanoindentation in conjunction with finite element modeling. *The Plant Journal* 73, 509–520.
- Franks, J., Cowan, I.R., Tyerman, S.D., Cleary, A.L., Lloyd, J., and Farquhar, G.D. (1995). Guard cell pressure / aperture characteristics measured with the pressure probe. *Plant, Cell and Environment* 18, 795–800.

- Franks, P.J., Buckley, T.N., Shope, J.C., and Mott, K.A. (2001). Guard Cell Volume and Pressure Measured Concurrently by Confocal Microscopy and the Cell Pressure Probe. *Plant Physiology* *125*, 1577–1584.
- Fry, S.C. (1998). Oxidative scission of plant cell wall polysaccharides by ascorbate-induced hydroxyl radicals. *Biochemical Journal* *332*: 507-515.
- Fry, S.C. (2004). Oxidative coupling of tyrosine and ferulic acid residues : Intra- and extra-protoplasmic occurrence , predominance of trimers and larger products , and possible role in inter-polymeric cross-linking. *Phytochemistry Reviews* *3*: 97–111.
- Fu, Y., Li, H., and Yang, Z. (2002). The ROP2 GTPase Controls the Formation of Cortical Fine F-Actin and the Early Phase of Directional Cell Expansion during Arabidopsis Organogenesis. *The Plant Cell* *14*, 777–794.
- Fu, Y., Gu, Y., Zheng, Z., Wasteneys, G., and Yang, Z. (2005). Arabidopsis Interdigitating Cell Growth Requires Two Antagonistic Pathways with Opposing Action on Cell Morphogenesis. *Cell* *120*, 687–700.
- Fu, Y., Xu, T., Zhu, L., Wen, M., and Yang, Z. (2009). A ROP GTPase signalling pathway controls cortical microtubule ordering and cell expansion in Arabidopsis. *Current Biology* *19*, 1827–1832.
- Galletti, R., and Ingram, G.C. (2015). Communication is key: Reducing DEK1 activity reveals a link between cell-cell contacts and epidermal cell differentiation status. *Communicative & Integrative Biology*, e1059979–e1059979.
- Gao, Y., Zhang, Y., Zhang, D., Dai, X., Estelle, M., and Zhao, Y. (2015). Auxin binding protein 1 (ABP1) is not required for either auxin signaling or Arabidopsis development. *PNAS* *112*, 2275–2280.
- Geitmann, A., and Ortega, J.K.E. (2009). Mechanics and modeling of plant cell growth. *Trends in Plant Science* *14*, 467–478.
- Glover, B.J. (2000). Differentiation in plant epidermal cells. *Journal of Experimental Botany* *51*, 497–505.
- Gomez, J.M., Chumakova, L., Bulgakova, N.A., and Brown, N.H. (2016). Microtubule organization is determined by the shape of epithelial cells. *Nature Communications* *7*, 13172.
- Gramüller, B., Köke, H., and Hühne, C. (2015). Holistic design and implementation of pressure actuated cellular structures. *Smart Mater. Struct.* *24*, 125027.
- Green, P.B. (1962). Mechanism for Plant Cellular Morphogenesis. *Science* *138*, 1404–1405.
- Guerriero, G., Hausman, J.-F., and Cai, G. (2014). No Stress! Relax! Mechanisms Governing Growth and Shape in Plant Cells. *Int J Mol Sci* *15*, 5094–5114.

- Guiducci, L., Fratzl, P., Bréchet, Y.J.M., and Dunlop, J.W.C. (2014). Pressurized honeycombs as soft-actuators: a theoretical study. *Journal of The Royal Society Interface* *11*, 20140458.
- Guillaume-Gentil, O., Potthoff, E., Ossola, D., Franz, C.M., Zambelli, T., and Vorholt, J.A. (2014). Force-controlled manipulation of single cells: from AFM to FluidFM. *Trends in Biotechnology* *32*, 381–388.
- Hamant, O., and Haswell, E.S. (2017). Life behind the wall: sensing mechanical cues in plants. *BMC Biology* *15*, 59.
- Hamant, O., Heisler, M.G., Jönsson, H., Krupinski, P., Uyttewaal, M., Bokov, P., Corson, F., Sahlin, P., Boudaoud, A., Meyerowitz, E.M., et al. (2008). Developmental patterning by mechanical signals in Arabidopsis. *Science* *322*, 1650–1655.
- Hamilton, E.S., Schlegel, A.M., and Haswell, E.S. (2015). United in diversity: mechanosensitive ion channels in plants. *Annu Rev Plant Biol* *66*, 113–137.
- Haupt, A., and Minc, N. (2018). How cells sense their own shape - mechanisms to probe cell geometry and their implications in cellular organization and function. *J. Cell. Sci.* *131*.
- Hayot, C.M., Forouzesh, E., Goel, A., Avramova, Z., and Turner, J. (2012). Viscoelastic properties of cell walls of single living plant cells determined by dynamic nanoindentation. *Journal of Experimental Botany* *63*, 2525–2540.
- Heisler, M.G., Hamant, O., Krupinski, P., Uyttewaal, M., Ohno, C., Jönsson, H., Traas, J., and Meyerowitz, E.M. (2010). Alignment between PIN1 polarity and microtubule orientation in the shoot apical meristem reveals a tight coupling between morphogenesis and auxin transport. *PLoS Biology* *8*, e1000516–e1000516.
- Hejnowicz, Z., Rusin, A., and Rusin, T. (2000). The Orientation of Cortical Microtubules in the Epidermis of Sunflower Hypocotyl. *Journal of Plant Growth Regulation* *19*: 31–44.
- Hemerly, A., Engler, J. de A., Bergounioux, C., Van Montagu, M., Engler, G., Inzé, D., and Ferreira, P. (1995). Dominant negative mutants of the Cdc2 kinase uncouple cell division from iterative plant development. *The EMBO Journal* *14*, 3925–3936.
- Hepler, P.K., Rounds, C.M., and Winship, L.J. (2013). Control of Cell Wall Extensibility during Pollen Tube Growth. *Molecular Plant* *6*, 998–1017.
- Hervieux, N., Dumond, M., Sapala, A., Routier-Kierzkowska, A.-L., Kierzkowski, D., Roeder, A.H.K., Smith, R.S., and Hamant, O. (2016). A mechanical feedback restricts sepal growth and shape in Arabidopsis. *Current Biology* *26*, 1019–1028.
- Hervieux, N., Tsugawa, S., Fruleux, A., Dumond, M., Routier-Kierzkowska, A.-L., Komatsuzaki, T., Boudaoud, A., Larkin, J.C., Smith, R.S., Li, C.-B., et al. (2017). Mechanical Shielding of Rapidly Growing Cells Buffers Growth Heterogeneity and Contributes to Organ Shape Reproducibility. *Current Biology* *27*, 3468–3479.
- Higaki, T., Kutsuna, N., Akita, K., and Takigawa-Imamura, H. (2016). A Theoretical Model of Jigsaw-Puzzle Pattern Formation by Plant Leaf Epidermal Cells. *PLOS Computational Biology* *12*: e1004833..

- Higaki, T., Takigawa-Imamura, H., Akita, K., Kutsuna, N., Kobayashi, R., Hasezawa, S., and Miura, T. (2017). Exogenous Cellulase Switches Cell Interdigitation to Cell Elongation in an RIC1-dependent Manner in *Arabidopsis thaliana* Cotyledon Pavement Cells. *Plant & Cell Physiology* 58, 106–119.
- Hisanaga, T., Kawade, K., and Tsukaya, H. (2015). Compensation: a key to clarifying the organ-level regulation of lateral organ size in plants. *Journal of Experimental Botany* 66, 1055–1063.
- Hofhuis, H., and Hay, A. (2017). Explosive seed dispersal. *New Phytologist* 216: 339-342.
- Hofhuis, H., Moulton, D., Lessinnes, T., Routier-Kierzkowska, A.-L., Bomphrey, R.J., Mosca, G., Reinhardt, H., Sarchet, P., Gan, X., Tsiantis, M., et al. (2016). Morphomechanical Innovation Drives Explosive Seed Dispersal. *Cell* 166, 222–233.
- Hong, L., Dumond, M., Tsugawa, S., Sapala, A., Routier-Kierzkowska, A.-L., Zhou, Y., Chen, C., Kiss, A., Zhu, M., Hamant, O., et al. (2016). Variable Cell Growth Yields Reproducible Organ Development through Spatiotemporal Averaging. *Developmental Cell* 38, 15–32.
- Horiguchi, G., Ferjani, A., Fujikura, U., and Tsukaya, H. (2006). Coordination of cell proliferation and cell expansion in the control of leaf size in *Arabidopsis thaliana*. *Journal of Plant Research* 119, 37–42.
- Hülkamp, M., Miséra, S., and Jürgens, G. (1994). Genetic dissection of trichome cell development in *Arabidopsis*. *Cell* 76, 555–566.
- Hunter, C., Willmann, M.R., Wu, G., Yoshikawa, M., Luz Gutierrez-Nava, M. and Poethig, S.R. (2006). *Development* 133: 2973-2981.
- Hussain, S., Wivagg, C.N., Szwedziak, P., Wong, F., Schaefer, K., Izoré, T., Renner, L.D., Holmes, M.J., Sun, Y., Bisson-Filho, A.W., et al. (2018). MreB filaments align along greatest principal membrane curvature to orient cell wall synthesis. *eLife*, e32471.
- Ito, K., and Akiyama, Y. (2005). Cellular functions, mechanism of action, and regulation of ftsH protease. *Annu. Rev. Microbiol.* 59, 211–231.
- Jacques, E., and Vissenberg, K. (2014). Review on shape formation in epidermal pavement cells of the *Arabidopsis* leaf. *Functional Plant Biology* 41, 914–921.
- Jönsson, H., Heisler, M.G., Shapiro, B.E., Meyerowitz, E.M., and Mjolsness, E. (2006). An auxin-driven polarized transport model for phyllotaxis. *Proceedings of the National Academy of Sciences of the United States of America* 103, 1633–1638.
- Julien, J.-D., and Boudaoud, A. (2018). Elongation and shape changes in organisms with cell walls: A dialogue between experiments and models. *The Cell Surface* 1, 34–42.
- Karimi, M., Inzé, D., and Depicker, A. (2002). GATEWAY vectors for *Agrobacterium*-mediated plant transformation. 7, 193–195.
- Kierzkowski, D., Nakayama, N., Routier-Kierzkowska, A.-L., Weber, A., Bayer, E., Schorderet, M., Reinhardt, D., Kuhlemeier, C., and Smith, R.S. (2012). Elastic Domains

Regulate Growth and Organogenesis in the Plant Shoot Apical Meristem. *Science* 335, 1096–1099.

Kim, G.T., Tsukaya, H., and Uchimiya, H. (1998). The ROTUNDIFOLIA3 gene of *Arabidopsis thaliana* encodes a new member of the cytochrome P-450 family that is required for the regulated polar elongation of leaf cells. *Genes and Development* 12, 2381–2391.

Kim, I., Kobayashi, K., Cho, E., and Zambryski, P.C. (2005). Subdomains for transport via plasmodesmata corresponding to the apical–basal axis are established during *Arabidopsis* embryogenesis. *PNAS* 102, 11945–11950.

Kimura, S., Laosinchai, W., Itoh, T., Cui, X., Linder, C.R., and Brown, R.M. (1999). Immunogold labeling of rosette terminal cellulose-synthesizing complexes in the vascular plant *vigna angularis*. *Plant Cell* 11, 2075–2086.

Kuchen, E.E., Fox, S., de Reuille, P.B., Kennaway, R., Bensmihen, S., Avondo, J., Calder, G.M., Southam, P., Robinson, S., Bangham, A., et al. (2012). Generation of leaf shape through early patterns of growth and tissue polarity. *Science* 335, 1092–1096.

Kutschera, U., and Niklas, K.J. (2007). The epidermal-growth-control theory of stem elongation: An old and a new perspective. *Journal of Plant Physiology* 164, 1395–1409.

Kwiatkowska, D., and Dumais, J. (2003). Growth and morphogenesis at the vegetative shoot apex of *Anagallis arvensis* L. *Journal of Experimental Botany* 54, 1585–1595.

Landrein, B., Kiss, A., Sassi, M., Chauvet, A., Das, P., Cortizo, M., Laufs, P., Takeda, S., Aida, M., Traas, J., et al. (2015). Mechanical stress contributes to the expression of the STM homeobox gene in *Arabidopsis* shoot meristems. *eLife* 4, e07811.

Le, J., Mallery, E.L., Zhang, C., Brankle, S., Szymanski, D.B., and Hall, L. (2006). *Arabidopsis* BRICK1 / HSPC300 Is an Essential WAVE-Complex Subunit that Selectively Stabilizes the Arp2 / 3 Activator SCAR2. *Current Biology* 16, 895–901.

Lee, G., Cheung, K., Chang, W., Lee, L.P. (2000). Mechanical interlocking with precisely controlled nano- and microscale geometries for implantable microdevices. 1st Annual International IEEE-EMBS Special Topic Conference on Microtechnologies in Medicine & Biology.

Lee, Y.K., Kim, G.-T., Kim, I.-J., Park, J., Kwak, S.-S., Choi, G., and Chung, W.-I. (2006). LONGIFOLIA1 and LONGIFOLIA2, two homologous genes, regulate longitudinal cell elongation in *Arabidopsis*. *Development* 133, 4305–4314.

Li, S., and Wang, K.W. (2015). Fluidic origami with embedded pressure dependent multi-stability: a plant inspired innovation. *Journal of The Royal Society Interface* 12, 20150639.

Li, H., Lin, D., Dhonukshe, P., Nagawa, S., Chen, D., Friml, J., and Scheres, B. (2011). Phosphorylation switch modulates the interdigitated pattern of PIN1 localization and cell expansion in *Arabidopsis* leaf epidermis. *Nature* 21, 970–978.

- Liang, H., Zhang, Y., Martinez, P., Rasmussen, C., Xu, T., and Yang, Z. (2018). The microtubule-associated protein IQ67 DOMAIN5 modulates microtubule dynamics and pavement cell shape. *Plant Physiology* pp.00558.2018.
- Lin, D., Cao, L., Zhou, Z., Zhu, L., Ehrhardt, D., Yang, Z., and Fu, Y. (2013). Rho GTPase Signaling Activates Microtubule Severing to Promote Microtubule Ordering in Arabidopsis. *Current Biology* 23, 290–297.
- Lintilhac, P.M., and Vesecky, T.B. (1984). Stress-induced alignment of division plane in plant tissues grown in vitro. *Nature* 307, 363–364.
- Lloyd, C., and Chan, J. (2004). Microtubules and the shape of plants to come. *Nat. Rev. Mol. Cell Biol.* 5, 13–22.
- Lockhart, J.A. (1965). An Analysis of Irreversible Plant Cell Elongation. *Journal of Theoretical Biology* 8, 264–275.
- Lockhart, J.A. (1967). Physical Nature of Irreversible Deformation of Plant Cells. *Plant Physiol.* 42; 1545–1552.
- Lockhart, J.A., Bretz, C., and Kenner, R. (1961). An analysis of cell wall extension. *Annals New York Academy of Sciences*: 19-33.
- Louveaux, M., Julien, J.-D., Mirabet, V., Boudaoud, A., and Hamant, O. (2016). Cell division plane orientation based on tensile stress in Arabidopsis thaliana. *PNAS* 113, E4294–E4303.
- Majda, M., Grones, P., Sintorn, I.M., Vain, T., Milani, P., Krupinski, P., Zagorska-Marek, B., Viotti, C., Jonsson, H., Mellerowicz, E., Hamant, O. and Robert, S. (2017). Mechanochemical Polarization of Contiguous Cell Article Mechanochemical Polarization of Contiguous Cell Walls Shapes Plant Pavement Cells. *Developmental Cell* 43, 290–304.
- Marga, F., Grandbois, M., Cosgrove, D.J., and Baskin, T.I. (2005). Cell wall extension results in the coordinate separation of parallel microfibrils: evidence from scanning electron microscopy and atomic force microscopy. *Plant J.* 43, 181–190.
- Mathur, J. (2006). Trichome cell morphogenesis in Arabidopsis : a continuum of cellular decisions. *Canadian Journal of Botany* 84, 604–612.
- Matthews, M. (2002). Physically based simulation of growing surfaces. MSc thesis. University of Calgary. <http://algorithmicbotany.org/papers/matthews.th2002.pdf>
- Milani, P., Gholamirad, M., Traas, J., Arnéodo, A., Boudaoud, A., Argoul, F., and Hamant, O. (2011). In vivo analysis of local wall stiffness at the shoot apical meristem in Arabidopsis using atomic force microscopy. *The Plant Journal* 67, 1116–1123.
- Mirabet, V., Krupinski, P., Hamant, O., Meyerowitz, E.M., Jönsson, H., and Boudaoud, A. (2018). The self-organization of plant microtubules inside the cell volume yields their cortical localization, stable alignment, and sensitivity to external cues. *PLOS Computational Biology* 14, 1–23.

- Mitra, D., Kumari, P., Quegwer, J., Klemm, S., Moeller, B., Poeschl, Y., Pflug, P., Stamm, G., Abel, S., and Bürstenbinder, K. (2018). Microtubule-associated protein IQ67 DOMAIN5 regulates interdigitation of leaf pavement cells in *Arabidopsis thaliana*. *BioRxiv* 268466.
- Möller, B., Poeschl, Y., Plötner, R., and Bürstenbinder, K. (2017). PaCeQuant: A Tool for High-Throughput Quantification of Pavement Cell Shape Characteristics. *Plant Physiology* 175: 998-1017.
- Mosca, G., Sapala, A., Strauss, S., Routier-Kierzkowska A.L. and Smith, R.S. (2017). On the micro-indentation of plant cells in a tissue context. *Physical Biology* 14: 015033.
- Nakayama, N., Smith, R.S., Mandel, T., Robinson, S., Kimura, S., Boudaoud, A., and Kuhlemeier, C. (2012). Mechanical regulation of auxin-mediated growth. *Current Biology* 22, 1468–1476.
- Ndamukong, I., Chetram, A., Saleh, A., and Avramova, Z. Wall-modifying genes regulated by the *Arabidopsis* homolog of trithorax, ATX1: repression of the XTH33 gene as a test case. *The Plant Journal* 58, 541–553.
- Niklas, K.J. (1992). *Plant Biomechanics: An Engineering Approach to Plant Form and Function* (The University of Chicago Press).
- Oparka, K.J. (1994). Plasmolysis: New insights into an old process. *New Phytologist* 126: 571–591.
- Paredez, A.R., Somerville, C.R., and Ehrhardt, D.W. (2006). Visualization of Cellulose Synthase Demonstrates Functional Association with Microtubules. *Science* 312, 1491–1496.
- Park, Y.B., and Cosgrove, D.J. (2012). A Revised Architecture of Primary Cell Walls Based on Biomechanical Changes Induced by Substrate-Specific Endoglucanases. *Plant Physiology* 158, 1933–1943.
- Peaucelle, A., Braybrook, S.A., Le Guillou, L., Bron, E., Kuhlemeier, C., and Höfte, H. (2011). Pectin-Induced Changes in Cell Wall Mechanics Underlie Organ Initiation in *Arabidopsis*. *Current Biology* 21, 1720–1726.
- Pien, S., Wyrzykowska, J., McQueen-Mason, S., Smart, C., and Fleming, a (2001). Local expression of expansin induces the entire process of leaf development and modifies leaf shape. *Proceedings of the National Academy of Sciences of the United States of America* 98, 11812–11817.
- Poethig, R.S., and Sussex, I.M. (1985). The cellular parameters of leaf development in tobacco: a clonal analysis. *Planta* 165, 170–184.
- Powell, A.E., and Lenhard, M. (2012). Control of Organ Size in Plants. *Current Biology* 22, 360–367.
- Proseus, T.E., and Boyer, J.S. (2005). Turgor pressure moves polysaccharides into growing cell walls of *Chara corallina*. *Ann. Bot.* 95, 967–979.

Prusinkiewicz, P. and Lindenmayer, A. (2012). The algorithmic beauty of plants. Springer Science & Business Media.

Qin, Y., and Yang, Z. (2011). Rapid tip growth: Insights from pollen tubes. *Semin Cell Dev Biol* 22, 816–824.

Qiu, J., Jilk, R., Marks, M.D., and Szymanski, D.B. (2002). The Arabidopsis SPIKE1 Gene Is Required for Normal Cell Shape Control and Tissue Development. *14*, 101–118.

Ralph, J., Bunzel, M., Marita, J.M., Hatfield, R.D., Lu, F., Schatz, P.F., Grabber, J.H., and Steinhart, H. (2004). Peroxidase-dependent cross-linking reactions of p - hydroxycinnamates in plant cell walls. *Phytochemistry Reviews* 3, 79–96.

Redmacher, M. (1997). Measuring the elastic properties of biological samples with the AFM. *IEE Engineering in Medicine and Biology* March/April: 47-57.

Reinhardt, D., Mandel, T., and Kuhlemeier, C. (2000). Auxin regulates the initiation and radial position of plant lateral organs. *The Plant Cell* 12, 507–518.

Rico, F., Gonzalez, L., Casuso, I., Puig-vidal, M., and Scheuring, S. (2013). High-Speed Force Spectroscopy Molecular Dynamics Simulations. *Science* 342, 741–743.

Robinson, S., Huflejt, M., Barbier de Reuille, P., Braybrook, S. a, Schorderet, M., Reinhardt, D., and Kuhlemeier, C. (2017). An automated confocal micro-extensometer enables in vivo quantification of mechanical properties with cellular resolution. *The Plant Cell* 29, 2959–2973.

Roeder, A.H.K., Chickarmane, V., Cunha, A., Obara, B., Manjunath, B.S., and Meyerowitz, E.M. (2010). Variability in the control of cell division underlies sepal epidermal patterning in Arabidopsis thaliana. *PLoS Biology* 8, e1000367–e1000367.

Roeder, A.H.K., Cunha, A., Ohno, C.K., and Meyerowitz, E.M. (2012). Cell cycle regulates cell type in the Arabidopsis sepal. *Development* 139, 4416–4427.

Routier-Kierzkowska, A.-L., and Smith, R.S. (2013). Measuring the mechanics of morphogenesis. *Current Opinion in Plant Biology* 16, 25–32.

Routier-Kierzkowska, A.-L., Weber, A., Kochova, P., Felekis, D., Nelson, B.J., Kuhlemeier, C., and Smith, R.S. (2012). Cellular force microscopy for in vivo measurements of plant tissue mechanics. *Plant Physiology* 158, 1514–1522.

Ruan, Y.L., Llewellyn, D.J., and Furbank, R.T. (2001). The control of single-celled cotton fiber elongation by developmentally reversible gating of plasmodesmata and coordinated expression of sucrose and K⁺ transporters and expansin. *The Plant Cell* 13, 47–60.

Rueden, C.T., Schindelin, J., Hiner, M.C., DeZonia, B.E., Walter, A.E., Arena, E.T., and Eliceiri, K.W. (2017). ImageJ2: ImageJ for the next generation of scientific image data. *BMC Bioinformatics* 18, 529.

Sager, R., and Lee, J.-Y. (2014). Plasmodesmata in integrated cell signalling: insights from development and environmental signals and stresses. *J Exp Bot* 65, 6337–6358.

- Sakai, Y., Yamazaki, T., Xu, Y., Kuzuya, A., and Komiyama, M. (2011). Nanomechanical DNA origami “single-molecule beacons” directly imaged by atomic force microscopy. *Nature Communications* 2, 448–449.
- Saladié, M., Rose, J.K.C., Cosgrove, D.J., and Catalá, C. (2006). Characterization of a new xyloglucan endotransglucosylase/hydrolase (XTH) from ripening tomato fruit and implications for the diverse modes of enzymic action. *Plant J.* 47, 282–295.
- Sampathkumar, A., Krupinski, P., Wightman, R., Milani, P., Berquand, A., Boudaoud, A., Hamant, O., Jönsson, H., and Meyerowitz, E.M. (2014). Subcellular and supracellular mechanical stress prescribes cytoskeleton behavior in *Arabidopsis* cotyledon pavement cells. *eLife*, e01967.
- Sánchez-Corrales, Y.E., Hartley, M., van Rooij, J., Marée, A.F.M., and Grieneisen, V.A. (2018). Morphometrics of complex cell shapes: lobe contribution elliptic Fourier analysis (LOCO-EFA). *Development* 145, dev156778.
- Sapala, A., Runions, A. and Smith, R.S. (2019) Mechanics, geometry and genetics of epidermal cell shape regulation: different pieces of the same puzzle. *Current Opinion in Plant Biology* 47, 1-8. Published online on 28.08.2018
- Sapala, A., Runions, A., Routier-Kierzkowska, A.L., Gupta, M.D., Hong, L., Hofhuis, H., Verger, S., Mosca, G., Li, C.B., Hay, A., et al. (2018). Why plants make puzzle cells, and how their shape emerges. *eLife*, e32794.
- Sapala, A. and Smith, R.S. (2018). Osmotic treatment for quantifying cell wall elasticity in the sepal of *Arabidopsis thaliana*. *Methods in Molecular Biology*. Submitted.
- Sassi, M., and Traas, J. (2015). New insights in shoot apical meristem morphogenesis: isotropy comes into play. *Plant Signaling & Behavior* 10:11, e1000150.
- Sauret-Güeto, S., Schiessl, K., Bangham, A., Sablowski, R., and Coen, E. (2013). JAGGED controls *Arabidopsis* petal growth and shape by interacting with a divergent polarity field. *PLoS Biology* 11, e1001550–e1001550.
- Savaldi-Goldstein, S., Peto, C., and Chory, J. (2007). The epidermis both drives and restricts plant shoot growth. *Nature* 446, 199–202.
- Scarpella, E., Barkoulas, M., and Tsiantis, M. (2010). Control of leaf and vein development by auxin. *Cold Spring Harbor Perspectives in Biology* 2010 2, a001511.
- Schindelin, J., Arganda-Carreras, I., Frise, E., Kaynig, V., Longair, M., Pietzsch, T., Preibisch, S., Rueden, C., Saalfeld, S., Schmid, B., et al. (2012). Fiji: an open-source platform for biological-image analysis. *Nature Methods* 9, 676–682.
- Schopfer, P. (2001). Hydroxyl radical-induced cell-wall loosening in vitro and in vivo : implications for the control of elongation growth. *The Plant Journal* 28, 679-688.
- Schopfer, P. (2006). Biomechanics of plant growth 1. *American Journal of Botany* 93, 1415–1425.

- Serna, L., Torres-Contreras, J., and Fenoll, C. (2002). Clonal Analysis of Stomatal Development and Patterning in Arabidopsis Leaves. *Developmental Biology* 241, 24–33.
- Shibata, M., Uchihashi, T., Ando, T., and Yasuda, R. (2015). Long-tip high-speed atomic force microscopy for nanometer-scale imaging in live cells. *Scientific Reports* 5, 8724.
- Shyer, A.E., Huycke, T.R., Mahadevan, L., Tabin, C.J., Shyer, A.E., Huycke, T.R., Lee, C., Mahadevan, L., and Tabin, C.J. (2015). Bending Gradients : How the Intestinal Stem Cell Article Bending Gradients : How the Intestinal Stem Cell Gets Its Home. *Cell* 161, 569–580.
- Smith, R.S., Guyomarc'h, S., Mandel, T., Reinhardt, D., Kuhlemeier, C., and Prusinkiewicz, P. (2006). A plausible model of phyllotaxis. *Proceedings of the National Academy of Sciences of the United States of America* 103, 1301–1306.
- Smyth, D.R., Bowman, J.L., and Meyerowitz, E.M. (1990). Early Flower Development in Arabidopsis. *The Plant Cell* 2, 755–767.
- Sotiriou, P., Giannoutsou, E., Panteris, E., Galatis, B., and Apostolakis, P. (2018). Local differentiation of cell wall matrix polysaccharides in sinuous pavement cells : its possible involvement in the flexibility of cell shape. *Plant Biology* 20, 223-237.
- Suslov, D., and Verbelen, J. (2006). Cellulose orientation determines mechanical anisotropy in onion epidermis cell walls. *Journal of Experimental Botany* 57, 2183–2192.
- Tomos, a. D., and Leigh, R. A. (1999). The Pressure Probe: A Versatile Tool in Plant Cell Physiology. *Annual Review of Plant Physiology and Plant Molecular Biology* 50, 447–472.
- Várkuti, B.H., Yang, Z., Kintsés, B., Erdélyi, P., Bárdos-nagy, I., Kovács, A.L., Hári, P., Kellermayer, M., Vellai, T., and Málnási-Csizmadia, A. (2012). A novel actin binding site of myosin required for effective muscle contraction. *Nature Structural & Molecular Biology* 19, 299–306.
- Vella, D., Ajdari, A., Vaziri, A., and Boudaoud, A. (2012). The indentation of pressurized elastic shells: from polymeric capsules to yeast cells. *J R Soc Interface* 9, 448–455.
- Verger, S., Long, Y., Boudaoud, A., and Hamant, O. (2018). A tension-adhesion feedback loop in plant epidermis. *eLife* 7, e34460.
- Vincken, J.-P., Schols, H.A., Oomen, R.J.F.J., McCann, M.C., Ulvskov, P., Voragen, A.G.J., and Visser, R.G.F. (2003). If homogalacturonan were a side chain of rhamnogalacturonan I. Implications for cell wall architecture. *Plant Physiol.* 132, 1781–1789.
- Vlad, D., Kierzkowski, D., Rast, M.I., Vuolo, F., Dello Ioio, R., Galinha, C., Gan, X., Hajheidari, M., Hay, A., Smith, R.S., et al. (2014). Leaf shape evolution through duplication, regulatory diversification, and loss of a homeobox gene. *Science* 343, 780–783.
- Vogel, G. (2013). When do organs know when they have reached the right size? *Science* 340, 1156–1161.

Wang, L., Hukin, D., Pritchard, J., and Thomas, C. (2006). Comparison of plant cell turgor pressure measurement by pressure probe and micromanipulation. *Biotechnology Letters* 28, 1147–1150.

Wang, Y., Xiong, G., Hu, J., Jiang, L., Yu, H., Xu, J., Fang, Y., Zeng, L., Xu, E., Xu, J., et al. (2015). Copy number variation at the GL7 locus contributes to grain size diversity in rice. *Nature* 47, 944–948.

Weber, A., Braybrook, S., Huflejt, M., Mosca, G., Routier-Kierzkowska, A.L., and Smith, R.S. (2015). Measuring the mechanical properties of plant cells by combining micro-indentation with osmotic treatments. *Journal of Experimental Botany* 66, 3229–3241.

Willats, W.G., Orfila, C., Limberg, G., Buchholt, H.C., van Alebeek, G.J., Voragen, A.G., Marcus, S.E., Christensen, T.M., Mikkelsen, J.D., Murray, B.S., et al. (2001). Modulation of the degree and pattern of methyl-esterification of pectic homogalacturonan in plant cell walls. Implications for pectin methyl esterase action, matrix properties, and cell adhesion. *J. Biol. Chem.* 276, 19404–19413.

Wolf, S., Hématy, K., and Höfte, H. (2012). Growth Control and Cell Wall Signaling in Plants. *Annual Review of Plant Biology* 63, 381–407.

Wu, T.-C., Belteton, S.A...Pack, J...Szymanski, D.B...Umulis, D.M. (2016). LobeFinder: a convex hull-based method for quantitative boundary analyses of lobed plant cells. *Plant Physiology* 171, 2331–2342.

Xu, T., Wen, M., Nagawa, S., Fu, Y., Chen, J., Wu, M.-J., Perrot-Rechenmann, C., Friml, J., Jones, A.M., and Yang, Z. (2010). Cell surface- and Rho GTPase-based auxin signalling controls cellular interdigitation in Arabidopsis. *Cell* 143, 99–110.

Yu, M.-F., Kowalewski, T., and Ruoff, R.S. (2001). Structural Analysis of Collapsed , and Twisted and Collapsed , Multiwalled Carbon Nanotubes by Atomic Force Microscopy. *Physical Review Letters* 86, 87–90.

Zhang, C., Halsey, L.E., and Szymanski, D.B. (2011). The development and geometry of shape change in Arabidopsis thaliana cotyledon pavement cells. *BMC Plant Biology* 11:27.

Zhang, T., Mahgoudy-Louyeh, S., Tittmann, B., and Cosgrove, D.J. (2014). Visualization of the nanoscale pattern of recently-deposited cellulose microfibrils and matrix materials in never-dried primary walls of the onion epidermis. *Cellulose* 21, 853–862.

Acknowledgements

When I first came to the Max Planck Institute in Cologne five years ago, I did not think I would ever arrive at the moment of writing my doctoral thesis, let alone the acknowledgements (which implies that I actually managed to finish writing my thesis). I thought: ‘I don’t have what it takes to make it’ and, indeed, at the time I did not have what it takes. It was only due to guidance, trust, challenges, mentorship and friendship of a large group of people I met here that I was able to ‘make it’ and have fun in the meantime. What follows is a poor attempt to do each and every one of them justice.

First and foremost, I would like to thank my supervisor Richard S. Smith for the countless opportunities to learn and grow he gave me. He provided me with all possible tools to develop as a scientist and taught me to not give up on an idea when others say it cannot be done. Whatever awaits me in my future career, it would not have been possible without him trusting me years ago as a very green internship student. The same applies to Milos Tsiantis who has supported my work and given me valuable advice during my stay in his department.

I thank Adam Runions for being my partner in crime in possibly the most fun project in the history of science. Together we looked into every nook and cranny of puzzle cell development. Our long discussions taught me a lot, but more importantly, inspired me to enjoy my job and my life. I have been very lucky to have you as a role model and a friend.

I am very grateful to Anne-Lise Routier-Kierzkowska and Daniel Kierzkowski – especially in the early days, they encouraged me to believe in myself, work hard and aim high.

I have been very lucky to collaborate with and get advice from very bright minds. I would like to thank Adrienne Roeder, Olivier Hamant, Arezki Boudaoud, Chun Biu Li, Angela Hay, Achim Tresch and Peter Huijser for their feedback on my work, many discussions and asking difficult questions. Furthermore, I want to acknowledge my junior collaborators: Lilan Hong, Mingyuan Zhu, Mathilde Dumond, Nathan Hervieux and Satoru Tsugawa. We worked side by side on our projects and spent great times in the most bizarre places – from a waterfall in New York State, through a seafood restaurant in Singapore, to a skiing resort in Japan. I very much value their professional help as well as friendship.

I cannot begin to describe what an amazing experience it has been to work in the Tsiantis Department, where everyone is free to be their true self. The result of that is an explosive mix of peculiar individuals in which we respect each other and enjoy each other’s company every day (and many evenings as well!). I want you all to know that you made Cologne feel like home and I will never forget this. A special ‘thank you’ goes to my fellow PhD students, supporting each other through the ups and downs: Lukas, Miguel, Hannah, Elizabeta, Leona, Yi, Shanda, Ziliang, Gaby, Stefan, Alessandro, Sébastien, Farnaz. The Smith Group: Sören, Gabriella, Brendan, Mateusz, Milad, Namrata, Nacho, Dorota and Hagen. Other members, whom I call a

collaborator, teacher, role model, office buddy, lunch companion, friend, or all of the above: Anahit, Mainak, Luke, Marie, Wolfram, Cristina, Rita B., Rita P., Remco, Juan, Mohsen, Madieh, Ute, Isa, Sigi, Claire, Janne, Britta, Bjorn, Christos, Samija, Rena, David, Ismene.

Luckily, I also made great friends outside of building J: next door (such as Paloma and Sayan) or ‘out in the real world’ (such as Henning, Helen, Carina, Rafa and Roussanna).

Now I would like to mention a very special trio. Actually, they deserve a whole dissertation dedicated to them exclusively. Chidi, Francesco and Vangelis (in alphabetical order, as no other order would be fair) – my big brothers, who made me laugh even when nobody else could and taught me how to stand tall at any circumstance (in- or outside the lab). I miss you every day but I’m so proud of the roads you’ve taken.

Last but not least, Alfredo – his contributions go way beyond proof-reading this boring thesis. He supports me in good and bad times, always with a charming smile on his face. Sei la più grande sorpresa della mia vita (e sai quanto amo le sorprese). Spero che possiamo vedere molte cose e molti posti insieme. Sono molto felice di essere nella tua vita.

Wreszcie, specjalne podziękowania dla osób które są ze mną od zawsze:

dla Sabinki i Waldka – za ogromne wsparcie i ufanie moim szalonym pomysłom na życie,

dla Asi, Doroty i Kuby – za przetarcie mi szlaków jak przystało na starsze rodzeństwo i dawanie przykładu (co robić, lub czego nie robić☺), nawet jeśli jesteśmy bardzo daleko od siebie.

Oraz osób które dołączyły trochę później:

dla Ani – za wszystko, za to, że jest od zawsze i na zawsze,

dla Ewy – za ponadczasowe mądrości życiowe które zaczęły się pod licealnym automatem do kawy w roku 2006, ale wciąż są aktualne,

dla Oli i Łukasza – za to, że zawsze mają dla mnie miejsce w swoich sercach i w swoim domu,

dla Marysi – za umilanie mi życia w Kolonii dobrym słowem i dobrym jedzeniem,

i dla Marty – za to, że można z nią konie kraść (już kilka ukradłyśmy), i za to, że zdała egzamin z Fizyki Atomów, Cząsteczek i Makrocząsteczek Biologicznych szybciej ode mnie i zmotywowała mnie tym do nauki.

Lebenslauf

Persönliche Angaben

Name: Aleksandra Sapala

Geburtsdatum: 05.09.1990

Geburtsort: Stettin, Polen

Nationalität: Polnisch



Berufserfahrung

2015-2018 **Doktorandin**

Max Planck Institut für Pflanzenzüchtungsforschung, Köln

Abteilung Vergleichende Entwicklungsgenetik (Direktor: Prof. M.Tsiantis)

Gruppenleiter Dr. Richard S. Smith

2014 **Diplomandin (Masterarbeit)**

Max Planck Institut für Pflanzenzüchtungsforschung, Köln

Arbeitsgruppe Entwicklung und Vielfalt der Pflanzen

2013 **Laborpraktika**

Max Planck Institut für Pflanzenzüchtungsforschung, Köln

2012 **Laborpraktikum**

Centre of New Technologies, Universität Warschau

Laboratory of Bioinformatics and Systems Biology

2011 **Laborpraktikum**

Research Institute of Horticulture, Skierniewice, Poland

Genetically Modified Organisms Research Laboratory

Ausbildung

- 2012-2014 Master of Sciences, Physik
 Universität Warschau
- 2010-2015 Bachelor of Engineering, Gartenbau
 Warschauer Naturwissenschaftliche Universität
- 2009-2012 Bachelor of Sciences, Physik
 Universität Warschau

Konferenzvorträge

- 2018 'Why do plants make puzzle cells?'
 9. Internationale Konferenz der Biomechanik der Pflanzen, Montreal, Canada
- 2014 'Quantification of plant morphogenesis using confocal image treatment software
 MorphoGraphX'
 3. Internationale Konferenz der Biophysik-Studenten, Krakau, Polen

Stipendien

- 2015 International Max Planck Research School Doktorandstipendium

Sprachkenntnisse

- Englisch verhandlungssicher in Wort und Schrift (C1-Zertifikat)
- Deutsch verhandlungssicher in Wort und Schrift (C1-Zertifikat)
- Italienisch Grundkenntnisse
- Polnisch Muttersprache

Publikationen

Sapala, A., Runions, A. and Smith, R.S. (2019) Mechanics, geometry and genetics of epidermal cell shape regulation: different pieces of the same puzzle. *Current Opinion in Plant Biology* 47, 1-8. Published online on 28.08.2018.

Sapala, A., Runions, A., Routier-Kierzkowska, A.L., Gupta, M.D., Hong, L., Hofhuis, H., Verger, S., Mosca, G., Li, C.B., Hay, A., et al. (2018). Why plants make puzzle cells, and how their shape emerges. *eLife* 7:e32794.

Sapala, A. and Smith, R.S. (2018). Osmotic treatment for quantifying cell wall elasticity in the sepal of *Arabidopsis thaliana*. *Methods in Molecular Biology*. Submitted.

Mosca, G., Adibi, M., Strauss, S., Runions, A., **Sapala, A.**, Smith, R.S. (2018). Modeling plant tissue growth and cell division. In: *Mathematical modeling in plant biology*, Springer Verlag, in press.

Tsugawa, S., Hervieux, N., Kierzkowski, D., Routier-Kierzkowska A.-L., **Sapala, A.**, Hamant, O., Smith, R.S., Roeder, A.H.K., Boudaoud, A., Li, C.-B (2017). Clones of cells switch from reduction to enhancement of size variability in *Arabidopsis* sepals. *Development* 144, 4398-4405.

Mosca, G., **Sapala, A.**, Strauss, S., Routier-Kierzkowska, AL., Smith, RS (2017). On the micro-indentation of plant cells in a tissue context. *Physical Biology* 14 (1), 015003.

Hong, L., Dumond, M., Tsugawa, S., **Sapala, A.**, Routier-Kierzkowska, AL., Zhou, Y., Chen, C., Kiss, A., Zhu, M., Hamant, O., Smith, RS, Komatsuzaki, T., Li, C-B, Boudaoud, A., Roeder, AHK. (2016). Variable cell growth yields reproducible organ development through spatiotemporal averaging. *Developmental Cell* 38 (1), 15-32.

Hervieux, N., Dumond, M., **Sapala, A.**, Routier-Kierzkowska, A.-L., Kierzkowski, D., Roeder, AHK., Smith, R.S., Boudaoud, A., Hamant, O. (2016). A mechanical feedback restricts sepal growth and shape in *Arabidopsis*. *Current Biology* 26 (8), 1019-1028.

Barbier de Reuille, P., Routier-Kierzkowska, A.-L., Kierzkowski, D., Bassel, G.W., Schüpbach, T., Tauriello, G., Bajpai, N., Strauss, S., Weber, A., Kiss, A., Burian, A., Hofhuis, H., **Sapala, A.**, Lipowczan, M., Heimlicher, M. B., Robinson, S., Bayer, E. M., Basler, K., Koumoutsakos, P., Roeder, A. H. K., Aegerter-Wilmsen, T., Nakayama, N., Tsiantis, M., Hay, A., Kwiatkowska, D., Xenarios, I., Kuhlemeier, C., Smith, R. S (2015). MorphoGraphX: A platform for quantifying morphogenesis in 4D. *eLife*, 4:e05864.

Affidavit / Eidesstaatliche Erklärung

Ich versichere, dass ich die von mir vorgelegte Dissertation selbständig angefertigt, die benutzten Quellen und Hilfsmittel vollständig angegeben und die Stellen der Arbeit – einschließlich Tabellen, Karten und Abbildungen –, die anderen Werken im Wortlaut oder dem Sinn nach entnommen sind, in jedem Einzelfall als Entlehnung kenntlich gemacht habe; dass diese Dissertation noch keiner anderen Fakultät oder Universität zur Prüfung vorgelegen hat; dass sie – abgesehen von unten angegebenen Teilpublikationen – noch nicht veröffentlicht worden ist, sowie, dass ich eine solche Veröffentlichung vor Abschluss des Promotionsverfahrens nicht vornehmen werde.

Die Bestimmungen der Promotionsordnung sind mir bekannt. Die von mir vorgelegte Dissertation ist von Prof. Dr. Miltos Tsiantis betreut worden.

Ich versichere, dass ich alle Angaben wahrheitsgemäß nach bestem Wissen und Gewissen gemacht habe und verpflichte mich, jedmögliche, die obigen Angaben betreffenden Veränderungen, dem Dekanat unverzüglich mitzuteilen

Köln, 24.09.2018

Aleksandra Sapala

Teilbublikationen

Sapala, A., Runions, A. and Smith, R.S. (2019). Mechanics, geometry and genetics of epidermal cell shape regulation: different pieces of the same puzzle. *Current Opinion in Plant Biology* 47, 1-8. Published online on 28.08.2018.

Sapala, A., Runions, A., Routier-Kierzkowska, A.L., Gupta, M.D., Hong, L., Hofhuis, H., Verger, S., Mosca, G., Li, C.B., Hay, A., et al. (2018). Why plants make puzzle cells, and how their shape emerges. *eLife* 7:e32794.

Mosca, G., Sapala, A., Strauss, S., Routier-Kierzkowska, AL., Smith, RS (2017). On the micro-indentation of plant cells in a tissue context. *Physical biology* 14 (1), 015003.

Hong, L., Dumond, M., Tsugawa, S., Sapala, A., Routier-Kierzkowska, AL., Zhou, Y., Chen, C., Kiss, A., Zhu, M., Hamant, O., Smith, RS, Komatsuzaki, T., Li, C-B, Boudaoud, A., Roeder, AHK. (2016). Variable cell growth yields reproducible organ development through spatiotemporal averaging. *Developmental Cell* 38 (1), 15-32.

Hervieux, N., Dumond, M., Sapala, A., Routier-Kierzkowska, A.-L., Kierzkowski, D., Roeder, AHK., Smith, R.S., Boudaoud, A., Hamant, O. (2016). A mechanical feedback restricts sepal growth and shape in *Arabidopsis*. *Current Biology* 26 (8), 1019-1028.